Visible-light triggered templated ligation on surface using furan-modified PNAs

Alex Manicardi‡*, Enrico Cadoni‡, and Annemieke Madder*

1. General

All reagents were purchased from Sigma-Aldrich, Fluka, Merck, TCI Europe, Fluorochem and used without further purification. Dry DMF was stored over 4 Å molecular sieves. TLCs were run on Merck silica 60 on aluminum sheets. Column chromatography was performed as flash chromatography on Grace silica 60 (0.060- 0.200 mm). DNA and RNA sequences were purchased from IDT (Leuven, Belgium).

3-(2-benzyl-1,3-dioxo-1,2,3,3a,7,7a-hexahydro-4H-4,7-epoxyisoindol-4-yl)propanoic acid was synthesized according to a procedure previously reported.[1]

NMR spectra were recorded on a Bruker Avance 300 or 400. δ values are expressed in ppm relatively either to $CDCl_3$ (7.29 ppm for proton and 76.9 ppm for carbon) or DMSO-d^6 (2.50 ppm for proton and 39.5 ppm for carbon). The following abbreviations are used to explain the multiplicities: s=singlet, d=doublet, t=triplet, q=quartet, m=multiplet, and br=broad.
HPLC-MS data were collected on an Agilent 1100 Series instrument equipped with a Phenomenex Kinetex C18 100 Å column (150 x 4.6 mm, 5 µm at 35 °C) connected to an ESMSD type VL mass detector (quadrupole ion trap mass spectrometer) with a flow rate of 1.5 ml/min was used with the following solvent systems: (A): 0.1% HCOOH in H_2O and (B) MeCN. Gradient: 100% A for 2 min, then a gradient from 0 to 100% B over 6 min was used, followed by 2 min of flushing with 100% B (further referred to as HPLC1 conditions) or 100% A for 0.5 min, a gradient from 0 to 10% B over 0.1 min and then from 10 % to 30 % B over 7.7 minutes was used, followed by 2 min of flushing with 100% B (further referred to as HPLC2 conditions).
HPLC-UV data were collected on an Agilent 1100 Series instrument equipped with a Waters XTERRA RP18 5µm column (250 x 2.1 mm at 40°C or 50°C) connected to a DAD using a flow rate of 0.35 ml/min with the following solvent systems: (A): 0.1% TFA in H_2O and (B) 0.1% TFA in MeCN. Gradient: 100% A for 1 min, then a gradient from 0 to 10% B in 1 min, then to 30% B in 10 min, and finally to 100% B in 1 min, followed by 3.5 min of flushing with 100% B (further referred to as HPLC3 conditions). PNA oligomers were purified using a Luna C18(2) (5 µm, 100 Å, 250x10 mm) (further referred to as HPLC4 conditions: 100% A for 5 min, then a gradient from 0 to 50% B over 30 min at a flow rate of 4.0 ml/min).
UV-VIS spectra were recorded using a Trinean DropSense96 UV/VIS droplet reader.
Thermal denaturation experiments were recorded on a Varian Cary 300 Bio instrument equipped with a six-cell thermostatted cell holder.
MALDI-TOF analysis was performed using an Applied Biosystems - 4800 Plus MALDI TOF/TOF™ Analyzer. As matrix, 100mg/ml 2,5-Dihydroxybenzoic acid (DHB) in mQ water : MeCN (1:2) + 0.1% TFA was used.
PAGE analysis was performed using CBS Scientific QNC-700 Quadra Mini-Vertical Combo System, connected to a Consort 202 EV power supply. Gels were prepared into Novex 8x8 cm Empty Cassettes (1.0 mm). Temperature control was ensured by a JULABO-F12 refrigerated circulator connected to the QNC.
Crosslinking experiments were performed using Eppendorf Thermomixer Comfort for temperature control and Euromex Illuminator EK-1 lamps (100W halogen lamp LE.5210), equipped with Euromex LE.5214 dual arm light conductor. Power of the lamps was measured using a TES 1335 light meter equipped with a custom fitting for the lamp bulbs.
Surface ligation experiments were performed using Stuart SSM1 mini orbital shaker for uniform shaking of the wells. The temperature control was ensured by a homemade thermostat incubation chamber.
Microarray slides were scanned with an Agilent G2565CA.
Densitometric measurements where performed using ImageJ 1.52p software.

2. Monomer and photosensitizer synthesis

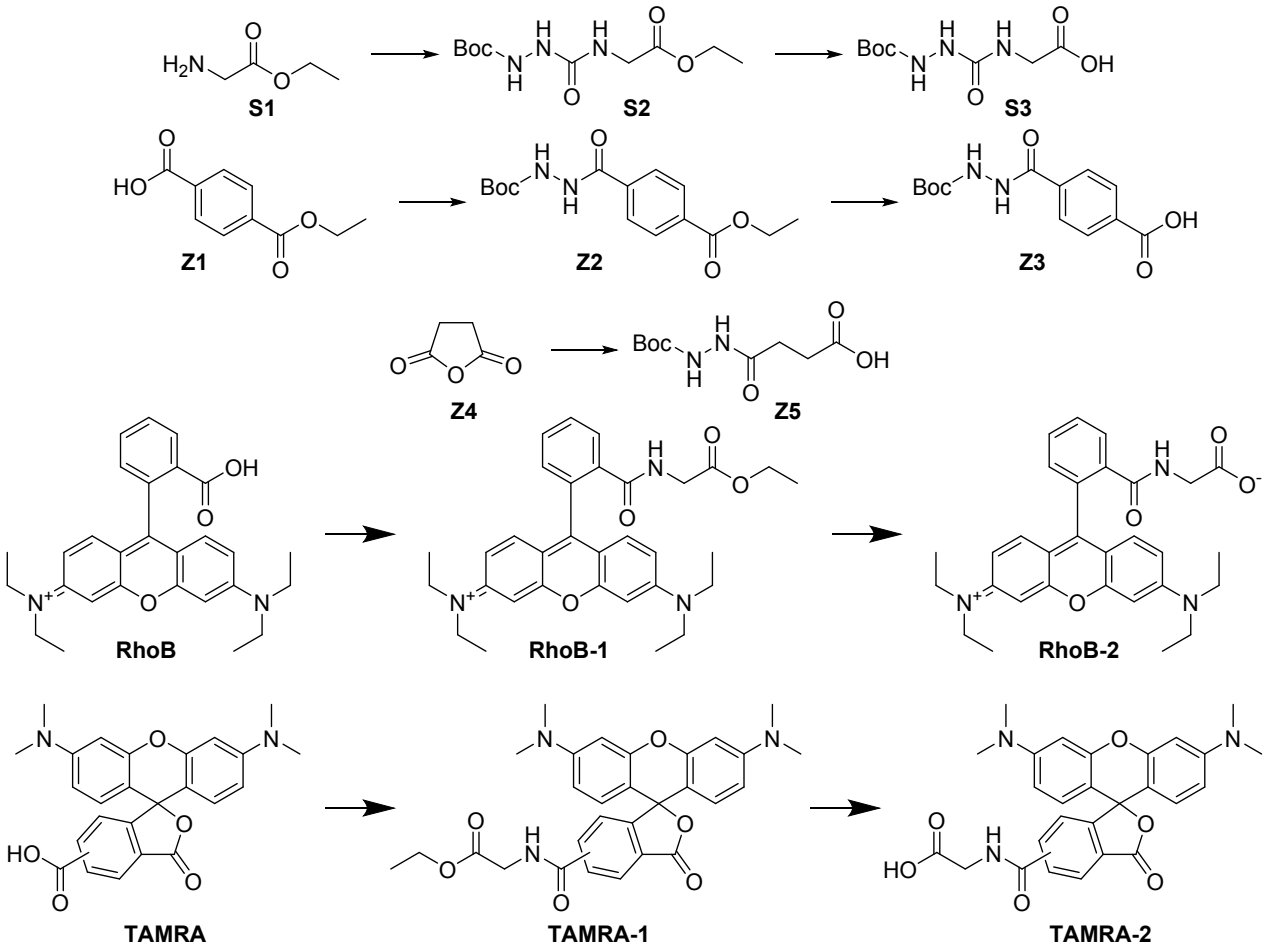

Scheme S1: overview of small molecules synthesized for this study.

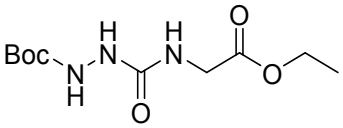

Ethyl N6-Boc-(hydrazinecarbonyl)glycinate (S2): in a round bottom flask glycine ethyl ester hydrochloride (984.1 mg, 7.050 mmol, 1 eq.) was dispersed in DCM (20 mL), then carbonyldiimidazole (1.20g, 7.40 mmol, 1.05 eq.) was added followed by DIPEA (3.69 mL, 21.15 mmol, 3 eq.). After 1h, the reaction became clear and tert-butylcarbazide (931.8 mg, 7.05mmol, 1 eq.) was added to the mixture and left react overnight. Solvent was then removed under reduced pressure and the resulting oil was taken up with AcOEt (100 mL) and washed with 0.1 M HCl (2x100 mL) and brine (100 mL). The organic layer was then dried over Na_2SO_4 and the solvent removed under reduced pressure, affording **S2** as a white powder (823.4 mg, 44.7% yield). **TLC** (AcOEt): Rf= 0.26; **^{1}H-NMR** ($CDCl_3$, 400 MHz) δ 6.82 (s, 1H), 6.64 (s, 1H), 5.98 (t, J = 5.3 Hz, 1H), 4.18 (q, J = 7.1 Hz, 2H), 3.99 (d, J = 5.5 Hz, 2H), 1.45 (s, 9H), 1.25 (t, J = 7.1 Hz, 3H); **^{13}C NMR** ($CDCl_3$, 101 MHz) δ 171.0, 158.6, 156.2, 82.2, 61.6, 42.0, 28.3, 14.3.; **MS** (ESI, MeOH) m/z calcd for $[C_{10}H_{19}N_3O_5]$ 261.13247, found: 260.4 $[M-H]^-$; **HRMS** (ESI, MeOH) found 260.1264 for $[C_{10}H_{18}N_3O_5]^+$.

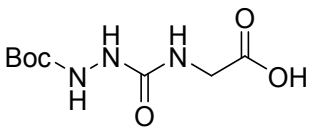

N6-Boc-(hydrazinecarbonyl)glycine (S3): in a round bottom flask **S2** (778.5 mg, 2.98 mmol, 1 eq.) was solubilized in MeOH (15 mL) and cooled down to 0°C with an ice bath before the addition of a NaOH solution (1.191 g, 29.8 mmol, 10 eq.) in water (15 mL). After 30 minutes the reaction was allowed to warm to r.t. and it was left to react for further 90 minutes. The volatile fraction was removed and the resulting aqueous phase was washed with DCM (2x30 mL). The pH was adjusted to 2.5 with HCl, then the aqueous phase was washed with AcOEt (5x20 mL). The merged organic fractions were dried over Na_2SO_4 and the solvent was removed under reduced pressure to afford **S3** as a white powder (445.5 mg,

64.1% yield). **TLC** (AcOEt/MEOH 9:1): Rf= 0.34; **^{1}H-NMR** (400 MHz, DMSO-d^6) δ 12.43 (s, 1H), 8.55 (s, 1H), 7.85 (s, 1H), 6.43 (s, 1H), 3.69 (d, J = 5.8 Hz, 2H), 1.39 (s, 9H); **^{13}C NMR** (101 MHz, DMSO-d^6) δ 172.06, 158.18, 155.95, 78.98, 41.28, 28.09; **MS** (ESI, MeOH) m/z calcd for $[C_8H_{15}N_3O_5]$ 233.10117, found: 467.2.2 $[2M+H]^+$, 489.2 $[2M+Na]^+$, 232.2 $[M-H]^-$, 465.2 $[2M-H]^-$; **HRMS** (ESI, MeOH) found 232.0942 for $[C_8H_{14}N_3O_5]^-$.

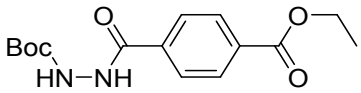

Ethyl 4-(2-Boc-hydrazinecarbonyl)benzoate (Z2): in a round bottom flask 4-(ethoxycarbonyl)benzoic acid (317.2 mg, 1.63 mmol, 1.2 eq.) was solubilized in DMF (3 mL) together with HBTU (593.8 mg, 1.57 mmol, 1.15 eq.) and the temperature was lowered to 0°C with an ice bath before the addition of DIPEA (522.3 µL, 2.99 mmol, 2.2 eq.). The reaction was left to react for 15 minutes at 0°C with formation of a milky solution, then allowed to warm to r.t. for further 15 minutes. The temperature is then reduced again to 0°C before the addition of tert-butylcarbazide (179.9 mg, 1.36 mmol, 1 eq.). In 15 minutes at 0°C the reaction turned clear, and then it was allowed to warm at r.t. and left to react for further 90 minutes. The reaction mixture was then diluted with AcOEt (100 mL) and washed with $KHSO_4$ (2x100 mL) and $NaHCO_3$ (2x100 mL) and brine (100 mL). The organic layer was then dried over Na_2SO_4 and the solvent removed under reduced pressure, affording **Z2** as a white powder (419.6 mg, 99.9% yield). **TLC** (AcOEt): Rf= 0.63; **^{1}H-NMR** ($CDCl_3$, 400 MHz) δ 8.38 (s, 1H), 8.07 (d, J = 8.4 Hz, 2H), 7.85 (d, J = 8.4 Hz, 2H), 6.82 (s, 1H), 4.40 (q, J = 7.1 Hz, 2H), 1.49 (s, 9H), 1.41 (t, J = 7.1 Hz, 3H); **^{13}C NMR** ($CDCl_3$, 101 MHz) δ 166.1, 165.8, 155.8, 135.6, 133.9, 130.0, 127.4, 82.5, 61.6, 28.3, 14.4; **MS** (ESI, MeOH) m/z calcd for $[C_{15}H_{20}N_2O_5]$ 308.13722, found: 307.3 $[M-H]^-$; **HRMS** (ESI, MeOH) found 307.1288 for $[C_{15}H_{19}N_2O_5]^-$.

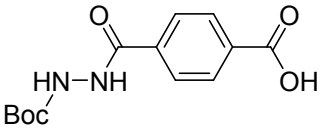

4-(2-Boc-hydrazinecarbonyl)benzoic acid (Z3): in a round bottom flask **Z2** (404.6 mg, 1.31 mmol, 1 eq.) was solubilized in MeOH (10 mL) and a NaOH solution (544 mg, 13.1 mmol, 10 eq.) in water (10 mL). After 30 minutes the volatile fraction was removed and the pH was adjusted to 1.5 with HCl, the solution was allowed to precipitate at 4°C for at least 2h. **Z3** was collected through Buchner filtration as a beige powder (302.1 mg, 82.1% yield). **TLC** (AcOEt): Rf= 0.24; **^{1}H-NMR** (DMSO-d^6, 400 MHz) δ 13.24 (s, 1H), 10.35 (s, 1H), 8.98 (s, 1H), 8.03 (d, J = 8.6 Hz, 2H), 7.94 (d, J = 8.1 Hz, 2H), 1.43 (s, 9H); **^{13}C NMR** (DMSO-d^6, 101 MHz) δ 166.7, 165.4, 155.4, 136.3, 133.5, 129.5, 129.4, 127.6, 79.3, 28.1; **MS** (ESI, MeOH) m/z calcd for $[C_{13}H_{16}N_2O_5]$ 280.10592, found: 279.3 $[M-H]^-$; **HRMS** (ESI, MeOH) found 279.0990 for $[C_{13}H_{15}N_2O_5]^-$.

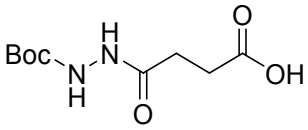

4-(2-Boc-hydrazineyl)-4-oxobutanoic acid (Z5): in a round bottom flask succinic anhydride (207.6 mg, 2.07 mmol, 1 eq.) and tert-butylcarbazide (301.6 mg, 2.28 mol, 1.1 eq.) were solubilized in DCM (5 mL). After 1h the reaction mixture was diluted with DCM (10 mL) and quenched with 20 mL $KHSO_4$. The mixture was transferred in a separatory funnel and the aqueous phase washed with additional 20 mL DCM. Finally, the aqueous phase was extracted with AcOEt (4x20 mL). The organic layer was then dried over Na_2SO_4 and the solvent removed under reduced pressure, affording **Z5** as a white hygroscopic foam (468.8 mg, 97.1% yield). **TLC** (AcOEt): Rf= 0.21; **^{1}H-NMR** (DMSO-d^6, 400 MHz) δ 12.09, 9.52, 8.68, 3.32, 2.44, 2.44, 2.43, 2.42, 2.42, 2.41, 2.37, 2.33, 2.33, 2.31, 2.30, 1.41, 1.38; **^{13}C NMR** ($CDCl_3$, 101 MHz) δ 173.5, 170.7, 155.2, 79.0, 28.7, 28.1, 28.0; **MS** (ESI, MeOH) m/z calcd for $[C_9H_{16}N_2O_5]$ 232.10592, found: 231.1 $[M-H]^-$; **HRMS** (ESI, MeOH) found 231.0990 for $[M-H]^-$.

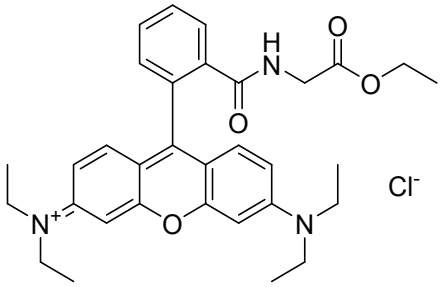

***N*-(6-(diethylamino)-9-(2-((2-ethoxy-2-oxoethyl)carbamoyl)phenyl)-3*H*-xanthen-3-ylidene)-*N*-ethylethanaminium chloride (Rhob-1):** in a round bottom flask, rhodamine B chloride (100.0 mg, 0.21 mmol, 1.0 eq.), glycine ethyl ester

hydrochloride (58.6 mg, 0.42 mmol, 2.0 eq.) and 4-dimethylaminopyridine (102.6 mg, 0.84 mmol, 4.0 eq.) were dissolved in DCM (3 mL) and the solution cooled down to 0°C with an ice bath, protected from light. Ethylcarbodiimide hydrochloride (80.5 mg, 0.42 mmol, 2.0 eq.) is added in a period of 5 minutes, after which the mixture was allowed to warm to r.t. and left react overnight. The reaction mixture was then diluted to 30 mL with DCM and washed with saturated $NaHCO_3$ (2x30 mL), HCl 0.1 M (2x30 mL), and brine (2x30 mL). The organic layer was then dried over Na_2SO_4 and passed through a small layer of silica before the removal of the solvent under reduced pressure to afford **Rhob-1** as red solid (100.7 mg, 85% yield). **TLC** (DCM): Rf=0.3; **^{1}H-NMR** (300 MHz, $CDCl_3$) δ 7.91 – 7.81 (m, 1H), 7.42 – 7.33 (m, 2H), 7.07 – 6.97 (m, 1H), 6.46 (d, *J* = 8.9 Hz, 2H), 6.29 (d, *J* = 2.6 Hz, 2H), 6.20 (dd, *J* = 8.9, 2.6 Hz, 2H), 3.82 (q, *J* = 7.1 Hz, 2H), 3.76 (s, 2H), 3.26 (q, *J* = 7.1 Hz, 8H), 1.08 (t, *J* = 7.0 Hz, 12H), 1.02 (t, *J* = 7.1 Hz, 3H); **^{13}C-NMR** (100 MHz, $CDCl_3$) δ 168.5, 168.0, 153.7, 153.6, 148.9, 132.7, 130.7, 129.6, 128.2, 124.0, 123.3, 108.1, 104.9, 97.7, 77.5, 76.8, 61.0, 44.5, 41.8, 29.8, 14.1, 12.7. **MS** (ESI, MeOH) m/z calcd for $[C_{32}H_{38}N_3O_4]^+$ 528.67245, found: 528.2 $[M+H]^+$; **HRMS** (ESI, MeOH) found 528.2854 for $[C_{32}H_{38}N_3O_4]^+$.

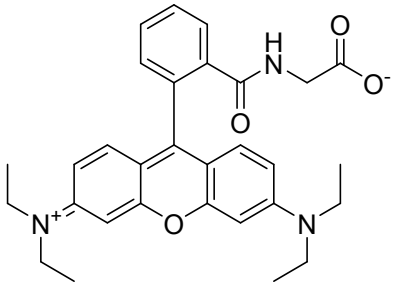

(2-(6-(diethylamino)-3-(diethyliminio)-3*H*-xanthen-9-yl)benzoyl)glycinate (Rhob-2): in a round bottom flask, **Rhob-1** (260 mg, 0.461 mmol, 1.0 eq.) was dissolved in MeOH (1 ml), a 1 ml NaOH (19.8 mg, 0.496 mmol, 1.08 eq.) aqueous solution was added dropwise. After 3 hours the volatile fraction was removed and the pH was adjusted to 2 with HCl 0.1 M. The precipitate was filtered was filtered and dried to obtain **R3** as pink powder (183 mg, 79.7% yield). **TLC** (DCM): Rf=0; **^{1}H NMR** (400 MHz, DMSO-*d*6) δ 12.37 (s, 1H), 7.83 – 7.77 (m, 1H), 7.54 – 7.47 (m, 2H), 7.04 – 6.98 (m, 1H), 6.42 (d, *J* = 8.7 Hz, 2H), 6.35 (d, *J* = 2.5 Hz, 2H), 6.32 (dd, *J* = 8.8, 2.6 Hz, 2H), 3.58 (s, 2H), 3.31 (q, *J* = 6.6 Hz *), 1.08 (t, *J* = 7.0 Hz, 12H). **^{13}C-NMR** (101 MHz, DMSO-d^6) δ 168.8, 166.8, 153.6, 152.7, 148.3, 132.8, 129.7, 128.9, 128.3, 123.6, 122.4, 107.8, 104.2, 97.0, 64.3, 43.6, 41.1, 12.4. **MS** (ESI, MeOH) m/z calcd for $[C_{30}H_{33}N_3O_4]$ 499.6, found: 500.1 $[M+H]^+$; **HRMS** (ESI, ACN) found 500.2559 for $[C_{30}H_{34}N_3O_4]^+$.
* Integral not defined due to signal overlap with water peak.

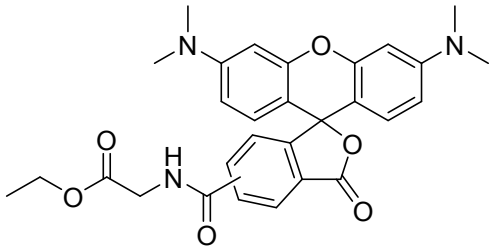

Ethyl (3',6'-bis(dimethylamino)-3-oxo-3*H*-spiro[isobenzofuran-1,9'-xanthene]-5(6)-carbonyl)glycinate (TAMRA-1): in a round bottom flask, 5(6)-carboxytetramethylrhodamine (100 mg, 0.242 mmol, 1.0 eq.) was dissolved in DMF (1ml). DIPEA (125 µl, 0.72 mmol, 3.1 eq.), glycine ethyl ester hydrochloride (67 mg, 0.48 mmol, 2.0 eq.) and HBTU (96.8 mg, 0.255 mmol, 1.1 eq.) are subsequently added and stirred under argon for 5 hours, shielded from the light. The solvent is removed under reduced pressure, the mixture solubilized in DCM (30 ml) and washed with HCl 0.1 M (3x30 mL), saturated $NaHCO_3$ (3x30 mL) and brine (1x30 mL) aqueous solutions. The organic layer was then dried over Na_2SO_4 and the solvent removed under reduced pressure to afford **TAMRA-1** in 93% yield (116 mg, 0.225 mmol). **TLC** (DCM:MeOH 9:1): Rf= 0.4; **^{1}H-NMR** (DMSO, 400 MHz, major regioisomer) δ 9.38 (t, *J* = 5.8 Hz, 1H), 8.71 (s, 1H), 8.32 (dd, *J* = 8.0, 1.8 Hz, 1H), 7.60 (d, *J* = 7.9 Hz, 1H), 7.03 (s, 3H), 6.94 (s, 2H), 4.16 (q, *J* = 7.1 Hz, 2H), 4.10 (t, *J* = 6.7 Hz, 2H), 3.25 (s, 12H), 1.24 (t, *J* = 7.1 Hz, 3H); δ ; **MS** (ESI, MeOH) m/z calcd for $[C_{29}H_{29}N_3O_6]$ 515.20564, found: 516.1 $[M + H]^+$; **HRMS** (ESI, MeOH) found 516.2133 for $[M + H]^+$.

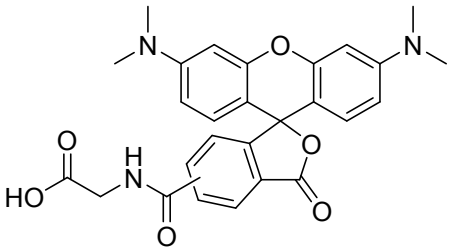

(3',6'-bis(dimethylamino)-3-oxo-3*H*-spiro[isobenzofuran-1,9'-xanthene]-5(6)-carbonyl)glycine (TAMRA-2): **TAMRA-1** (100 mg, 0.194 mmol, 1.0 eq.) was dissolved in MeOH (1 ml) and 1 ml of aqueous NaOH solution (15.5 mg, 0.388 mmol, 2 eq.) slowly added dropwise. The mixture was reacted for two hours, after which all the starting material was consumed. MeOH was then removed under reduced pressure and the aqueous residue acidified with HCl 2 M to pH 3. The solution was stored at -22 °C until a pink precipitate appeared. The precipitate was filtered and washed with acetone. The procedure was repeated once again with the residual acetone solution, and the solid obtained collected together to afford **R6** in 70.1 % yield (0.136 mmol 68.5 mg)**. TLC** (DCM:MeOH 1:1): Rf= 0.1; **^{1}H-NMR**, two regioisomers (D_2O, 400 MHz) δ 8.15 – 8.10 (m, 1H), 7.95 (d, *J* = 8.5 Hz, 1H), 7.92 (d, *J* = 8.4 Hz, 1H), 7.77 (d, *J* = 8.2 Hz, 1H), 7.60 (s, 1H), 7.37 (d, *J* = 7.9 Hz, 1H), 7.07 – 7.00 (m, 2H), 6.98 (m, 2H), 6.72 – 6.51 (m, 4H), 6.17 (dd, *J* = 25.1, 2.4 Hz, 4H), 3.91 (s, 2H), 3.76 (s, 2H), 2.89 (s, 24H). **^{13}C NMR**, two regioisomers (D_2O, 100 MHz) δ 157.71, 156.73, 156.63, 134.90, 133.95, 133.64, 130.93, 130.88, 130.56, 130.22, 129.32, 128.72, 128.05, 127.26, 113.75, 113.69, 112.74, 112.67, 96.08, 43.98, 39.98; **MS** (ESI, MeOH) m/z calcd for $[C_{27}H_{25}N_3O_6]$ 487.17434, found: 488.2 $[M+H]^+$; **HRMS** (ESI, ACN) found 488.1820 for $[C_{27}H_{26}N_3O_6]^+$.

3. PNA synthesis

The synthesis of the PNA probes was performed with standard manual Fmoc-based solid-phase synthesis using HBTU/DIPEA as coupling mixture and commercially available Fmoc-PNA-OH monomers (Biosearch Technologies, Scotland). Rinkamide-ChemMatrix resin was first loaded with Fmoc-Arg$_{(Pbf)}$-OH, Fmoc-Lys$_{(Mtt)}$-OH or Fmoc-Lys$_{(Dde)}$-OH as first monomer (0.2 mmol/g). Modifications of lysine side chains were performed after Dde (for a 5 µmol scale: shake vigorously the resin for 1h in a solution containing 250 mg hydroxylamine hydrochloride and 184 mg imidazole in 1.2 mL NMP/DMF 5:1)[2] or Mtt (for a 5 µmol scale: 0.5 mL off 0.5% BtOH·H_2O in HFIP/DCM 1:1, 4 x 3 minutes)[3] deprotection for furan and TAMRA insertion, respectively. All coupling steps are performed using HBTU/DIPEA as activating mixture except for **Z5** where a DIC/DhBtOH mixture was used. More in detail, for all furan-containing probes a Fmoc-Lys$_{(Dde)}$-OH was introduced at the C-terminus of the PNA sequence and, after probe elongation, the Dde protective group was removed to allow the coupling of 3-(2-benzyl-1,3-dioxo-1,2,3,3a,7,7a-hexahydro-4H-4,7-epoxyisoindol-4-yl)propanoic acid (in order to safeguard the acid sensitive furan moiety during the final cleavage, a Diels-Alder adduct was formed between 3-(furan-2-yl)propanoic acid and N-benzyl maleimide); final Fmoc deprotection was performed before probe cleavage from the solid support. For the nucleophilic probes, Fmoc-Lys$_{(Mtt)}$-OH was coupled to the resin after the PNA sequence, the Mtt protective group was removed and the resulting free amine was acetylated or coupled to the TAMRA; removal of the Fmoc protective group allowed the final introduction of the desired protected nucleophile. For **PNA-Am3**, **PNA-Ac3**, and **PNA-Hy3** a resin bearing a Fmoc-Lys$_{(Dde)}$-OH as first residue was employed, the Fmoc group was removed to allow the introduction of the Biot-PEG$_4$ reporter, while subsequent Dde removal allowed the synthesis of the remainder of the probe.

Cleavages were performed using a TFA/m-cresol (9:1) cleavage cocktail. After RP-HPLC purification (HPLC4 conditions, *vide supra* general), the purity and identity of the PNAs were evaluated by LC-MS (HPLC1 conditions).

Retro Diels-Alder protocol: the crude PNA obtained after cleavage was solubilized in mQ water at a final PNA concentration of 1 mM (based on synthesis scale). If necessary, the pH of the solution can be increased from ~3 to 11.5 with carbonate buffer (add 10 µL of saturate sodium carbonate solution for each µmol of crude, then adjust with 1M NaOH). The solution was then aliquoted in 1.5 mL Eppendorf and submitted to the retro Diels-Alder temperature ramp: (A) pH ~3: from 25°C to 90°C in 30 minutes, then 90°C for 4.5h and finally to 15°C in 20 minutes; (B) pH ~11.5: from 25°C to 90°C in 30 minutes, then 90°C for 90 minutes and finally to 15°C in 20 minutes. In case of presence of PEG-based spacers, the retro-Diels-Alder has to be carried out in basic conditions to avoid ether bond hydrolysis.[1]

Table S1: PNA sequences synthesized for this study. Capital letters indicate PNA monomers, small letters indicate L-amino acids, modifications on the lysine side chain are indicated inserted inside brackets: Fur: 3-(furan-2-yl)propanoyl; O: 2-(2-aminoethoxy)ethoxyacetyl (AEEA spacer); Ahx: 6-aminohexanoyl; TAMRA: carboxytetramethylrhodamine;

PNA/DNA/RNA	Sequence
PNA-Fur0-5mer	Ac-GATCT-k$_{(Fur)}$rr-NH_2
PNA-Fur0-9mer	Ac-GCATGATCT-k$_{(Fur)}$rr-NH_2
PNA-Fur0-11mer	Ac-GGGCATGATCT-k$_{(Fur)}$rr-NH_2
PNA-Fur1	Ac-ATGATCT-k$_{(Fur)}$rr-NH_2
PNA-Fur2	Ac-ATCATGT-k$_{(Fur)}$rr-NH_2
PNA-Fur3	Ac-TTATCAG-k$_{(Fur)}$rr-NH_2
PNA-Fur4	H-OO-GGGCATGATCT-k$_{(Fur)}$rr-NH2
PNA-Fur5	H-OO-GTCTTGAGCAG-k$_{(Fur)}$rr-NH2
PNA-Am0	H-AGATCATGCCC-k$_{(Dde)}$rr-NH_2
PNA-Am1	H-β-Ala-k$_{(Ac)}$-AGATCATGCCC-rrr-NH_2
PNA-Am2(TAMRA-6)	H-β-Ala-k$_{(6\text{-}TAMRA)}$-AGATCATGCCC-rrr-NH_2
PNA-Am2(TAMRA-5)	H-β-Ala-k$_{(5\text{-}TAMRA)}$-AGATCATGCCC-rrr-NH_2
PNA-Am3	Biot-PEG_4-k(H-g-k$_{(5\text{-}TAMRA)}$-AGATCATGCCC-rrr-->)-NH_2
PNA-Ac0	Ac-AGATCATGCCC-rrr-NH_2
PNA-Ac1	Ac-β-Ala-k$_{(Ac)}$-AGATCATGCCC-rrr-NH_2
PNA-Ac2(TAMRA-6)	Ac-β-Ala-k$_{(6\text{-}TAMRA)}$-AGATCATGCCC-rrr-NH_2
PNA-Ac2(TAMRA-5)	Ac-β-Ala-k$_{(5\text{-}TAMRA)}$-AGATCATGCCC-rrr-NH_2
PNA-Ac3	Biot-PEG_4-k(Ac-g-k$_{(5\text{-}TAMRA)}$-AGATCATGCCC-rrr-->)-NH_2
PNA-Hy0	H_2N-NH-CH_2CO-g-Ahx-AGATCATGCCC-k$_{(Dde)}$-rr-NH_2
PNA-Hy1	H_2N-NH-CH_2CO-k$_{(Ac)}$-AGATCATGCCC-rrr-NH_2
PNA-Hy2(TAMRA-6)	H_2N-NH-CH_2CO-k$_{(6\text{-}TAMRA)}$-AGATCATGCCC-rrr-NH_2
PNA-Hy2(TAMRA-5)	H_2N-NH-CH_2CO-k$_{(5\text{-}TAMRA)}$-AGATCATGCCC-rrr-NH_2

PNA-Hy3	Biot-PEG_4-k(H_2N-g-$k_{(5\text{-}TAMRA)}$-AGATCATGCCC-rrr-->)-NH_2
PNA-Sc0	H_2N-NH-CO-NH-CH_2CO-g-Ahx-AGATCATGCCC-$k_{(Dde)}$-rr-NH_2
PNA-Sc1	H_2N-NHCONH-CH2CO-$k_{(Ac)}$-AGATCATGCCC-rrr-NH_2
PNA-Hd0	H_2N-NHCO-(4)Ph(1)-CO-g-Ahx-AGATCATGCCC-$k_{(Dde)}$-rr-NH_2
PNA-Hd1	H_2N-NHCO(CH_2)$_2$CO-$k_{(Ac)}$-AGATCATGCCC-rrr-NH_2
DNA 1	5’-ATGATCTCTGATAA-3’
DNA 2	5’-ATGATCTCAGTTAA-3’
DNA 3	5'-GGGCATGATCTCTGCTCAAGAC-3'
DNA 4	5'-GGGCATGATCTCCGCGTAATAC-3'
DNA 5	5'-GGCCAGGATTTCCGCGTAATAC-3'
DNA 6	5'-AATGTGTGCGCTACACGCTAGC-3'
RNA 1	5’-AUGAUCUCUGAUAA-3’
RNA 2	5’-AUGAUCUCAGUUAA-3’
RNA 3	5'-GGGCAUGAUCUCUGCUCAAGAC-3'
RNA 4	5'-GGGCAUGAUCUCCGCGUAAUAC-3'
RNA 5	5'-GGGCAUGAUCUUACACGCUAGC-3'
RNA 6	5'-AAUGUGUGCGCUACACGCUAGC-3'

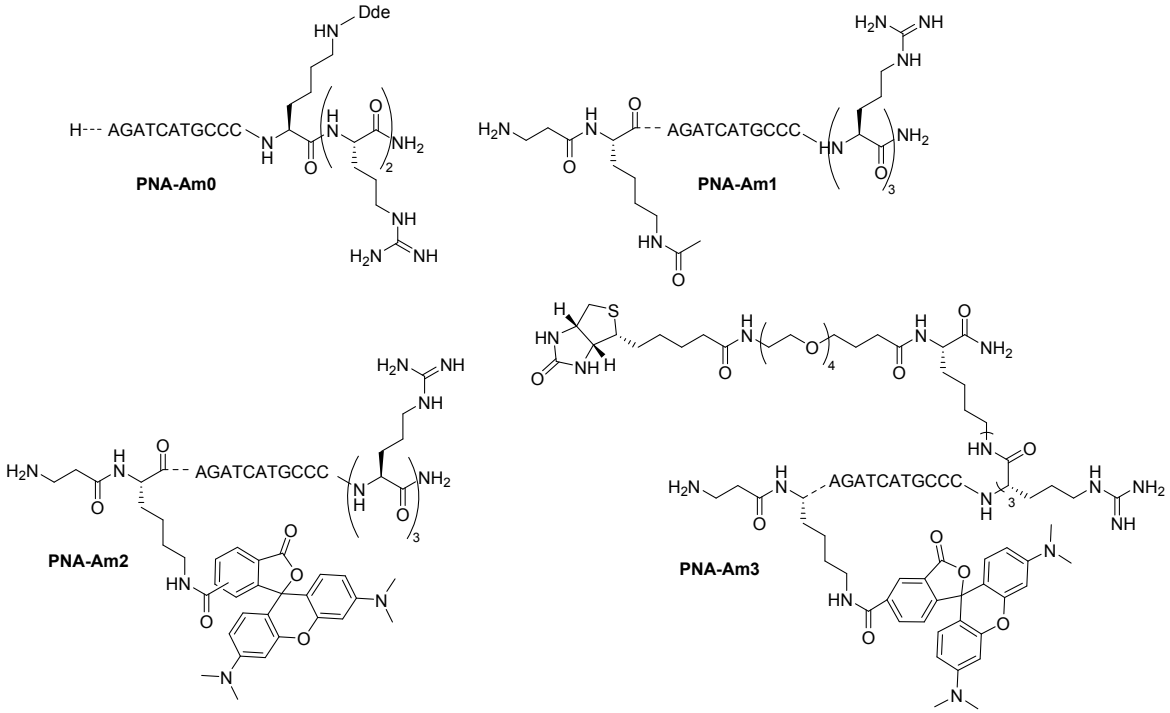

Figure S1: structure and sequence of the amino-PNA probes used in this study.

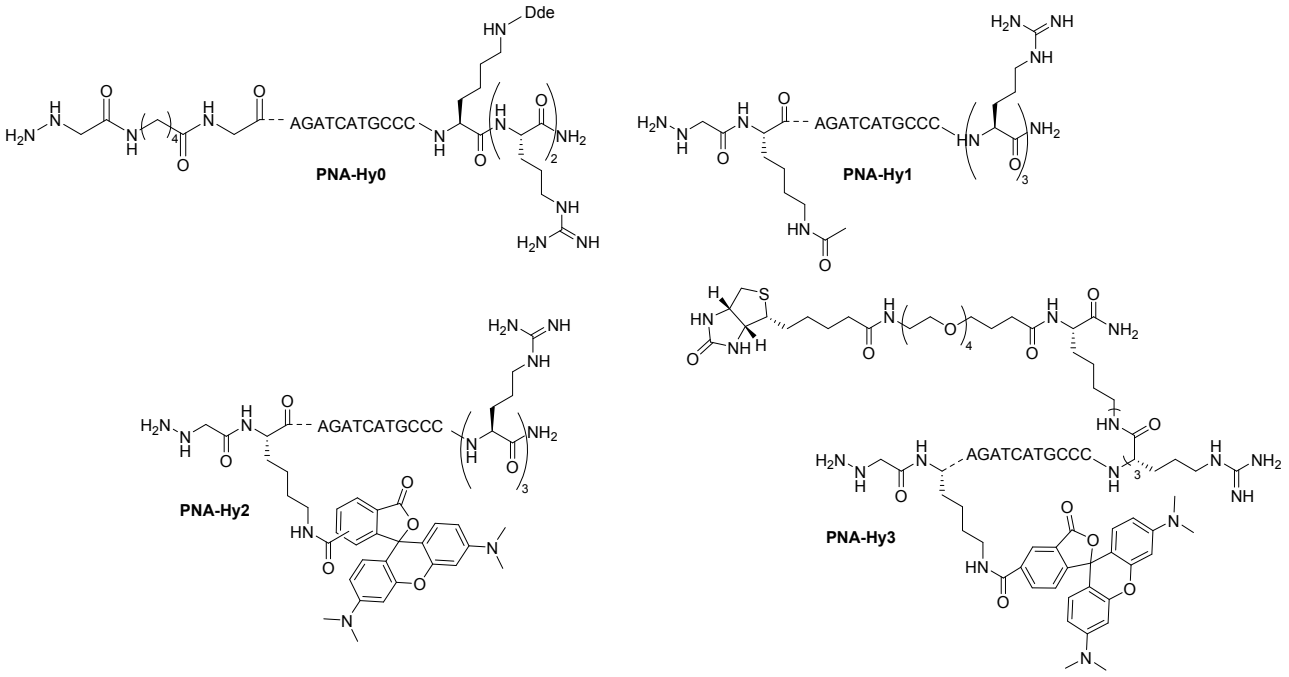

Figure S2: structure and sequence of the hydrazino-PNA probes used in this study.

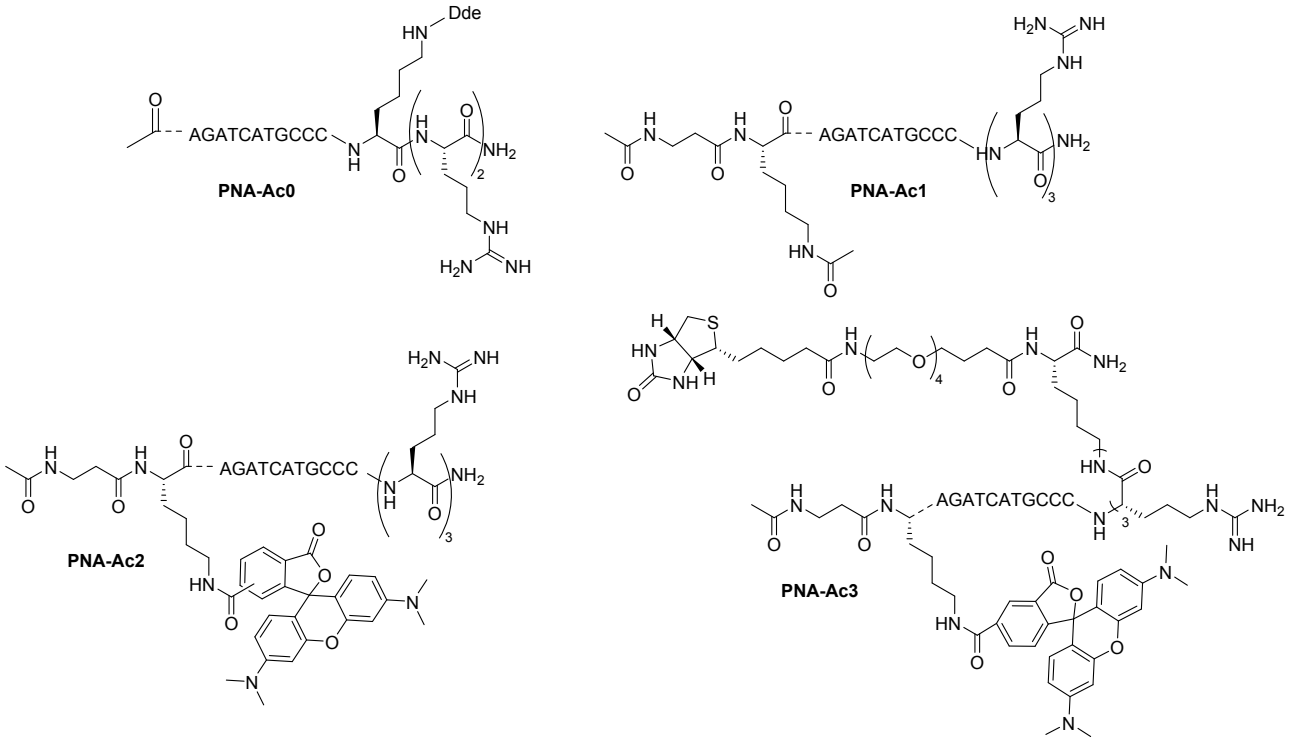

Figure S3: structure and sequence of the acetylated PNA probes used in this study.

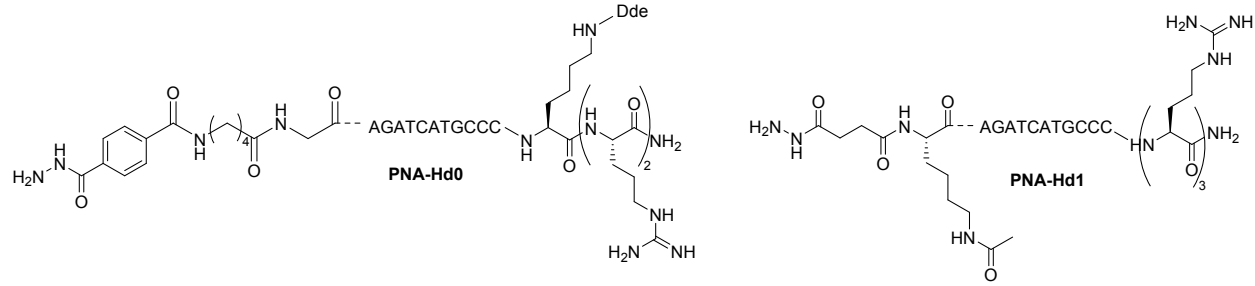

Figure S4: structure and sequence of the hydrazido-PNA probes used in this study.

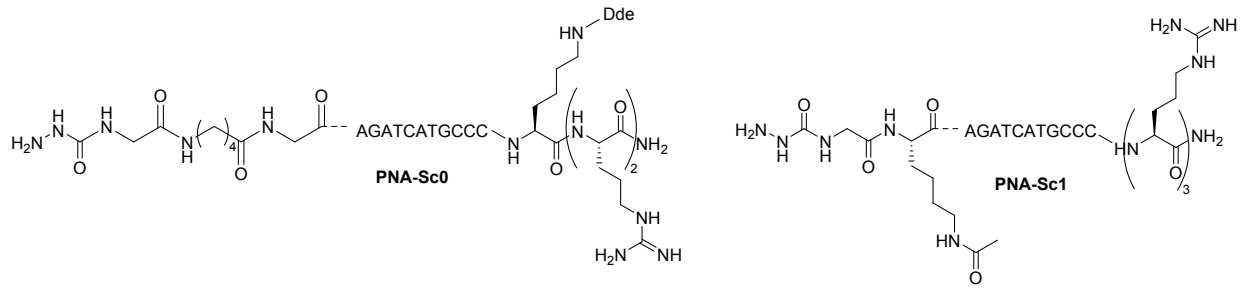

Figure S5: structure and sequence of the semicarbazido-PNA probes used in this study.

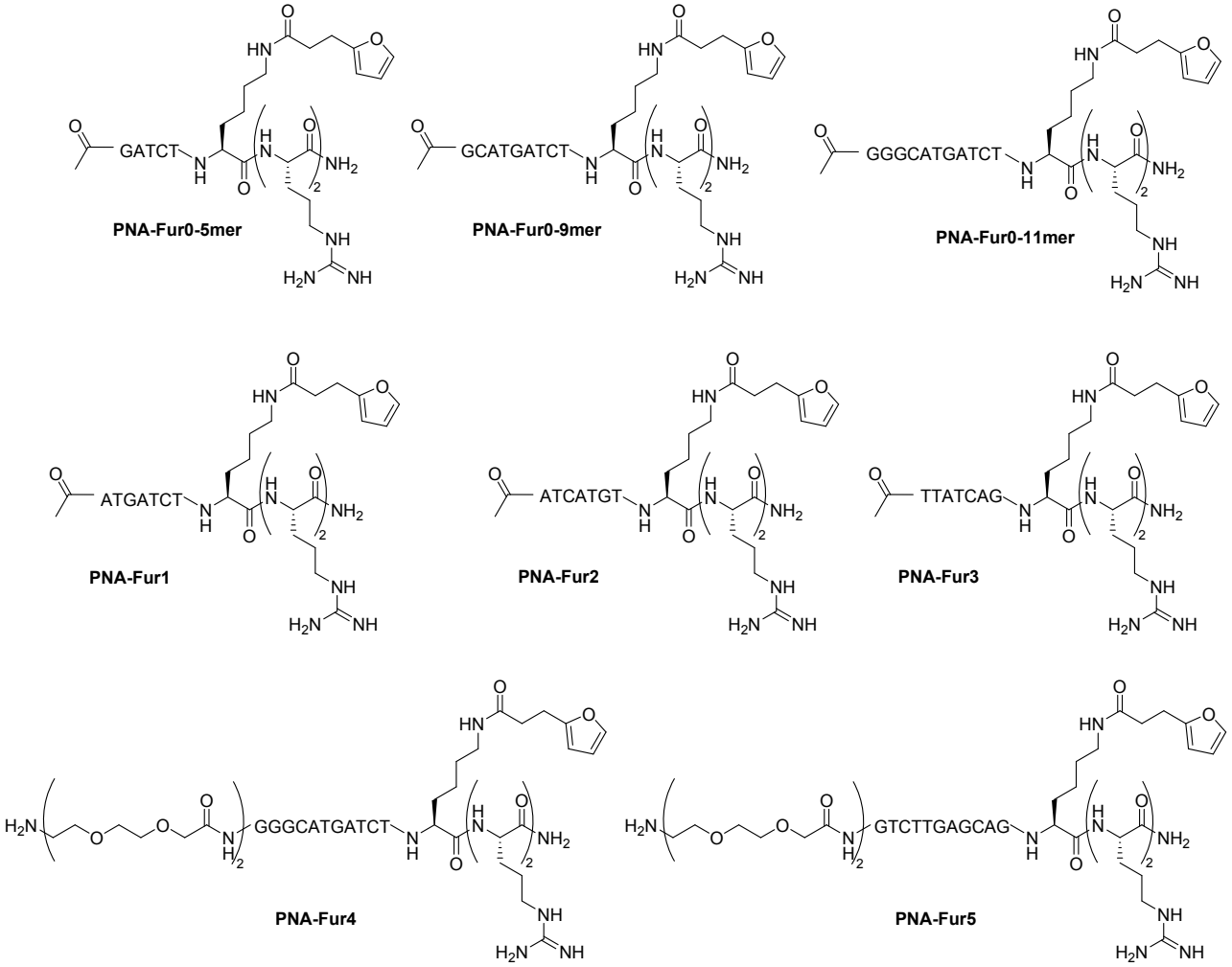

Figure S6: structure and sequence of the furan-PNA probes used in this study.

PNA-Fur0-5mer: 7.2%; t_r: 3.24 min; ε = 49200 $M^{-1}cm^{-1}$; ESI-MS: *m/z* calcd 1972.05 [M]: 986.7 $[M+2H]^{2+}$, 658.2 $[M+3H]^{3+}$, 494.0 $[M+4H]^{4+}$, 395.4 $[M+5H]^{5+}$. **PNA-Fur0-9mer:** 5.6%; t_r: 3.23 min; ε = 89800 $M^{-1}cm^{-1}$; ESI-MS: *m/z* calcd 3056.10 [M]: 1528.6 $[M+2H]^{2+}$, 1019.4 $[M+3H]^{3+}$, 764.8 $[M+4H]^{4+}$, 612.2 $[M+5H]^{5+}$, 510.3 $[M+6H]^{6+}$, 437.5 $[M+7H]^{7+}$. **PNA-Fur0-11mer:** 3.1%; t_r: 3.27 min; ε = 113200 $M^{-1}cm^{-1}$; ESI-MS: *m/z* calcd 3638.64 [M]: 1213.5 $[M+3H]^{3+}$, 910.3 $[M+4H]^{4+}$, 728.5 $[M+5H]^{5+}$, 607.3 $[M+6H]^{6+}$, 520.7 $[M+7H]^{7+}$. **PNA-Fur1:** 7.6%; t_r: 3.25 min; ε = 71500 $M^{-1}cm^{-1}$; ESI-MS: *m/z* calcd 2513.58 [M]: 1257.3 $[M+2H]^{2+}$, 838.5 $[M+3H]^{3+}$, 629.2 $[M+4H]^{4+}$, 503.7 $[M+5H]^{5+}$, 419.9 $[M+6H]^{6+}$. **PNA-Fur2:** 9.8%; t_r: 3.18 min; ε = 71500 $M^{-1}cm^{-1}$; ESI-MS**:** *m/z* calcd 2513.6 [M]: 1257.3 $[M+2H]^{2+}$, 838.7 $[M+3H]^{3+}$, 629.2 $[M+4H]^{4+}$, 503.7 $[M+5H]^{5+}$. **PNA-Fur3:** 17.18%; t_r: 3.18 min; ε = 71500 $M^{-1}cm^{-1}$; ESI-MS**:** *m/z* calcd 2513.6 [M]: 1257.3 $[M+2H]^{2+}$, 838.7 $[M+3H]^{3+}$, 629.4 $[M+4H]^{4+}$, 503.7 $[M+5H]^{5+}$, 419.9 $[M+6H]^{6+}$. **PNA-Fur4:** 6.36%, t_r 3.18 min; ε = 113200 $M^{-1}cm^{-1}$; ESI-MS**:** *m/z* calcd 3886.92 [M]: 1296.4 $[M+3H]^{3+}$, 972.6 $[M+4H]^{4+}$, 778.3 $[M+5H]^{5+}$, 648.7 $[M+6H]^{6+}$, 556.2 $[M+7H]^{7+}$, 486.9 $[M+8H]^{8+}$. **PNA-Fur5:** 12.97%, t_r 3.16 min; ε = 113200 $M^{-1}cm^{-1}$; ESI-MS**:** *m/z* calcd 3886.92 [M]: 1296.3 $[M+3H]^{3+}$, 972.6 $[M+4H]^{4+}$, 778.3 $[M+5H]^{5+}$, 648.7 $[M+6H]^{6+}$, 556.2 $[M+7H]^{7+}$, 486.9 $[M+8H]^{8+}$. **PNA-Am0:** 13.9%; t_r: 3.13 min; ε = 108100 $M^{-1}cm^{-1}$; ESI-MS: *m/z* calcd 3567.66 [M]: 1189.7 $[M+3H]^{3+}$, 892.7 $[M+4H]^{4+}$, 714.3 $[M+5H]^{5+}$, 595.5 $[M+6H]^{6+}$, 510.6 $[M+7H]^{7+}$, 446.9 $[M+8H]^{8+}$. **PNA-Am1:** 13.9%;

t_r: 2.90 min; ε = 108100 $M^{-1}cm^{-1}$; ESI-MS**:** *m/z* calcd 3672.8 [M]: 1224.9 $[M+3H]^{3+}$, 918.9 $[M+4H]^{4+}$, 735.3 $[M+5H]^{5+}$, 612.9 $[M+6H]^{6+}$, 525.6 $[M+7H]^{7+}$, 460.0 $[M+8H]^{8+}$. **PNA-Am2(6-TAMRA):** 6.1%; t_r: 3.11 min; ε = 140080 $M^{-1}cm^{-1}$; ESI-MS**:** *m/z* calcd 4042.85 [M]: 1011.5 $[M+4H]^{4+}$, 809.4 $[M+5H]^{5+}$, 674.7 $[M+6H]^{6+}$, 578.4 $[M+7H]^{7+}$, 506.2 $[M+8H]^{8+}$, 450.1 $[M+9H]^{9+}$. **PNA-Am2(5-TAMRA):** 6.0%; t_r: 3.21 min; ε = 140080 $M^{-1}cm^{-1}$; ESI-MS**:** *m/z* calcd 4042.85 [M]: 1011.5 $[M+4H]^{4+}$, 809.4 $[M+5H]^{5+}$, 674.7 $[M+6H]^{6+}$, 578.4 $[M+7H]^{7+}$, 506.2 $[M+8H]^{8+}$, 450.1 $[M+9H]^{9+}$. **PNA-Am3:** 10.2%; t_r: 3.32 min; ε = 140080 $M^{-1}cm^{-1}$; ESI-MS**:** *m/z* calcd 4644.92 [M]: 1548.9 $[M+3H]^{3+}$, 1161.9 $[M+4H]^{4+}$, 929.7 $[M+5H]^{5+}$, 775.0 $[M+6H]^{6+}$, 664.5 $[M+7H]^{7+}$, 581.5 $[M+8H]^{8+}$, 517.0 $[M+9H]^{9+}$, 465.5 $[M+10H]^{10+}$. **PNA-Ac0:** 12.7%; t_r: 3.24 min; ε = 140080 $M^{-1}cm^{-1}$; ESI-MS**:** *m/z* calcd 3609.70 [M]: 1203.7 $[M+3H]^{3+}$, 903.2 $[M+4H]^{4+}$, 722.7 $[M+5H]^{5+}$, 602.4 $[M+6H]^{6+}$, 516.5 $[M+7H]^{7+}$, 452.1 $[M+8H]^{8+}$. **PNA-Ac1:** 9.4%; t_r: 2.96 min; ε = 108100 $M^{-1}cm^{-1}$; ESI-MS**:** *m/z* calcd 3714.8 [M]: 1238.8 $[M+3H]^{3+}$, 929.4 $[M+4H]^{4+}$, 743.7 $[M+5H]^{5+}$, 620.0 $[M+6H]^{6+}$, 531.6 $[M+7H]^{7+}$, 465.3 $[M+8H]^{8+}$. **PNA-Ac2(6-TAMRA):** 1.1%; t_r: 3.10 min; ε = 140080 $M^{-1}cm^{-1}$; ESI-MS**:** *m/z* calcd 4084.89 [M]: 1022.0 $[M+4H]^{4+}$, 817.8 $[M+5H]^{5+}$, 681.6 $[M+6H]^{6+}$, 584.4 $[M+7H]^{7+}$, 511.5 $[M+8H]^{8+}$, 454.8 $[M+9H]^{9+}$. **PNA-Ac2(5-TAMRA):** 2.0%; t_r: 3.21 min; ε = 140080 $M^{-1}cm^{-1}$; ESI-MS**:** *m/z* calcd 4084.89 [M]: 1022.0 $[M+4H]^{4+}$, 817.8 $[M+5H]^{5+}$, 681.7 $[M+6H]^{6+}$, 584.5 $[M+7H]^{7+}$, 511.5 $[M+8H]^{8+}$, 454.8 $[M+9H]^{9+}$. **PNA-Ac3:** 7.7 %; t_r: 3.41 min; ε: 140080 $M^{-1}cm^{-1}$; ESI-MS: *m/z* calcd 4687.0 [M]: 1562.9 $[M+3H]^{3+}$, 1172.4 $[M+4H]^{4+}$, 938.1 $[M+5H]^{5+}$, 782.0 $[M+6H]^{6+}$, 670.5 $[M+7H]^{7+}$, 586.8 $[M+8H]^{8+}$, 521.7 $[M+9H]^{9+}$, 469.6 $[M+10H]^{10+}$. **PNA-Hy0:** 7.7%; t_r: 3.11 min; ε = 108100 $M^{-1}cm^{-1}$; ESI-MS**:** *m/z* calcd 3809.94 [M]: 1270.5 $[M+3H]^{3+}$, 953.1 $[M+4H]^{4+}$, 762.8 $[M+5H]^{5+}$, 635.8 $[M+6H]^{6+}$, 545.1 $[M+7H]^{7+}$, 477.1 $[M+8H]^{8+}$, 424.2 $[M+9H]^{9+}$. **PNA-Hy1:** 8.1%; t_r: 2.89 min; ε = 108100 $M^{-1}cm^{-1}$; ESI-MS**:** *m/z* calcd 3673.8 [M]: 1225.2 $[M+3H]^{3+}$, 919.0 $[M+4H]^{4+}$, 735.5 $[M+5H]^{5+}$, 613.2 $[M+6H]^{6+}$, 525.8 $[M+7H]^{7+}$, 460.0 $[M+8H]^{8+}$. **PNA-Hy2(6-TAMRA):** 1.5%; t_r: 3.11 min; ε = 140080 $M^{-1}cm^{-1}$; ESI-MS**:** *m/z* calcd 4043.80 [M]: 1011.6 $[M+4H]^{4+}$, 809.5 $[M+5H]^{5+}$, 674.8 $[M+6H]^{6+}$, 578.5 $[M+7H]^{7+}$, 506.4 $[M+8H]^{8+}$, 450.3 $[M+9H]^{9+}$. **PNA-Hy2(5-TAMRA):** 2.9%; t_r: 3.21 min; ε = 140080 $M^{-1}cm^{-1}$; ESI-MS**:** *m/z* calcd 4043.80 [M]: 1011.6 $[M+4H]^{4+}$, 809.5 $[M+5H]^{5+}$, 674.8 $[M+6H]^{6+}$, 578.5 $[M+7H]^{7+}$, 506.4 $[M+8H]^{8+}$, 450.3 $[M+9H]^{9+}$. **PNA-Hy3:** 8.8%; t_r: 3.32 min; ε = 140080 $M^{-1}cm^{-1}$; ESI-MS**:** *m/z* calcd 4645.92 [M]: 1549.2 $[M+3H]^{3+}$, 1162.1 $[M+4H]^{4+}$, 930.0 $[M+5H]^{5+}$, 775.2 $[M+6H]^{6+}$, 664.7 $[M+7H]^{7+}$, 581.7 $[M+8H]^{8+}$, 517.2 $[M+9H]^{9+}$, 465.6 $[M+10H]^{10+}$. **PNA-Hd0**: 6.3%; tr: 3.21 min; ε = 108100 $M^{-1}cm^{-1}$; ESI-MS: m/z calcd 3900.02 [M]: 1300.5 $[M+3H]^{3+}$, 975.7 $[M+4H]^{4+}$, 780.8 $[M+5H]^{5+}$, 650.8 $[M+6H]^{6+}$, 558.0 $[M+7H]^{7+}$, 488.4 $[M+8H]^{8+}$. **PNA-Hd1**: 4.5%; tr: 2.93 min; ε = 108100 $M^{-1}cm^{-1}$; ESI-MS: m/z calcd 3715.9 [M]: 1239.2 $[M+3H]^{3+}$, 929.7 $[M+4H]^{4+}$, 743.8 $[M+5H]^{5+}$, 620.1 $[M+6H]^{6+}$, 531.7 $[M+7H]^{7+}$, 465.3 $[M+8H]^{8+}$. **PNA-Sc0**: 5.6%; tr: 3.14 min; ε = 108100 $M^{-1}cm^{-1}$; ESI-MS: *m/z* calcd 3852.96 [M]: 1284.9 $[M+3H]^{3+}$, 964.0 $[M+4H]^{4+}$, 771.5 $[M+5H]^{5+}$, 643.0 $[M+6H]^{6+}$, 551.2 $[M+7H]^{7+}$, 482.5 $[M+8H]^{8+}$, 429.0 $[M+9H]^{9+}$. **PNA-Sc1:** 3.3%; t_r: 2.93 min; ε = 108100 $M^{-1}cm^{-1}$; ESI-MS**:** *m/z* calcd 3716.8 [M]: 1239.4 $[M+3H]^{3+}$, 930.2 $[M+4H]^{4+}$, 744.2 $[M+5H]^{5+}$, 620.2 $[M+6H]^{6+}$, 531.9 $[M+7H]^{7+}$, 465.5 $[M+8H]^{8+}$.

4. Extended discussion on preliminary optimization

As described in the main text the neutral polyamidic backbone of PNA renders the resulting PNA:PNA duplexes more stable than classical dsDNA duplexes. Different lengths of PNA probes were synthesized and UV melting experiments of the different PNA:PNA duplexes were performed at different urea concentrations in order to evaluate the complex stability under different conditions. From the melting temperatures of dsPNAs reported in Figure S7 and Table S2, the expected destabilization effect induced by the presence of chaotropic agent is evident as well as the very high stability of short dsPNAs. Correct Tm and ΔG° values for the 11mer dsPNA can be extrapolated by linear regression of the available data. PAGE conditions where then optimized to ensure that the observed spots represents a covalently connected PNA-PNA rather than a stable dsPNA, and in order to obtain satisfactory band resolution.
Finally, in PNA-PNA ligation experiments the behavior of the different nucleophiles under different pH conditions was analyzed as the large influence of the pH on the reaction was previously described by us when this reaction was exploited for peptide ligation.

Solving the analytical problem: development of USDS-PAGE conditions

For the fast and reliable qualitative evaluation of ligation product formation, the classical HPLC-based approaches failed to provide the desired resolution of the different species involved in the reaction and did not allow to discriminate between the nature of the chromatographic peaks. Polyacrylamide gel electrophoresis (PAGE) was then selected for the identification of the ligation product which can be easily achieved thanks to its reduced electrophoretic mobility.
In order to fully characterize all the steps involved in the realization of the light triggered templated ligation, we tested the series of PNA probes previously employed for the evaluation of the complex stability and evaluated the possibility to follow the formation of a crosslinked product in an efficient way by PAGE. In contrast to DNA and RNA analysis, this technique is rarely employed for PNA characterization in view of the general absence of charges in the PNA probes. PAGE analysis has been employed for PNA characterization or purification, but is generally described to lack in sensitivity (LOD in the order of 0.2 μmol or 3-10 μg) and only performed with single stranded PNA probes.[4,5]
Classical SDS-PAGE analysis of the aforementioned PNA probes shows no complex melting when a 9mer dsPNA is used, and do not allow to discriminate between a covalently connected PNA-PNA and a non-covalent PNA:PNA hybridization complex, as they both show identical electrophoretic migration behavior. Partial melting was obtained with a 7mer dsPNA. The addition of 7 M urea during gel polymerization (urea and SDS PAGE, USDS-PAGE) allowed complete complex melting for the 7mer while only partial melting for the 9mer was observed, as shown in Figure S8. The band shape improvement upon urea addition, in combination with the application of a silver staining protocol for band visualization, ensured a detection limit of about 7.3 ng (see Figure S11). Using these optimized conditions, we are able to distinguish between ligated complex and standard duplexes by USDS-PAGE-analysis on 7mer dsPNA. For this reason we decided to use a 7mer PNA for the ligation optimization.

Preliminary ligation experiments

In the subsequent exploratory PNA-PNA ligation tests different experimental parameters were evaluated and optimized in order to obtain reproducible singlet oxygen production (i.e. air bubbling, light geometry and intensity, reaction volume). Ligation optimization started using all components at 5 μM and varying the concentration of singlet oxygen in the solution by means of two different PS with drastically different singlet oxygen quantum yield,[8] namely Rose Bengal (RB) and Rhodamine B (RhoB). In the light setup employed, we here evaluated the ability of RB to generate singlet oxygen to be 20 fold more efficient than RhoB (see Table S7), with quantum yields in line with those reported in literature.[9]
In a first ligation experiment between the 7mer **PNA-Fur1** and hydrazine containing **PNA-Hy0**, the formation of a covalent bond was demonstrated via USDS-PAGE (see Figure S12). The higher singlet oxygen production in presence of RB (as compared to RhoB) is clearly reflected in the faster activation of **PNA-Fur1** probe and formation of the crosslink product, but it is also associated with a fast disappearing of the bands associated with both starting material as well as product, clear indication of probe degradation under these conditions. In addition, the presence of the product band in absence of direct light irradiation indicates the possibility to trigger the reaction by ambient light. This effect seems to be more pronounced in acidic solution (in the absence of buffer, the pH of the PNA solutions resides around 3) than in neutral conditions (Figure S12), although we measured lower singlet oxygen production at low pH (Table S7).
Further characterization and optimization of the system was then performed using RhoB as PS for its ease to control reaction conditions.
It was earlier reported that hydrazide and semicarbazide nucleophiles are more efficient at lower pH as compared to hydrazine. We thus tested the behavior of the different nucleophiles (**PNA-Hy0**, **PNA-Sc0** and **PNA-Hd0**) at three different pHs (4.7, 6.0, and 7.4) in presence of **PNA-Fur1**, observing only a minor influence of the experimental conditions on desired product formation, as shown in Figure S13. This contrasts with our previous findings in peptide labelling. However, in the current context, the observed lower influence of pH on the reaction outcome can be attributed

to the enhanced kinetics induced by the increase in the effective concentration of the reactive moieties. Same behavior was obtained using shorter **PNA-Fur0-5mer** and longer **PNA-Fur0-9mer** and confirmed by HPLC-UV (Figure S14).
To confirm the formation of the ligation product via the terminal nucleophile and exclude the possible formation of an interstrand crosslink with the terminal adenine of the nucleophilic probe, the behavior of **PNA-Fur0-5mer÷3** in presence of a PNA bearing a capped or free amino function at the N-term (**PNA-Ac0** and **PNA-Am0**, respectively) was also tested. As expected, in the former case no ligation product was obtained (data not shown) due to the absence of available nucleophilic functional groups. In the latter case, USDS-PAGE analysis shows product formation, as reported for the α-nucleophiles (Figure S15). The induced proximity clearly compensates for the lower nucleophilicity and allows covalent bond formation with the oxidized furan probe. Similar behavior was also recently shown in a different context where spatial proximity between the two reactive units was ensured.[10]

5. PNA:PNA stability evaluation

Thermal denaturation profiles were measured by monitoring the absorbance at 260 nm from 15 °C to 90 °C and from 90 °C to 15 °C with a heating/cooling rate of 1 °C/min and recording every 0.1 °C. Measurement conditions: strand concentration = 5 µM in pH 7.4 PBS buffer (100 mM NaCl, 10 mM phosphate) at different urea concentrations. Melting temperatures were calculated from the first order derivative of a 10th order polynomial fitting function.

Free energy variation calculation

Gibbs' free energy variation (ΔG°) for the PNA:PNA duplexes was calculated at 37°C, adopting the procedures reported in literature [11,12].

$$\Delta G° = \Delta H° + T\Delta S° \qquad (1)$$

where ΔH° is the enthalpy variation, ΔS° is the entropy variation of the transition, and T is the temperature expressed in Kelvin.
The thermodynamic parameters were calculated with the hypochromicity method, using van't Hoff plot:

$$\ln K_T = \left(\frac{-\Delta H°}{R}\right)\frac{1}{T} + \frac{\Delta S°}{R} \qquad (2)$$

where K_T is defined as the equilibrium constant at the temperature T (in K) and R is gas constant.
Considering the system as a two-state model, the equilibrium constant can be calculated from:

$$K_T = \frac{2\alpha_{(T)}}{(1 - \alpha_{(T)})^2 c_s} \qquad (3)$$

Where $\alpha_{(T)}$ is defined as the molar fraction of single stranded PNA and c_s is the total concentration of strands in the system (10 µM in this case).
To calculate the value of $\alpha_{(T)}$ for each temperature, we used the formula:

$$\alpha_{(T)} = \frac{A_s - A_T}{A_s - A_d} \qquad (4)$$

where A_T is the measured absorbance of the experiment at a specific temperature T, A_s and A_d are, respectively, the absorbance of the fully unhybridized single strand and the fully hybridized duplex.
Only values of $0.85 > \alpha_{(T)} > 0.15$ were considered for the Van't Hoff plot for a better fitting (cit).
When all the parameters were extrapolated, the ΔH° and ΔS° values were calculated from the slope and the intercept on y axis of the Van't Hoff plot, respectively, as reported in *Eq. (2)*.

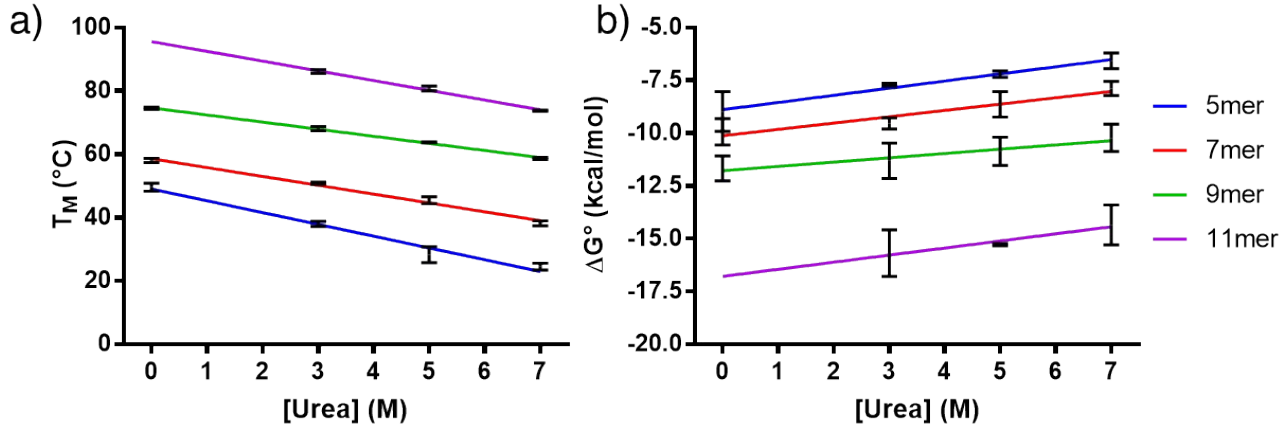

Figure S7: PNA:PNA stability studies measured at 5 µM strand concentration in PBS buffer pH 7.4 in presence of different urea concentrations. (a) Urea effect on melting temperature; (b) Urea effect on ΔG°(37°C).

Table S2. Melting temperature and thermodynamic parameters of dsPNA formation at different urea concentrations.

dsPNA length	Urea (M)	T_M (°C)	ΔH° (kcal/mol)	$\Delta G°_{(37°C)}$ (kcal/mol)
5 mer	0	49.6 ± 1.3	-3.1 ± 0.3	-9.0 ± 0.9
	3	38.0 ± 0.9	-3.3 ± 0.5	-7.7 ± 0.1
	5	28.3 ± 2.5	-3.9 ± 0.1	-7.2 ± 0.1
	7	24.5 ± 1.1	-5.6 ± 0.2	-6.6 ± 0.4
7 mer	0	54.0 ± 0.7	-3.5 ± 0.1	-10.0 ± 0.6
	3	50.9 ± 0.4	-4.6 ± 0.1	-9.5 ± 0.3
	5	45.5 ± 1.1	-5.1 ± 0.3	-8.6 ± 0.6
	7	38.2 ± 0.7	-5.2 ± 0.5	-7.9 ± 0.35
9 mer	0	74.5 ± 0.4	-3.4 ± 0.4	-11.7 ± 0.6
	3	68.1 ± 0.7	-4.8 ± 0.1	-11.3 ± 0.9
	5	63.8 ± 0.2	-5.6 ± 0.6	-10.9 ± 0.7
	7	58.7 ± 0.3	-5.3 ± 0.2	-10.2 ± 0.7
11 mer	0	95.6*	-	-16.8**
	3	86.1 ± 0.6	-6.1 ± 0.3	-15.9 ± 1.1
	5	80.8 ± 0.8	-6.5 ± 0.7	-15.3 ± 0.1
	7	73.8 ± 0.2	-7.1 ± 1.0	-14.3 ± 1.0

* Extrapolated data from graph reported in Figure S7a. ** Extrapolated value from the graph in Figure S7b.

6. Optimization of Urea-SDS-PAGE (USDS-PAGE) conditions

Optimized USDS-PAGE conditions: 15% polyacrylamide gels (15% T) with 5% crosslinker (5% C, 19:1 acrylamide/bisacrylamide) were prepared in 1x Tris-Acetate buffer (50mM Tris-Acetate, pH 7.6) containing 7 M urea and 0.1% SDS. The temperature of the gel was stabilized with a Julabo F12 at 25°C. The power supply used for gel electrophoresis was a consort EV202 and a voltage of 200 V for 0.75 mm thickness or 100 V for 1.0 mm thickness were used to run the gels (15 minutes pre-run). 2 µL of sample solution were mixed with 3 µL formamide and 5 µL loading buffer (100 mM Tris-Acetate pH 7.6, 7 M urea, 20 % formamide, 2 % SDS) from this mixture 5/8 µL were loaded on the gel. Gels were stained with Pierce Silver Stain (Thermo Fisher Scientific) and pictures were scanned with an HP Photosmart B110.

Table S3: lane loading used during USDS-PAGE optimization experiments.

Lane	Loaded sample	Lane description	Amount	Amount
2	Color	\	\	\
3	PNA-Am0	Target strand	8 pmol	28.5 ng
4	PNA-Fur0-5mer	5mer complementary strand	8 pmol	15.2 ng
5	PNA-Fur0-5mer + PNA-Am0	5mer dsPNA	4 pmol	21.8 ng
6	PNA-Fur1	7mer complementary strand	8 pmol	20.1 ng
7	PNA-Fur1 + PNA-Am0	7mer dsPNA	4 pmol	24.3 ng
8	PNA-Fur0-9mer	9mer complementary strand	8 pmol	24.5 ng
9	PNA-Fur0-9mer + PNA-Am0	9mer dsPNA	4 pmol	26.5 ng
10	PNA-Fur0-11mer	11mer complementary strand	8 pmol	29.1 ng
11	PNA-Fur0-11mer + PNA-Am0	11mer dsPNA	4 pmol	28.8 ng
12	Color	\	\	\

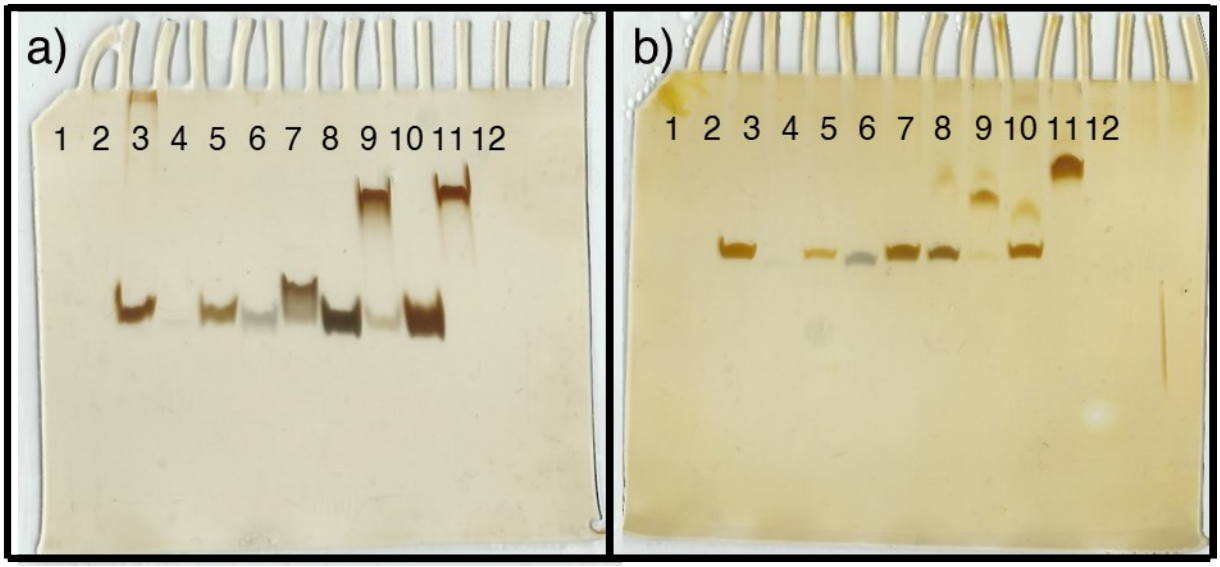

Figure S8: influence of urea concentration: (a) 0 M and (b) 7 M. Gel composition: 15% T, 5% C.

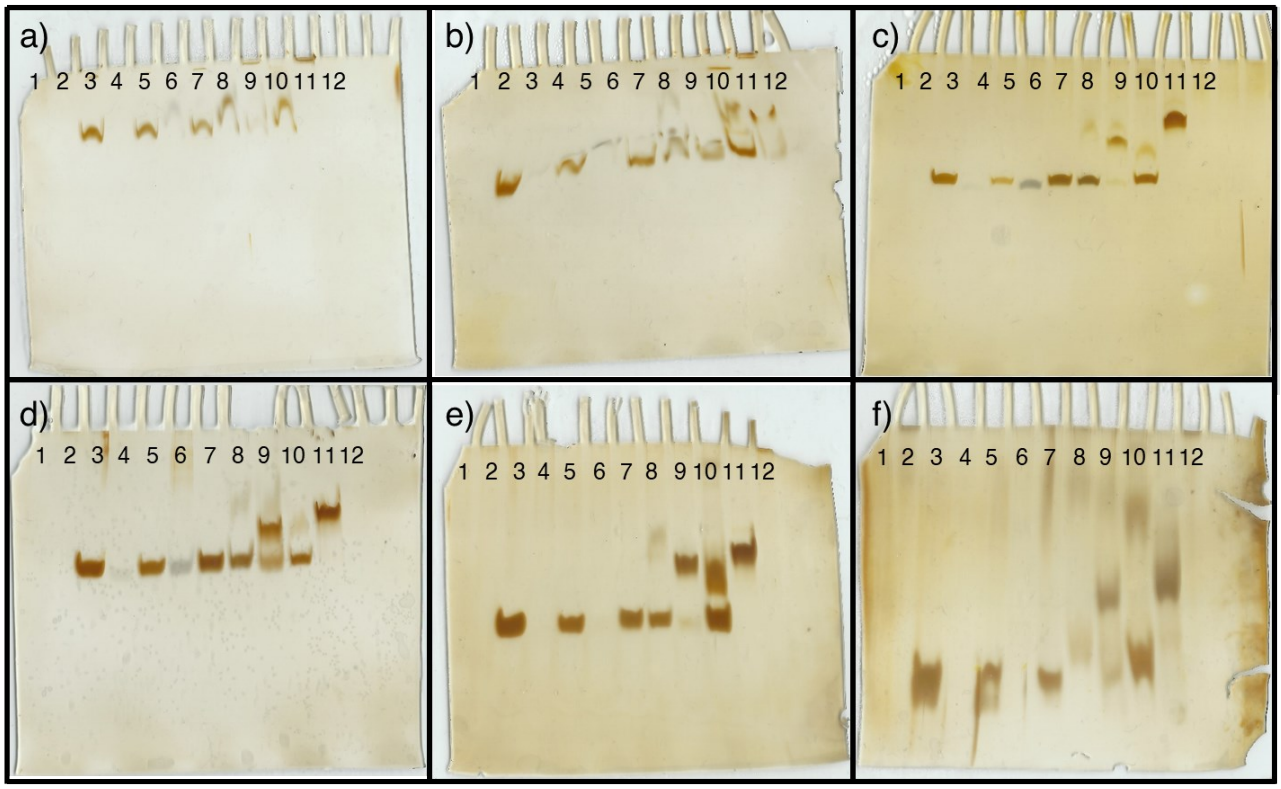

Figure S9: influence of acrylamide and bis-acrylamide concentration. (a) 20% T, 5% C; (b) 20% T, 2.5% C; (c) 15% T, 5% C; (d) 15% T, 2.5% C; (e) 10% T, 5% C; (f) 7% T, 5% C. Voltage applied: 250 V for (a), 200 V for the others; gels composition: 7 M urea and 0.1% SDS.

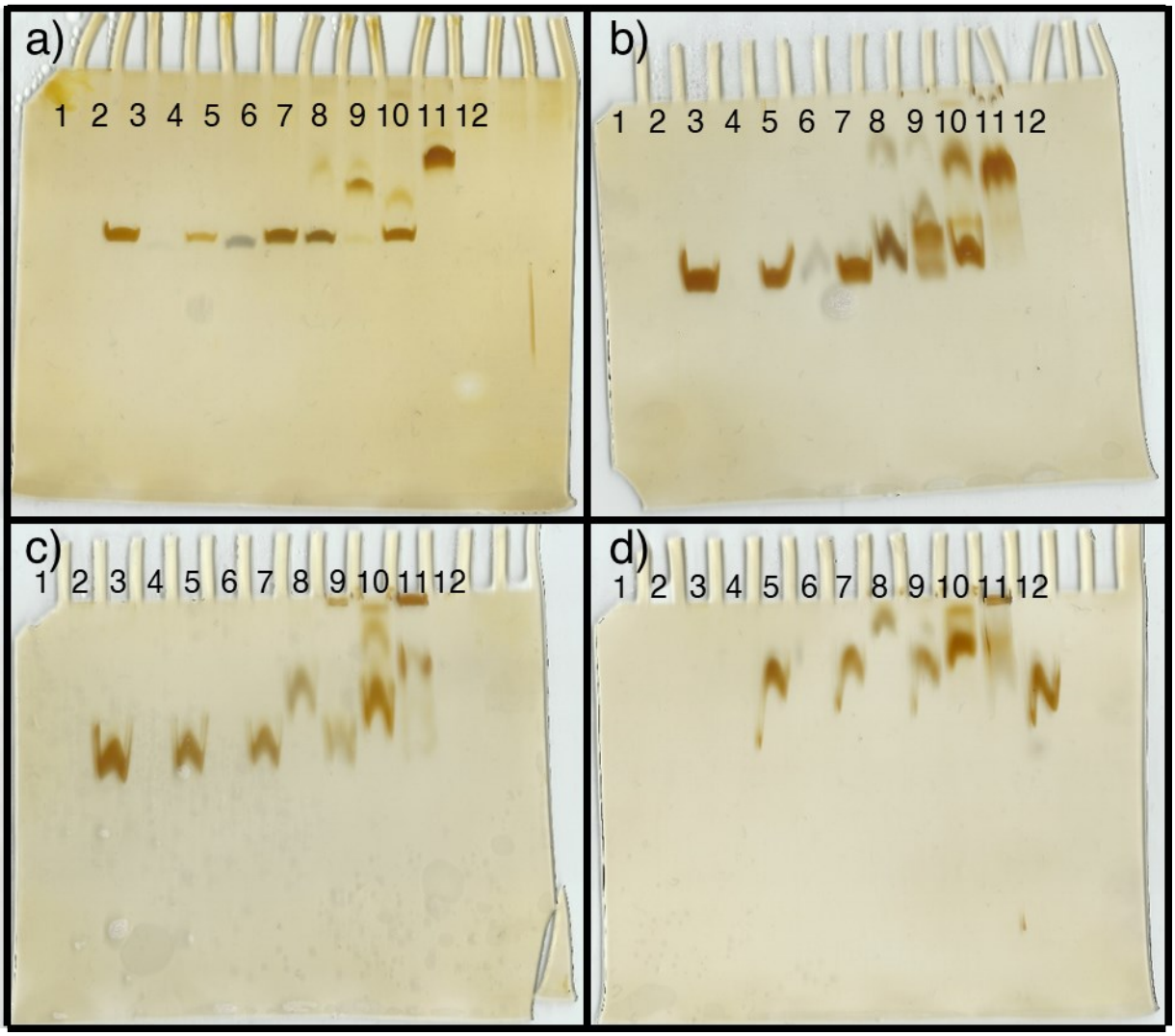

Figure S10: influence of temperature. (a) 25 °C; (b) run start at 25°C, then temperature increased to 40°C; (c) 40°C; (d) 55°C. Gel composition: 15% T, 5% C, 7 M urea, 0.1% SDS.

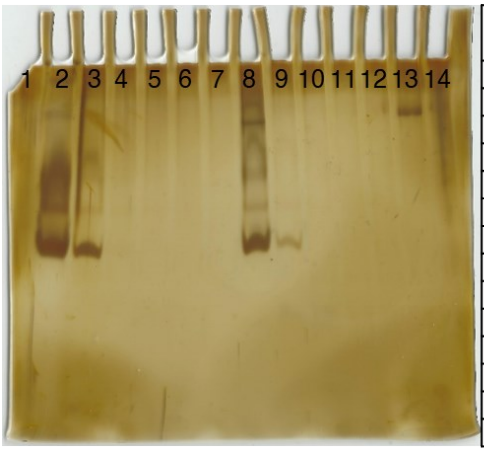

Lane	Sample concentration	Sample preparation	Moles	Amount
1	Color			
2	5 μM	PNA sample + Loading buffer 1:1	12.5 pmol	45.5 ng
3	2 μM		5 pmol	18.2 ng
4	1 μM		2.5 pmol	9.1 ng
5	500 nM		1.25 pmol	4.6 ng
6	200 nM		500 fmol	1.8 ng
7	100 nM		250 fmol	900 pg
8	5 μM	PNA sample + formamide + Loading buffer 2:3:5	5 pmol	18.2 ng
9	2 μM		2 pmol	7.3 ng
10	1 μM		1 pmol	3.6 ng
11	500 nM		500 fmol	1.82 ng
12	200 nM		200 fmol	728 pg
13	100 nM		100 fmol	364 ng
14	Color			

Figure S11: limit of detetion of USDS-PAGE. Gel composition: 15% T, 5% C, 7 M urea, 0.1% SDS; PNA sample: **PNA-Fur0-11mer**.

7. Preliminary screening of light triggered ligation

In a typical experiment a solution containing the PNA probes at 5.26 µM concentration in PBS (for pH 6.0 and 7.4) or acetate buffer (for pH 4.7) was cooled to 10°C and saturated with air for 20 minutes through bubbling at 10 mL/min. To this solution, the PS is then added and the light irradiation started (final concentration of probes and PS: 5 µM). 50 µL aliquots of reaction mixture were sampled at different irradiation times and left to react overnight at 25°C before the eventual quenching with methylhydrazine (5 µL, 5 mM in mQ). Results were then analyzed via PAGE experiments.

Table S4: lane loading of PAGE experiments shown in Figure S12.

Lane 1	Color	Lane 8	t = 30 min, quenched experiment
Lane 2	PNA references	Lane 9	t = 45 min
Lane 3	t = 0 min	Lane 10	t = 45 min, quenched experiment
Lane 4	t = 0 min, quenched experiment	Lane 11	t = 60 min
Lane 5	t = 15 min	Lane 12	t = 60 min, quenched experiment
Lane 6	t = 15 min, quenched experiment	Lane 13	Color
Lane 7	t = 30 min	Lane 14	\

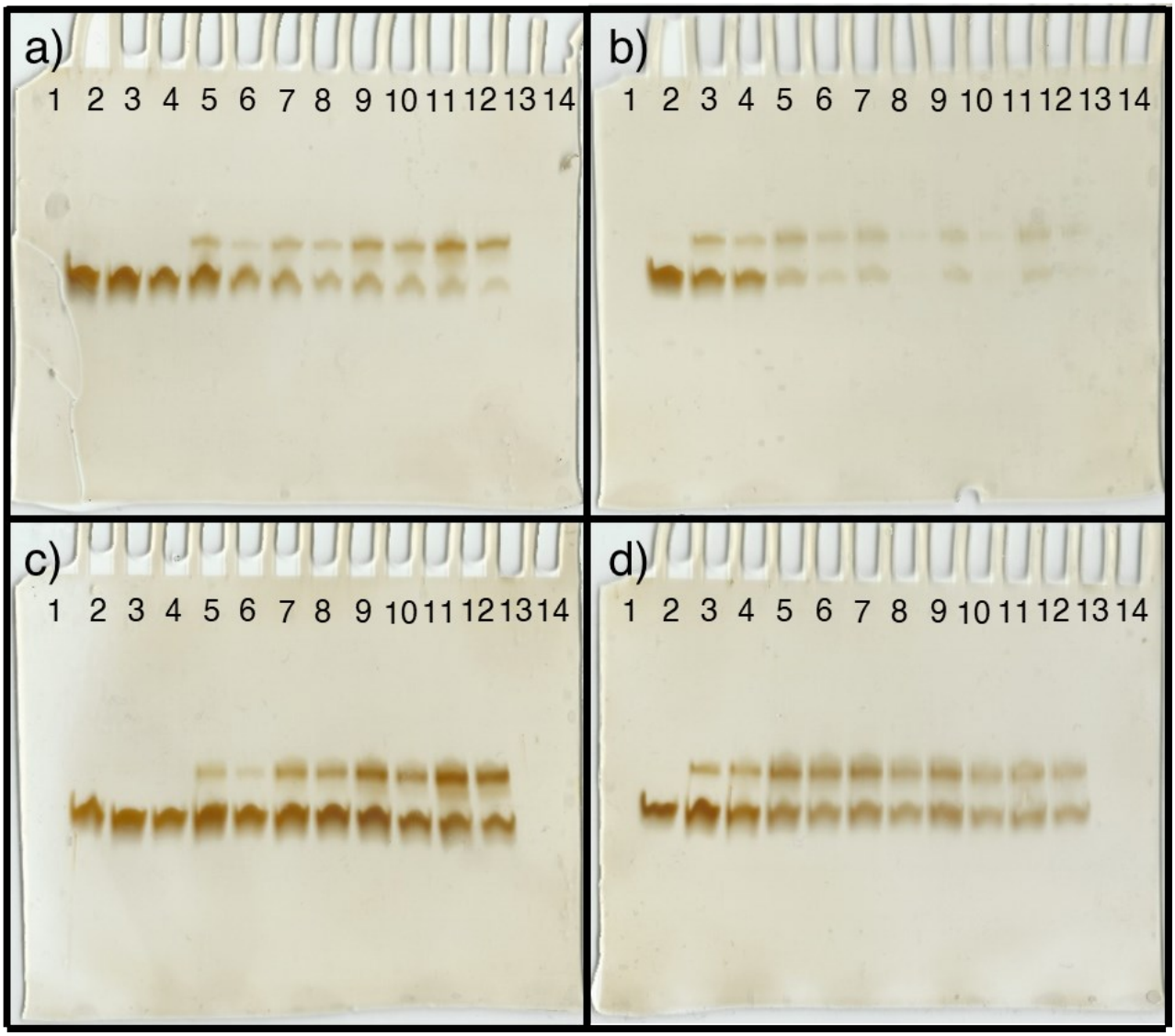

Figure S12: influence of PS in the ligation experiments between **PNA-Hy0** and **PNA-Fur1** in absence of buffer (a/b) or in PBS pH 7.4 (c/d). (a/c): rhodamine B; (b/d): rose bengal.

Table S5: lane loading of PAGE experiments shown in Figure S13.

Lane 1	color	Lane 8	pH 6.0, t = 30 min
Lane 2	pH 4.7, t = 0 min	Lane 9	pH 6.0, t = 60 min
Lane 3	pH 4.7, t = 15 min	Lane 10	pH 7.4, t = 0 min
Lane 4	pH 4.7, t = 30 min	Lane 11	pH 7.4, t = 15 min
Lane 5	pH 4.7, t = 60 min	Lane 12	pH 7.4, t = 30 min
Lane 6	pH 6.0, t = 0 min	Lane 13	pH 7.4, t = 60 min
Lane 7	pH 6.0, t = 15 min	Lane 14	PNA references

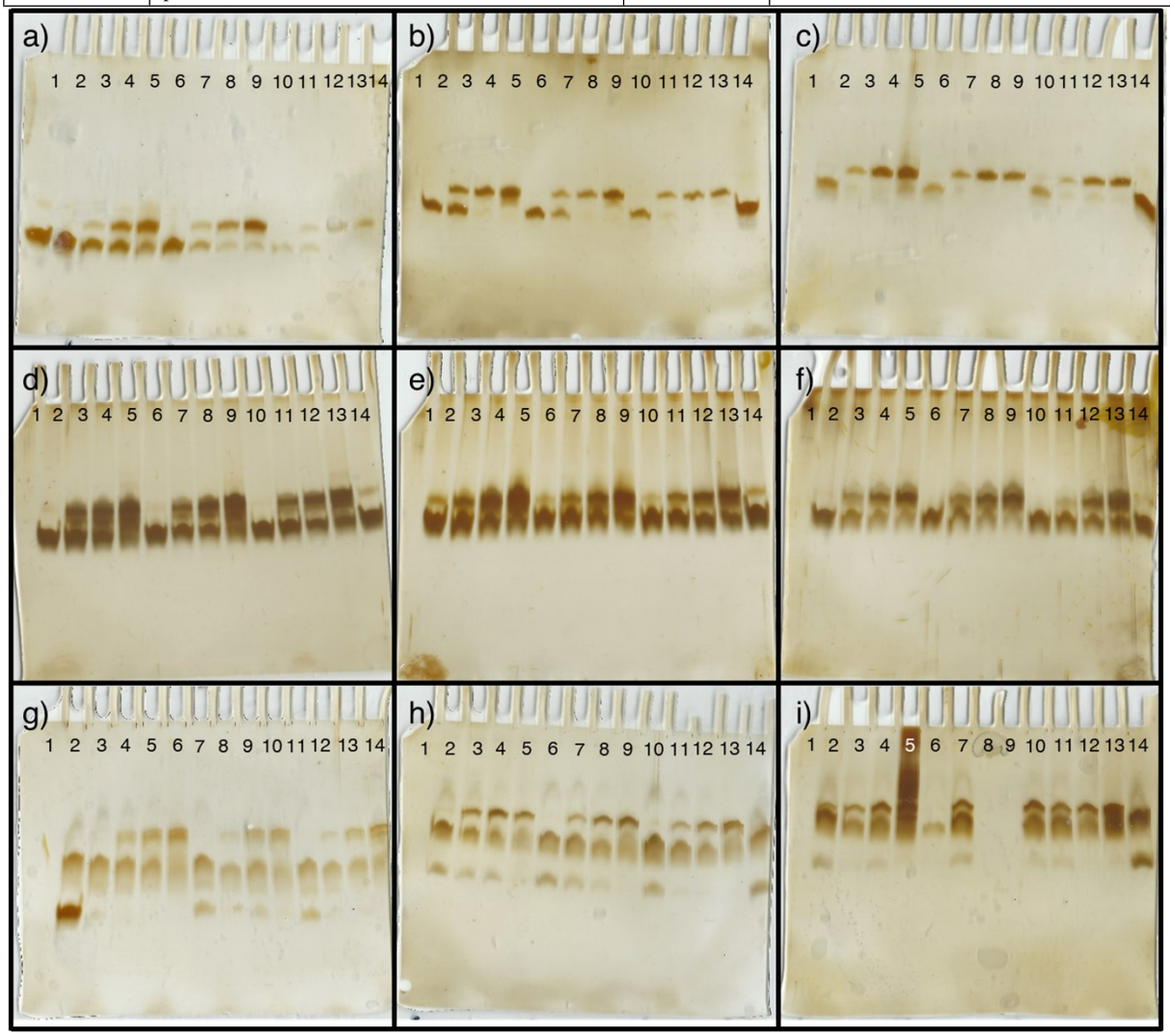

Figure S13: influence of pH in the ligation experiments between **PNA-Hy0** (a, d, g), **PNA-Hd0** (b, e, h), or **PNA-Sc0** (c, f, i) and **PNA-Fur0-5mer** (a, b, c) , **PNA-Fur1** (d, e, f), or **PNA-Fur0-9mer** (g, h, i).

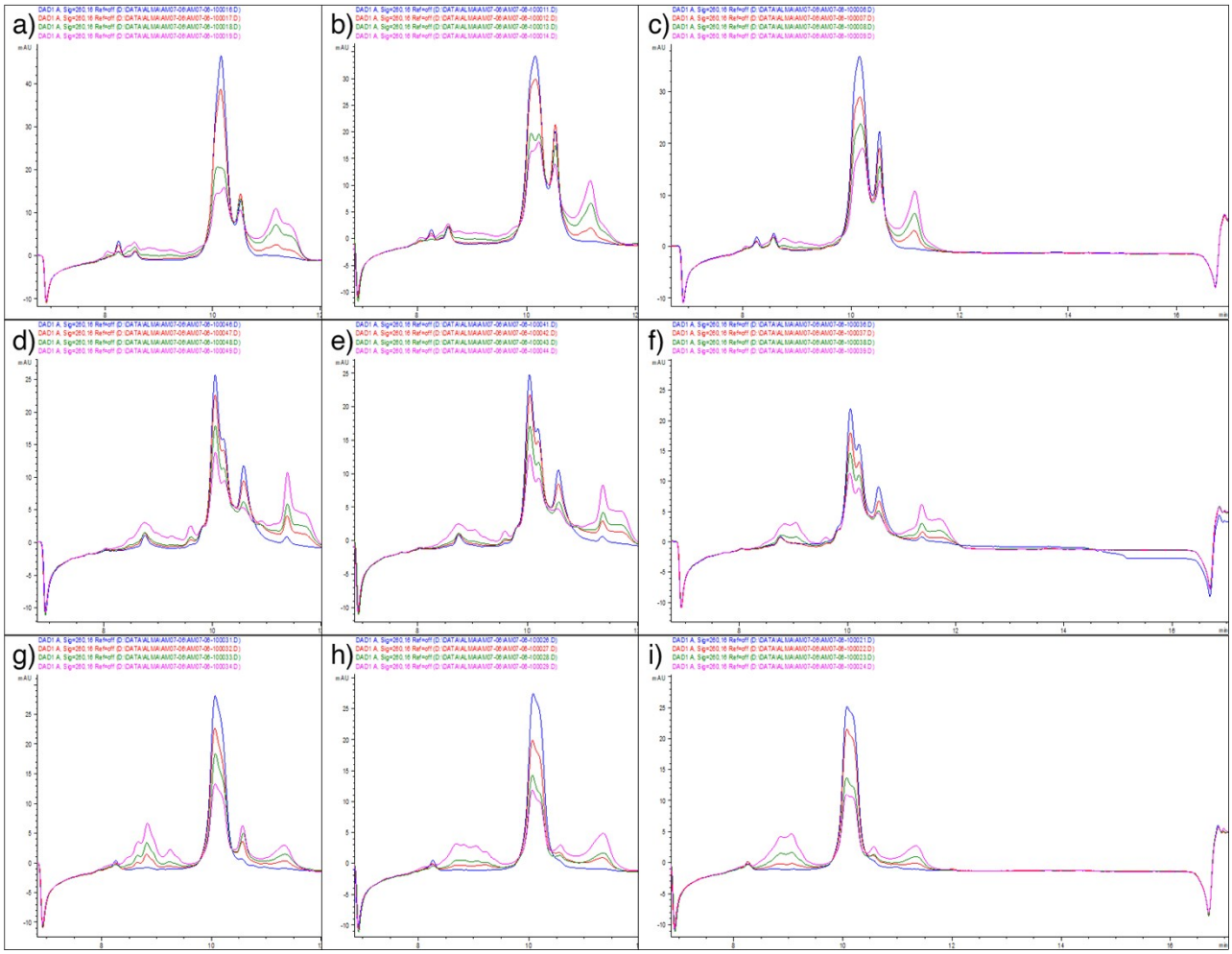

Figure S14: influence of pH in the ligation experiments of **PNA-Fur1**. **PNA-Hy0** at pH 4.7 (a), pH 6.0 (b), and pH 7.4 (c); **PNA-Hd0** at pH 4.7 (d), pH 6.0 (e), and pH 7.4 (f); **PNA-Sc0** at pH 4.7 (g), pH 6.0 (h), and pH 7.4 (i). HPLC3 traces after 0, 15, 30, and 60 minutes light irradiation are shown for every experiment. Starting probes R_t ~ 10 minutes, ligation product R_t ~ 11.5 minutes, degradation products R_t ~ 9 minutes (oxidized furan, degraded nucleophiles).

Table S6: lane loading of PAGE experiments shown in Figure S15.

Lane 1	color	Lane 8	PNA-Am0 + PNA-Fur1, 30min
Lane 2	PNA-Am0 + PNA-Fur0-5mer, 0min	Lane 9	PNA-Am0 + PNA-Fur1, 60min
Lane 3	PNA-Am0 + PNA-Fur0-5mer, 15min	Lane 10	PNA-Am0 + PNA-Fur0-9mer, 0min
Lane 4	PNA-Am0 + PNA-Fur0-5mer, 30min	Lane 11	PNA-Am0 + PNA-Fur0-9mer, 15min
Lane 5	PNA-Am0 + PNA-Fur0-5mer, 60min	Lane 12	PNA-Am0 + PNA-Fur0-9mer, 30min
Lane 6	PNA-Am0 + PNA-Fur1, 0min	Lane 13	PNA-Am0 + PNA-Fur0-9mer, 60min
Lane 7	PNA-Am0 + PNA-Fur1, 15min	Lane 14	PNA-Am0 + PNA-Fur1 references

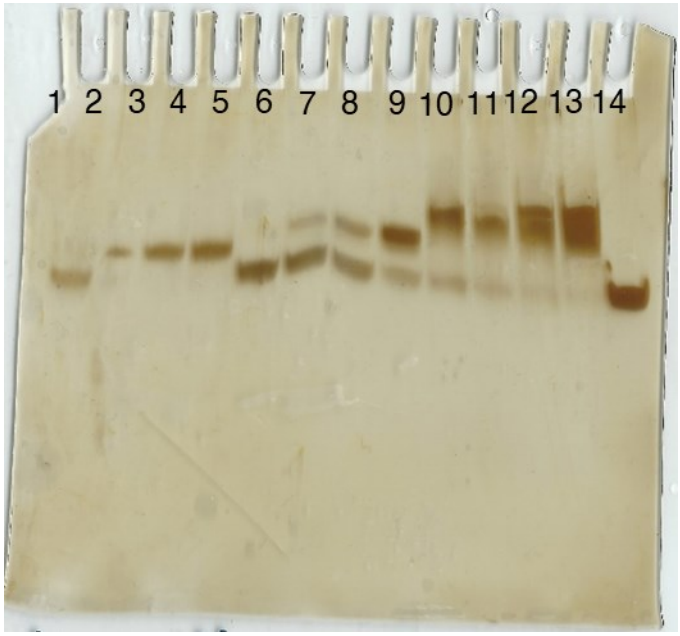

Figure S15: ligation experiments of **PNA-Am0** with **PNA-Fur0-5mer**, **PNA-Fur1**, and **PNA-Fur0-9mer** at pH 7.4.

8. PNA:PNA ligation

In a typical experiment a 100 µM stock solution of PS was freshly prepared from a 1 mM stock solution. In a 1.5 mL Eppendorf vial, 300 µL of an air saturated buffered solution (PBS, pH 7.4) containing probes at 5 µM concentration was prepared and allowed to equilibrate for 10 minutes at 25 °C, before the addition of the PS at 5 µM final concentration. The lamp (*vide supra*, general) is then placed on top of the Eppendorf vial for the entire duration of the experiment. 50 µL aliquots of reaction mixture were sampled at different irradiation times and left to react overnight at 25°C. Results were analyzed via USDS-PAGE and HPLC-UV experiments.

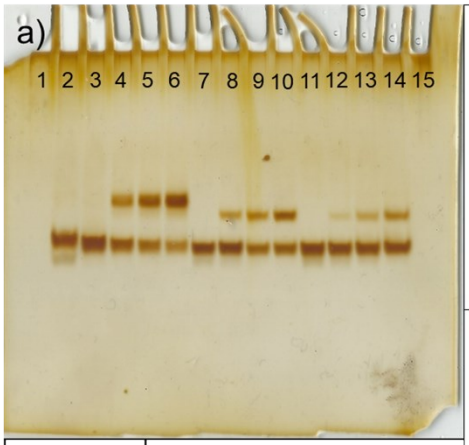

Lane 2	PNA reference
Lane 3	PNA-Am1 + PNA-Fur1, 0 min
Lane 4	PNA-Am1 + PNA-Fur1, 15 min
Lane 5	PNA-Am1 + PNA-Fur1, 30 min
Lane 6	PNA-Am1 + PNA-Fur1, 60 min
Lane 7	PNA-Am1 + PNA-Fur2, 0 min
Lane 8	PNA-Am1 + PNA-Fur2, 15 min
Lane 9	PNA-Am1 + PNA-Fur2, 30 min
Lane 10	PNA-Am1 + PNA-Fur2, 60 min
Lane 11	PNA-Am1 + PNA-Fur3, 0 min
Lane 12	PNA-Am1 + PNA-Fur3, 15 min
Lane 13	PNA-Am1 + PNA-Fur3, 30 min
Lane 14	PNA-Am1 + PNA-Fur3, 60 min
Lane 15	Color

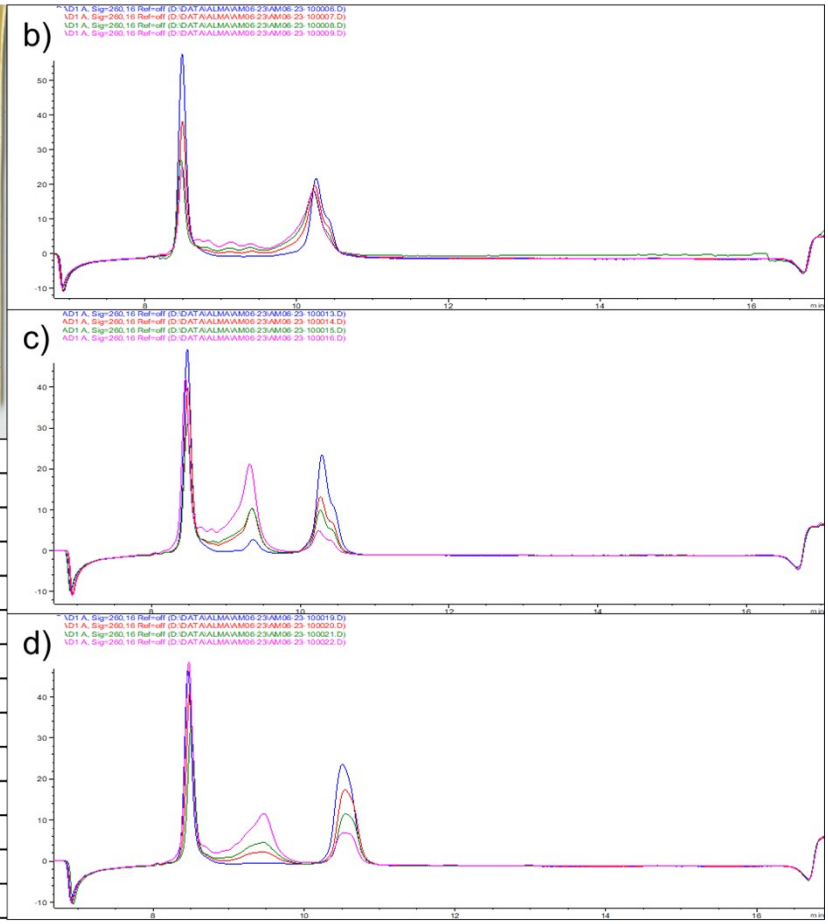

Figure S16: sequence selectivity of **PNA-Am1**. a) USDS-PAGE experiments and table with lane loading; b) HPLC3 traces of ligation experiment in presence of **PNA-Fur1**; c) HPLC3 traces of ligation experiment in presence of **PNA-Fur2**; d) HPLC3 traces of ligation experiment in presence of **PNA-Fur3**. HPLC3 traces after 0, 15, 30, and 60 minutes light irradiation are shown for every experiment.

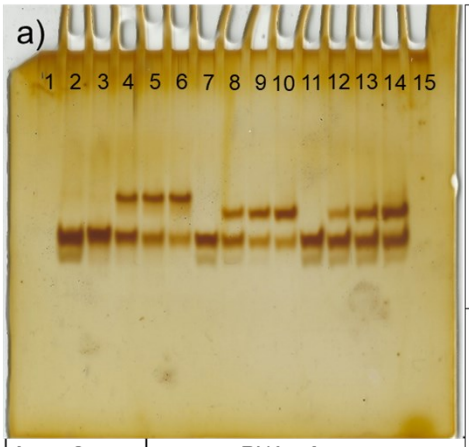

Lane 2	PNA refernce
Lane 3	PNA-Hy1 + PNA-Fur1, 0 min
Lane 4	PNA-Hy1 + PNA-Fur1, 15 min
Lane 5	PNA-Hy1 + PNA-Fur1, 30 min
Lane 6	PNA-Hy1 + PNA-Fur1, 60 min
Lane 7	PNA-Hy1 + PNA-Fur2, 0 min
Lane 8	PNA-Hy1 + PNA-Fur2, 15 min
Lane 9	PNA-Hy1 + PNA-Fur2, 30 min
Lane 10	PNA-Hy1 + PNA-Fur2, 60 min
Lane 11	PNA-Hy1 + PNA-Fur3, 0 min
Lane 12	PNA-Hy1 + PNA-Fur3, 15 min
Lane 13	PNA-Hy1 + PNA-Fur3, 30 min
Lane 14	PNA-Hy1 + PNA-Fur3, 60 min
Lane 15	Color

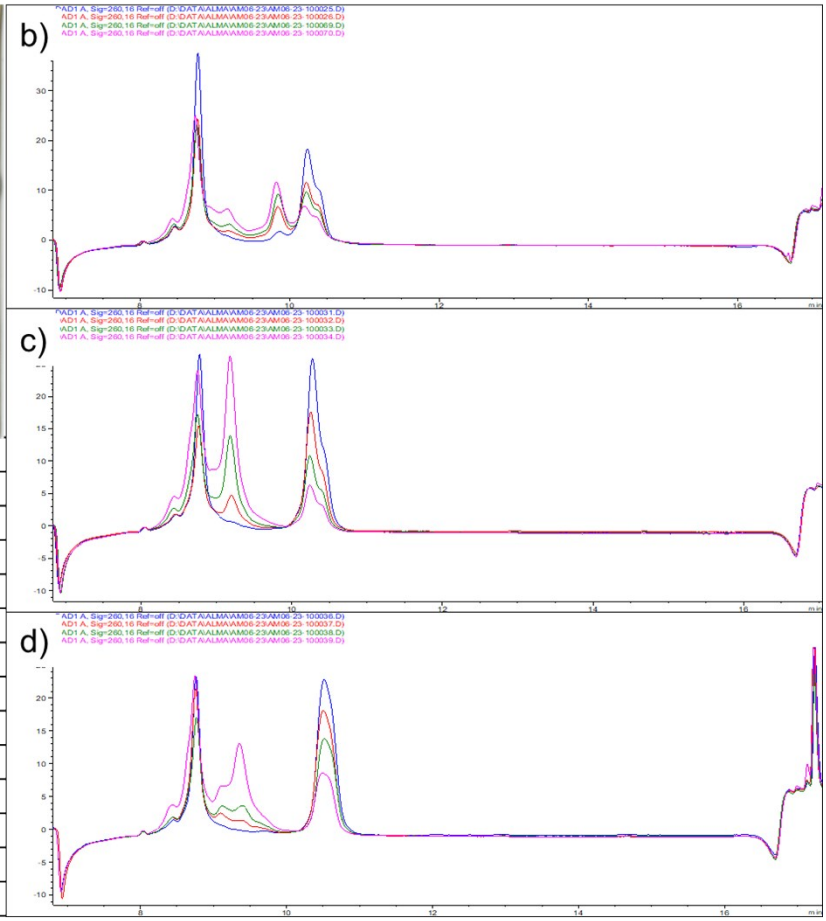

Figure S17: sequence selectivity of **PNA-Hy1**. a) USDS-PAGE experiments and table with lane loading; b) HPLC3 trace of ligation experiment in presence of **PNA-Fur1**; c) HPLC3 trace of ligation experiment in presence of **PNA-Fur2**; d) HPLC3 trace of ligation experiment in presence of **PNA-Fur3**. HPLC3 traces after 0, 15, 30, and 60 minutes light irradiation are shown for every experiment.

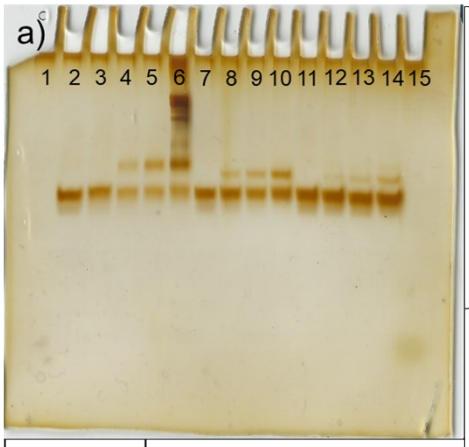

Lane 2	PNA reference
Lane 3	PNA-Hd1 + PNA-Fur1, 0 min
Lane 4	PNA-Hd1 + PNA-Fur1, 15 min
Lane 5	PNA-Hd1 + PNA-Fur1, 30 min
Lane 6	PNA-Hd1 + PNA-Fur1, 60 min
Lane 7	PNA-Hd1 + PNA-Fur2, 0 min
Lane 8	PNA-Hd1 + PNA-Fur2, 15 min
Lane 9	PNA-Hd1 + PNA-Fur2, 30 min
Lane 10	PNA-Hd1 + PNA-Fur2, 60 min
Lane 11	PNA-Hd1 + PNA-Fur3, 0 min
Lane 12	PNA-Hd1 + PNA-Fur3, 15 min
Lane 13	PNA-Hd1 + PNA-Fur3, 30 min
Lane 14	PNA-Hd1 + PNA-Fur3, 60 min
Lane 15	Color

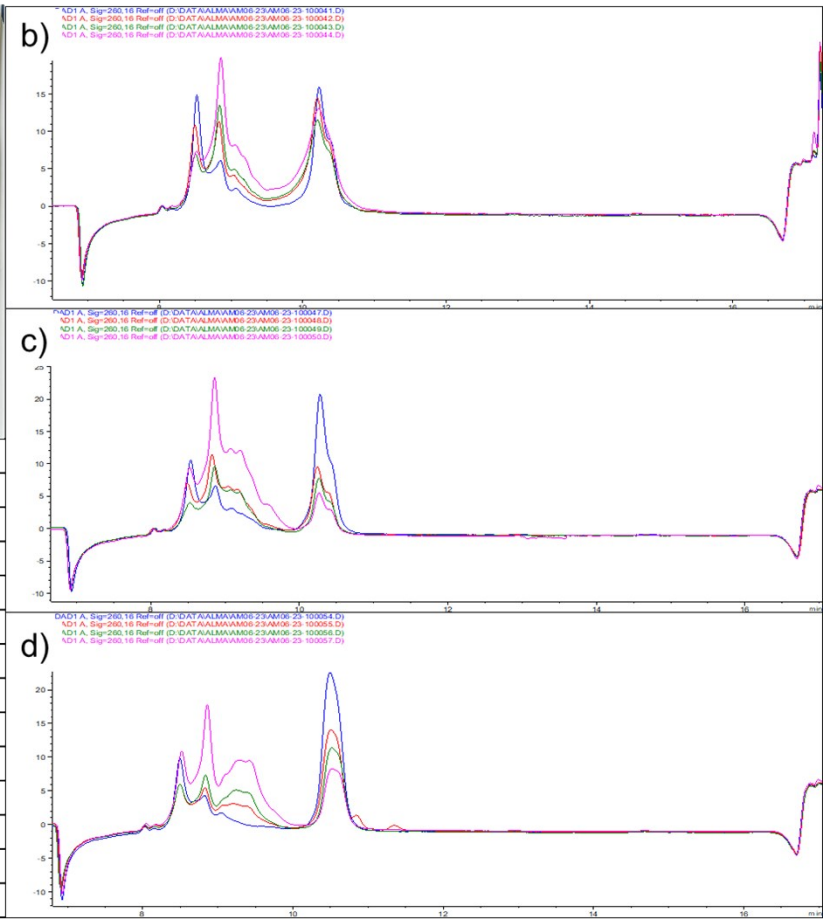

Figure S18: sequence selectivity of **PNA-Hd1**. a) USDS-PAGE experiments and table with lane loading; b) HPLC3 trace of ligation experiment in presence of **PNA-Fur1**; c) HPLC3 trace of ligation experiment in presence of **PNA-Fur2**; d) HPLC3 trace of ligation experiment in presence of **PNA-Fur3**. HPLC3 traces after 0, 15, 30, and 60 minutes light irradiation are shown for every experiment.

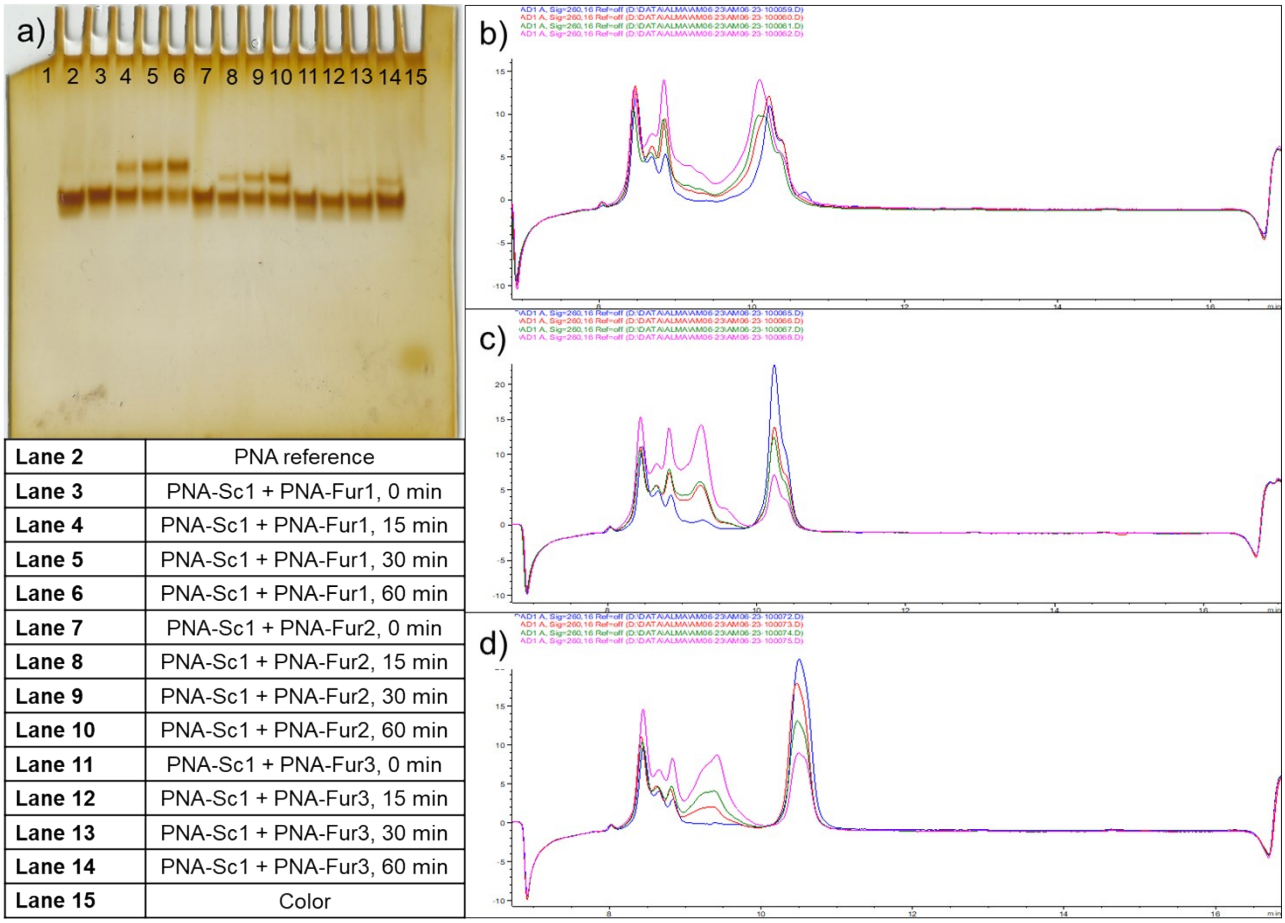

Lane 2	PNA reference
Lane 3	PNA-Sc1 + PNA-Fur1, 0 min
Lane 4	PNA-Sc1 + PNA-Fur1, 15 min
Lane 5	PNA-Sc1 + PNA-Fur1, 30 min
Lane 6	PNA-Sc1 + PNA-Fur1, 60 min
Lane 7	PNA-Sc1 + PNA-Fur2, 0 min
Lane 8	PNA-Sc1 + PNA-Fur2, 15 min
Lane 9	PNA-Sc1 + PNA-Fur2, 30 min
Lane 10	PNA-Sc1 + PNA-Fur2, 60 min
Lane 11	PNA-Sc1 + PNA-Fur3, 0 min
Lane 12	PNA-Sc1 + PNA-Fur3, 15 min
Lane 13	PNA-Sc1 + PNA-Fur3, 30 min
Lane 14	PNA-Sc1 + PNA-Fur3, 60 min
Lane 15	Color

Figure S19: sequence selectivity of **PNA-Sc1**. a) USDS-PAGE experiments and table with lane loading; b) HPLC3 traces of ligation experiment in presence of **PNA-Fur1**; c) HPLC3 traces of ligation experiment in presence of **PNA-Fur2**; d) HPLC3 traces of ligation experiment in presence of **PNA-Fur3**. HPLC3 traces after 0, 15, 30, and 60 minutes light irradiation are shown for every experiment.

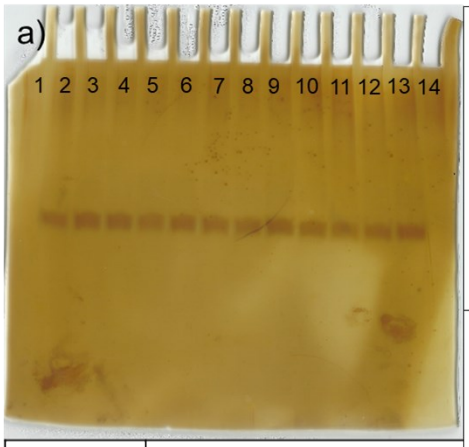

Lane 1	Color
Lane 2	PNA-Ac1 + PNA-Fur1, 0 min
Lane 3	PNA-Ac1 + PNA-Fur1, 15 min
Lane 4	PNA-Ac1 + PNA-Fur1, 30 min
Lane 5	PNA-Ac1 + PNA-Fur1, 60 min
Lane 6	PNA-Ac1 + PNA-Fur2, 0 min
Lane 7	PNA-Ac1 + PNA-Fur2, 15 min
Lane 8	PNA-Ac1 + PNA-Fur2, 30 min
Lane 9	PNA-Ac1 + PNA-Fur2, 60 min
Lane 10	PNA-Ac1 + PNA-Fur3, 0 min
Lane 11	PNA-Ac1 + PNA-Fur3, 15 min
Lane 12	PNA-Ac1 + PNA-Fur3, 30 min
Lane 13	PNA-Ac1 + PNA-Fur3, 60 min
Lane 14	\

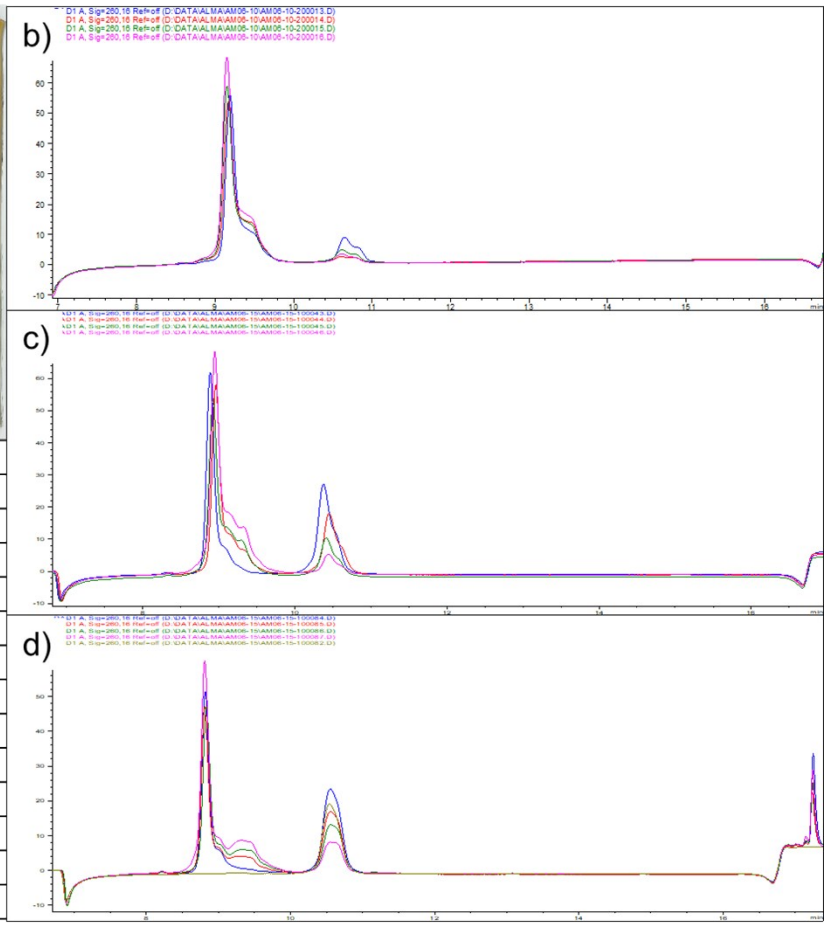

Figure S20: sequence selectivity of **PNA-Ac1**. a) USDS-PAGE experiments and table with lane loading; b) HPLC3 trace of ligation experiment in presence of **PNA-Fur1**; c) HPLC3 trace of ligation experiment in presence of **PNA-Fur2**; d) HPLC3 trace of ligation experiment in presence of **PNA-Fur3**. HPLC3 traces after 0, 15, 30, and 60 minutes light irradiation are shown for every experiment.

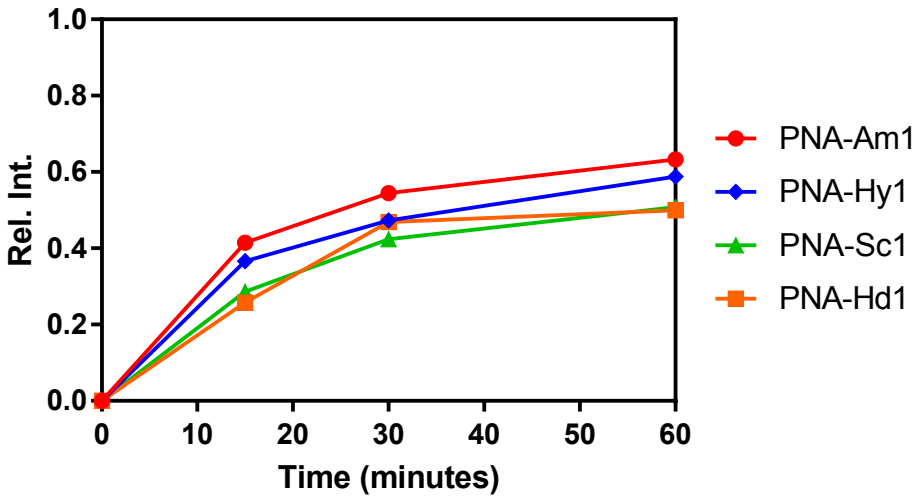

Figure S21: densitometric analysis of the ligation products band of the different nucleophilic PNAs in presence of **PNA-Fur1**. Densitometric analysis was performed on the USDS-PAGE presented in Figure S16-S20; values are expressed as relative intensity of the product band as compared to the sum of starting materials and products band intensities of each lane.

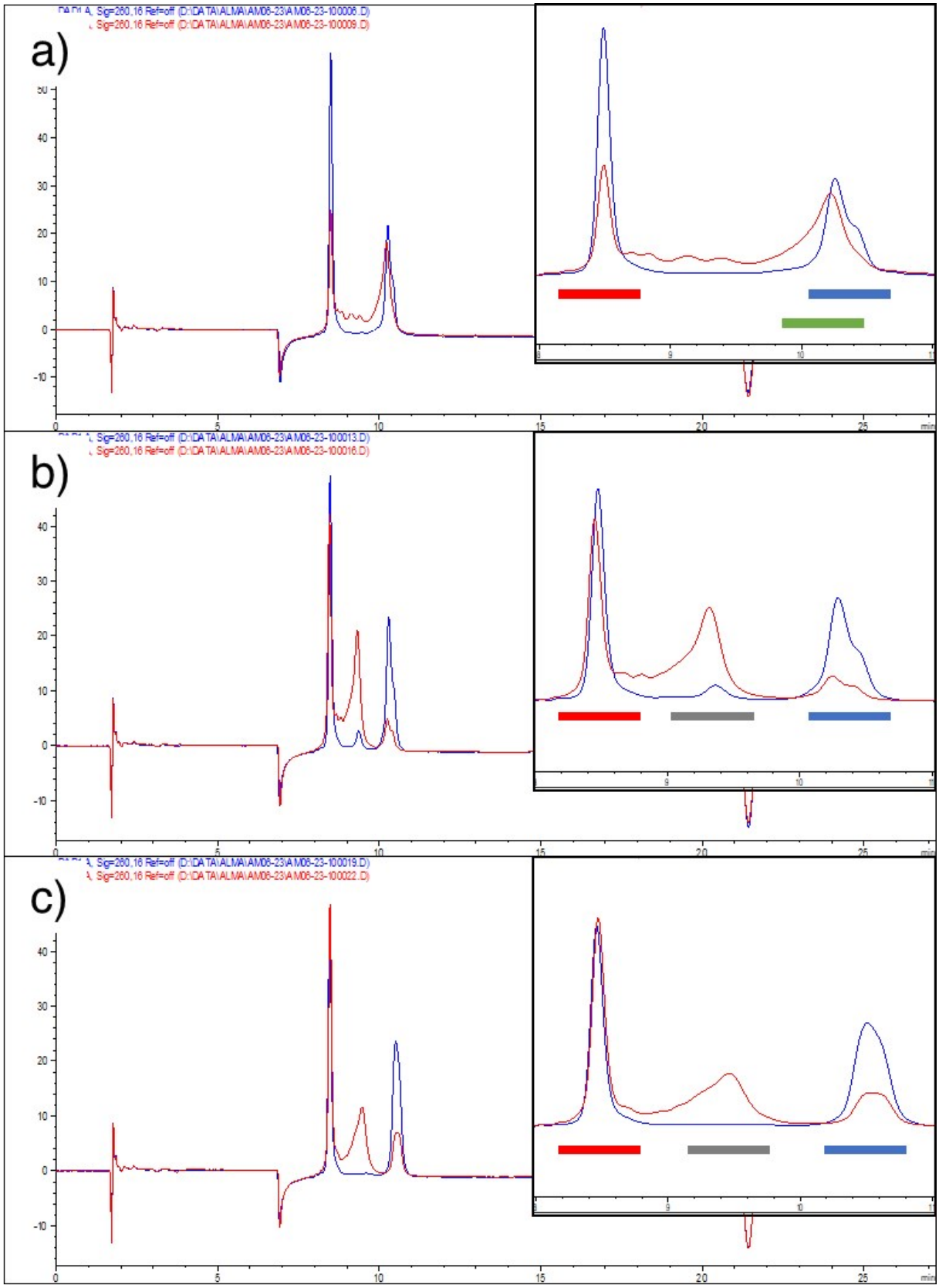

Figure S22: HPLC3 traces of **PNA-Am1** in presence of **PNA-Fur1** (a), **PNA-Fur2** (b), and **PNA-Fur3** (c) at 0 (blue trace) and 60 (red trace) minutes of irradiation. In each panel the insert represent a zoom of the 8-11 minutes region. Red bar: PNA-Nu; blue bar: PNA-Fur; green bar: ligation product; grey bar: oxidation products.

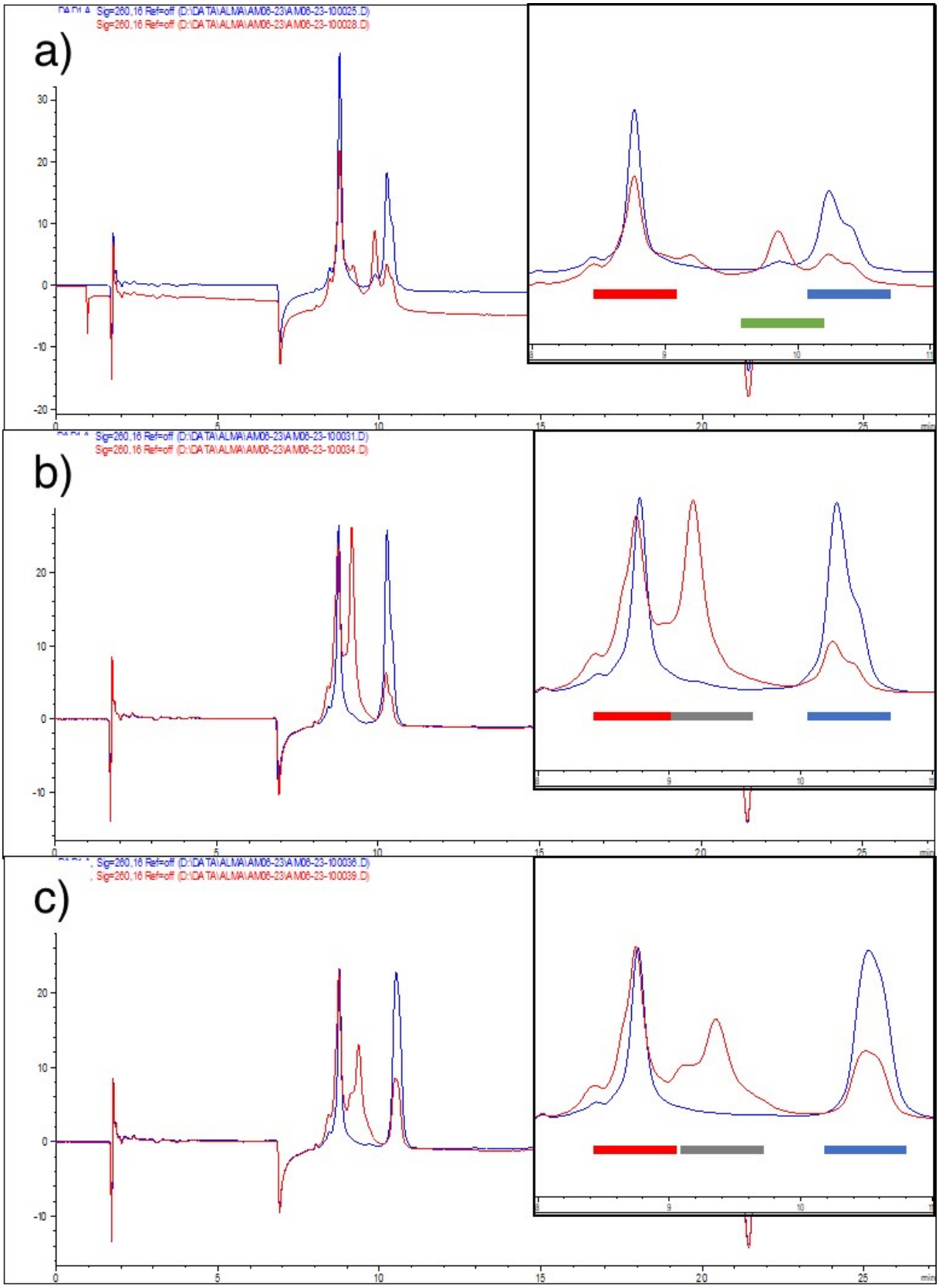

Figure S23: HPLC3 traces of **PNA-Hy1** in presence of **PNA-Fur1** (a), **PNA-Fur2** (b), and **PNA-Fur3** (c) at 0 (blue trace) and 60 (red trace) minutes of irradiation. In each panel the insert represents a zoom of the 8-11 minutes region. Red bar: PNA-Nu; blue bar: PNA-Fur; green bar: ligation product; grey bar: oxidation products.

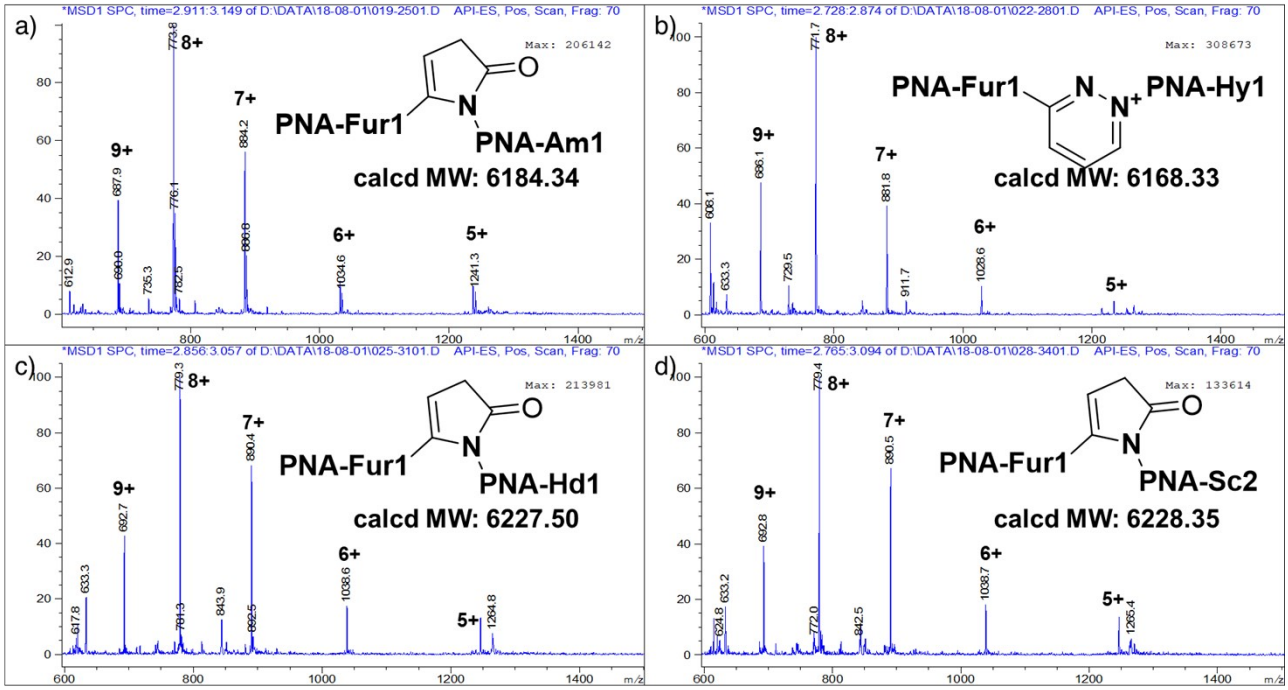

Figure S24: ESI-MS spectra of the peak corresponding to the formed product. a) **PNA-Fur1** + **PNA-Am1** calcd MW 6184.34: 1237.3 $[M+5H]^{5+}$, 1031.4 $[M+6H]^{6+}$, 884.2 $[M+7H]^{7+}$, 773.8 $[M+8H]^{8+}$, 687.9 $[M+9H]^{9+}$; calcd MW (hydrated form) 6202.35: 1241.3 $[M+5H]^{5+}$, 1034.6 $[M+6H]^{6+}$, 886.8 $[M+7H]^{7+}$, 776.1 $[M+8H]^{8+}$, 690.0 $[M+9H]^{9+}$; b) **PNA-Fur1** + **PNA-Hy1** calcd MW 6168.33: 1234.05 $[M+5H]^{5+}$, 1028.6 $[M+6H]^{6+}$, 881.8 $[M+7H]^{7+}$, 771.7 $[M+8H]^{8+}$, 686.1 $[M+9H]^{9+}$; c) **PNA-Fur1** + **PNA-Hd1** calcd MW 6227.50: 1246.2 $[M+5H]^{5+}$, 1038.6 $[M+6H]^{6+}$, 890.4 $[M+7H]^{7+}$, 779.3 $[M+8H]^{8+}$, 692.7 $[M+9H]^{9+}$; d) **PNA-Fur1** + **PNA-Sc1** calcd MW 6228.35: 1246.3 $[M+5H]^{5+}$, 1038.7 $[M+6H]^{6+}$, 890.5 $[M+7H]^{7+}$, 779.4 $[M+8H]^{8+}$, 692.8 $[M+9H]^{9+}$.

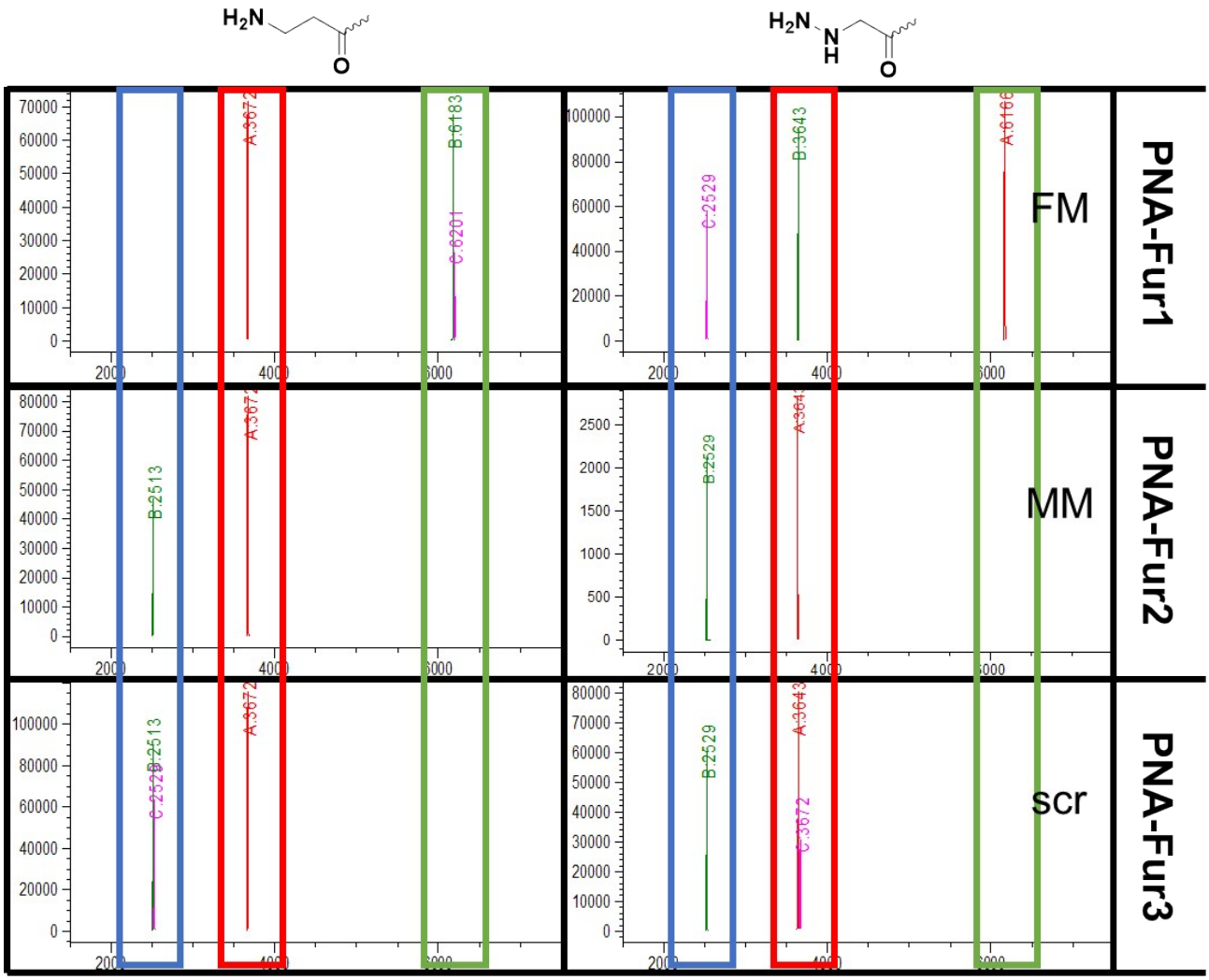

Figure S25: deconvolution of the sum of all MS spectra of PNA peaks obtained from HPLC-ESI-MS analysis of the reaction crude between PNA-Am1 (left column) and PNA-Hy1 (right column) and the different furan containing PNAs. For clarity, the MW regions of the different probes are boxed in blue (furan or oxidation products, 2513 and 2529 respectively), red (nucleophiles, 3672 for PNA-Am1 and 3673 for PNA-Hy1) and green (products, 6184 for PNA-Am1 and 6168 for PNA-Hy1).

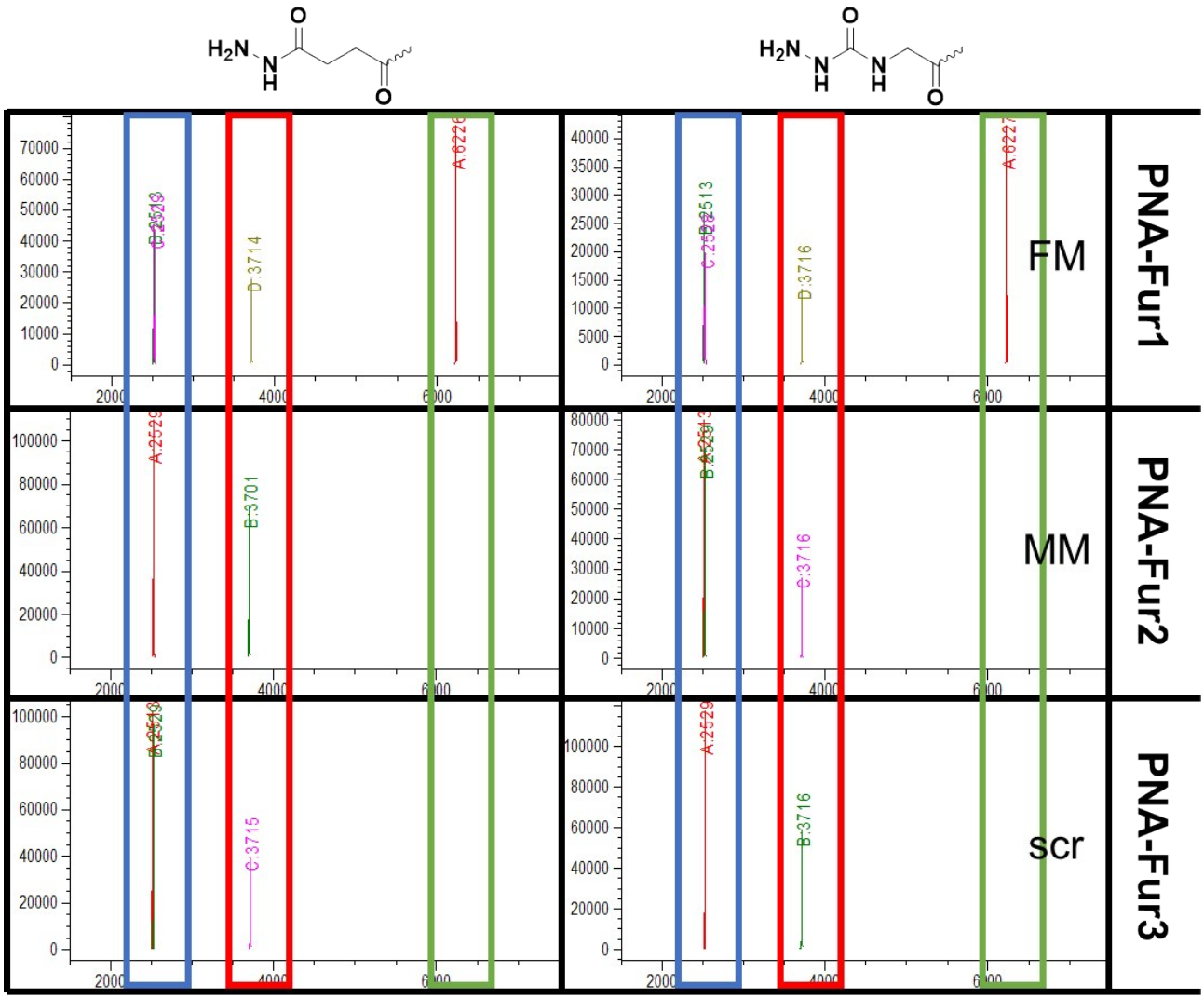

Figure S26: deconvolution of the sum of all MS spectra of PNA peaks obtained from HPLC-ESI-MS analysis of the reaction crude between PNA-Hd1 (left column) and PNA-Sc1 (right column) and the different furan containing PNAs. For clarity, the MW regions of the different probes are boxed in blue (furan or oxidation products, 2513 and 2529 respectively), red (nucleophiles, 3716 for PNA-Hd1 and 3717 for PNA-Sc1) and green (products, 6227 for PNA-Hd1 and 6228 for PNA-Sc1).

9. Templated PNA-PNA ligation

In a typical experiment a 100 µM stock solution of PS was freshly prepared from a 1 mM stock solution. In a 1.5 mL Eppendorf vial, 300 µL of an air saturated buffered solution (PBS, pH 7.4) containing all probes at 5 µM concentration was prepared and allowed to equilibrate for 10 minutes at 25 °C, before the addition of the PS at 5 µM final concentration. The lamp (*vide supra*, general) is then placed on top of the Eppendorf vial for the entire duration of the experiment. 50 µL aliquots of reaction mixture were sampled at different irradiation times and left to react overnight at 25°C. Results were analyzed via USDS-PAGE and HPLC-UV experiments.

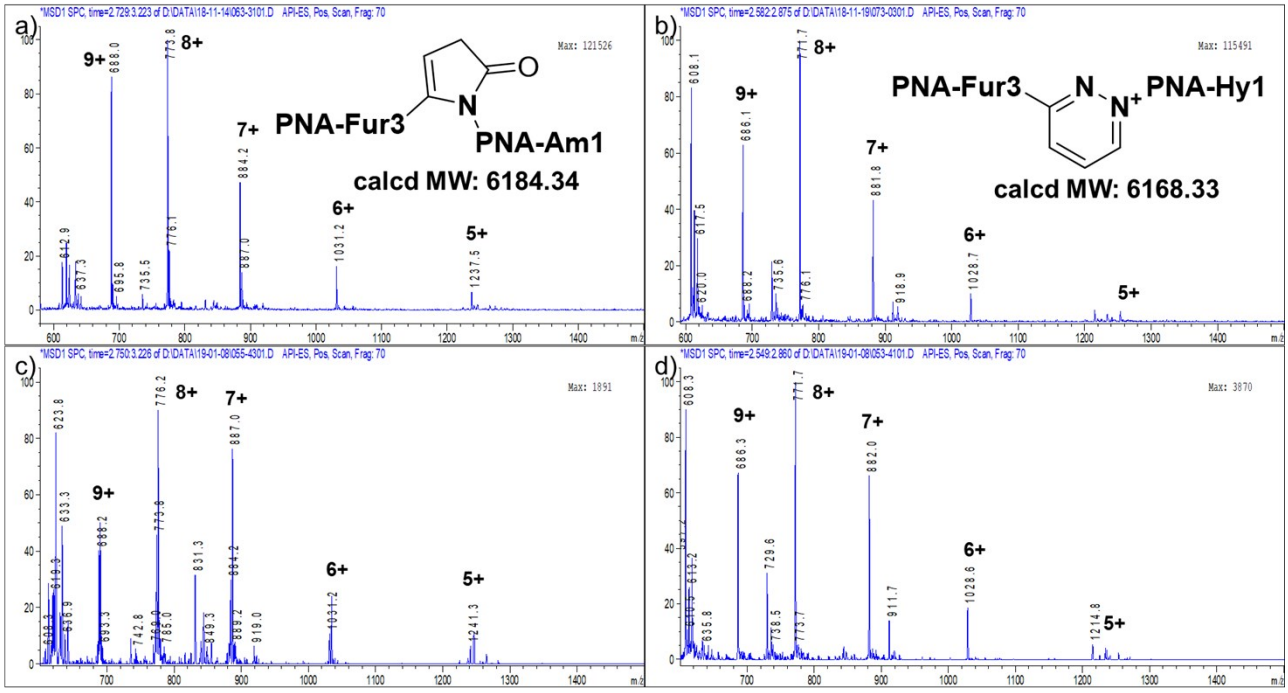

Figure S27: ESI-MS spectra of the peak corresponding to product formed in templated experiments. a) **PNA-Fur3** + **PNA-Am1** + **DNA-1** calcd MW 6184.34: 1237.3 $[M+5H]^{5+}$, 1031.4 $[M+6H]^{6+}$, 884.2 $[M+7H]^{7+}$, 773.8 $[M+8H]^{8+}$, 687.9 $[M+9H]^{9+}$; calcd MW (hydrated form) 6202.35: 1241.3 $[M+5H]^{5+}$, 1034.6 $[M+6H]^{6+}$, 886.8 $[M+7H]^{7+}$, 776.1 $[M+8H]^{8+}$, 690.0 $[M+9H]^{9+}$; b) **PNA-Fur3** + **PNA-Hy1** + **DNA-1** calcd MW 6168.33: 1234.05 $[M+5H]^{5+}$, 1028.6 $[M+6H]^{6+}$, 881.8 $[M+7H]^{7+}$, 771.7 $[M+8H]^{8+}$, 686.1 $[M+9H]^{9+}$; c) **PNA-Fur3** + **PNA-Am1** + **RNA-1** calcd MW 6184.34: 1237.3 $[M+5H]^{5+}$, 1031.4 $[M+6H]^{6+}$, 884.2 $[M+7H]^{7+}$, 773.8 $[M+8H]^{8+}$, 687.9 $[M+9H]^{9+}$; calcd MW (hydrated form) 6202.35: 1241.3 $[M+5H]^{5+}$, 1034.6 $[M+6H]^{6+}$, 886.8 $[M+7H]^{7+}$, 776.1 $[M+8H]^{8+}$, 690.0 $[M+9H]^{9+}$; d) **PNA-Fur3** + **PNA-Hy1** + **RNA-1** calcd MW 6168.33: 1234.05 $[M+5H]^{5+}$, 1028.6 $[M+6H]^{6+}$, 881.8 $[M+7H]^{7+}$, 771.7 $[M+8H]^{8+}$, 686.1 $[M+9H]^{9+}$.

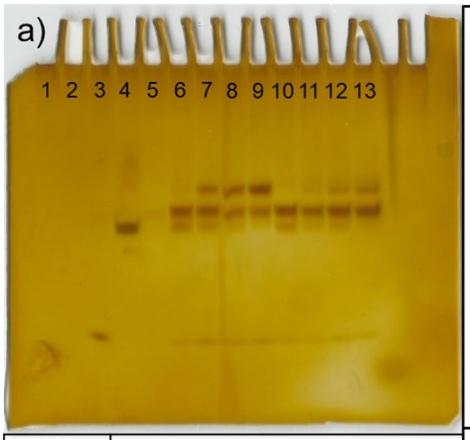

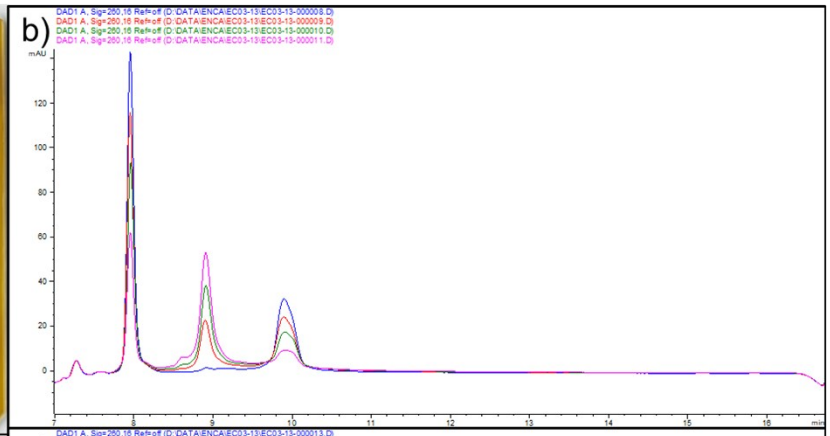

Lane 2	Color
Lane 3	DNA-1 Ref
Lane 4	PNA-Fur3 + DNA-1 Ref
Lane 5	PNA-Am1 + DNA-1 Ref
Lane 6	PNA-Am1 + PNA-Fur3 + DNA-1, 0’
Lane 7	PNA-Am1 + PNA-Fur3 + DNA-1, 15’
Lane 8	PNA-Am1 + PNA-Fur3 + DNA-1, 30’
Lane 9	PNA-Am1 + PNA-Fur3 + DNA-1, 60’
Lane 10	PNA-Am1 + PNA-Fur3 + DNA-2, 0’
Lane 11	PNA-Am1 + PNA-Fur3 + DNA-2, 15’
Lane 12	PNA-Am1 + PNA-Fur3 + DNA-2, 30’
Lane 13	PNA-Am1 + PNA-Fur3 + DNA-2, 60’

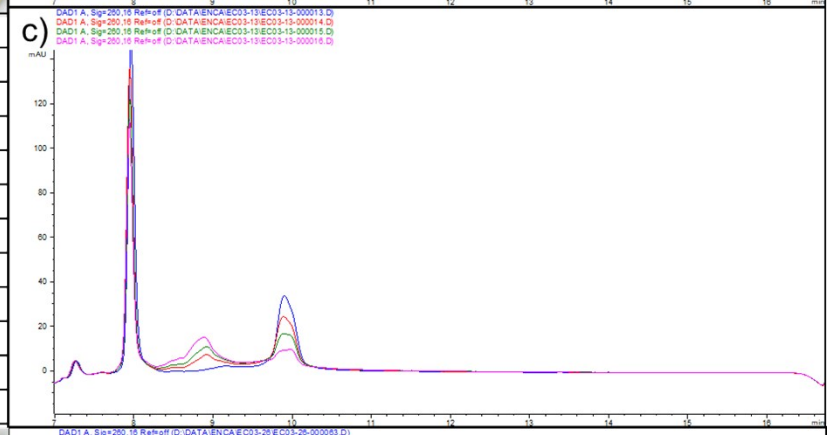

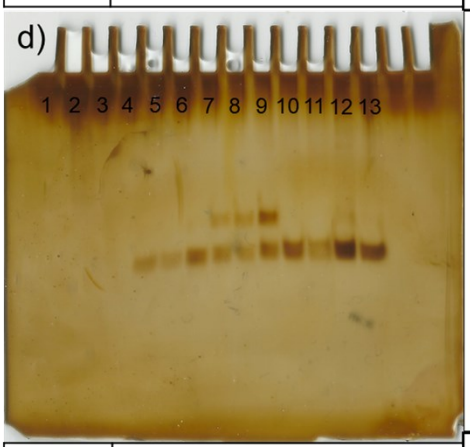

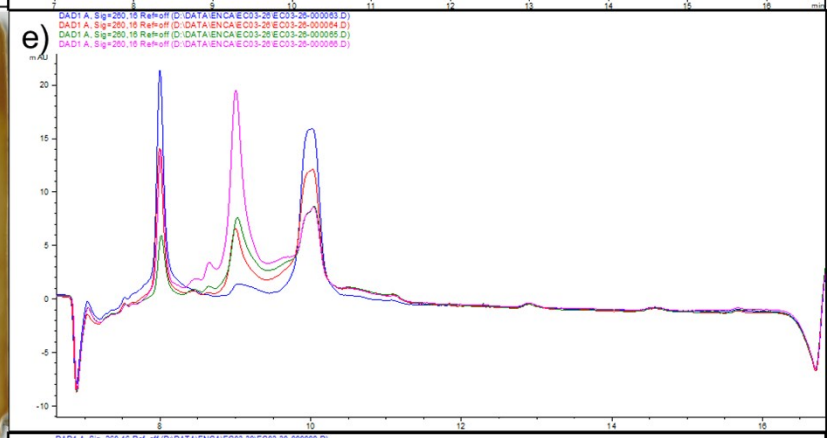

Lane 2	DNA-1 Ref
Lane 3	PNA-Fur3 + DNA-1 Ref
Lane 4	PNA-Am1 + DNA-1 Ref
Lane 5	PNA-Am1 + PNA-Fur3 Ref
Lane 6	PNA-Am1 + PNA-Fur3 + DNA-1, 0’
Lane 7	PNA-Am1 + PNA-Fur3 + DNA-1, 15’
Lane 8	PNA-Am1 + PNA-Fur3 + DNA-1, 30’
Lane 9	PNA-Am1 + PNA-Fur3 + DNA-1, 60’
Lane 10	PNA-Am1 + PNA-Fur3 + DNA-2, 0’
Lane 11	PNA-Am1 + PNA-Fur3 + DNA-2, 15’
Lane 12	PNA-Am1 + PNA-Fur3 + DNA-2, 30’
Lane 13	PNA-Am1 + PNA-Fur3 + DNA-2, 60’

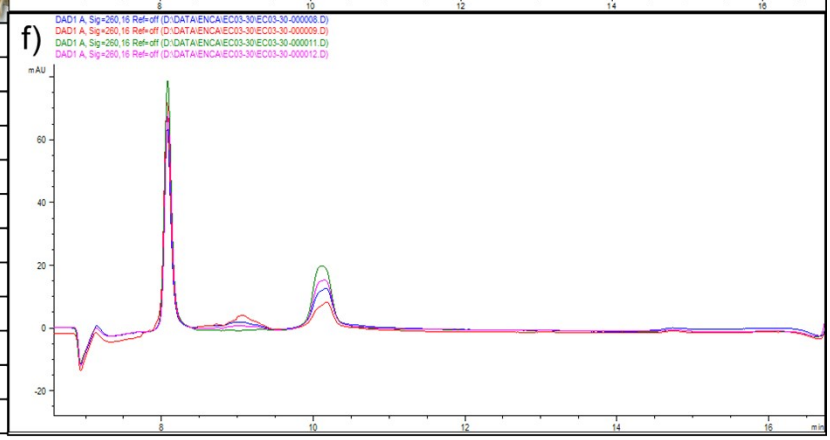

Figure S28: sequence selectivity of **PNA-Am1** and **PNA-Fur3** in a DNA templated setup performed at 5μM (a-c) and 1 μM (d-f) probe concentration. a,d) USDS-PAGE experiments and table with lane loading; b,e) HPLC3 trace of ligation experiment in presence of **DNA-1**; c,f) HPLC3 trace of ligation experiment in presence of **DNA-2**.

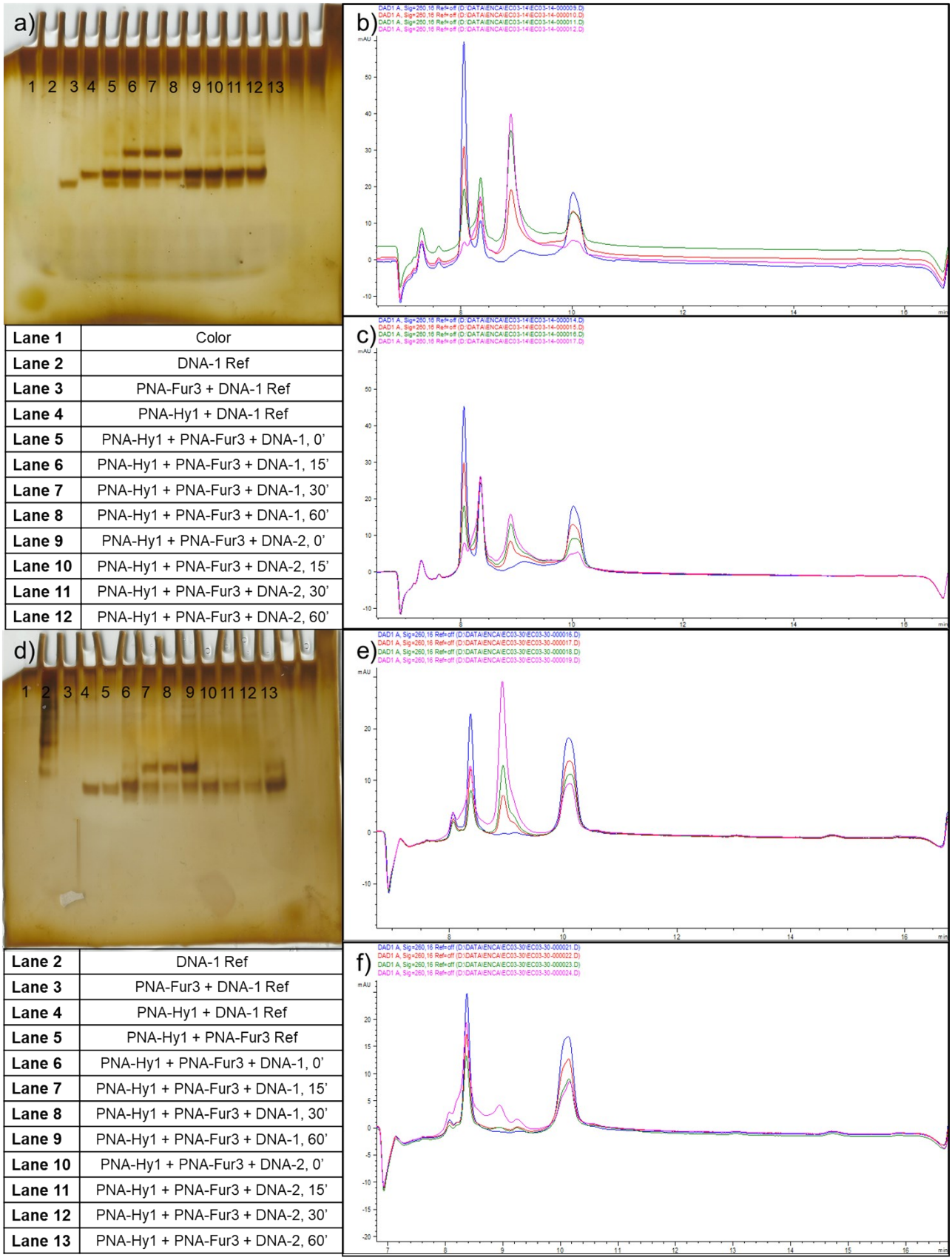

Lane 1	Color
Lane 2	DNA-1 Ref
Lane 3	PNA-Fur3 + DNA-1 Ref
Lane 4	PNA-Hy1 + DNA-1 Ref
Lane 5	PNA-Hy1 + PNA-Fur3 + DNA-1, 0’
Lane 6	PNA-Hy1 + PNA-Fur3 + DNA-1, 15’
Lane 7	PNA-Hy1 + PNA-Fur3 + DNA-1, 30’
Lane 8	PNA-Hy1 + PNA-Fur3 + DNA-1, 60’
Lane 9	PNA-Hy1 + PNA-Fur3 + DNA-2, 0’
Lane 10	PNA-Hy1 + PNA-Fur3 + DNA-2, 15’
Lane 11	PNA-Hy1 + PNA-Fur3 + DNA-2, 30’
Lane 12	PNA-Hy1 + PNA-Fur3 + DNA-2, 60’

Lane 2	DNA-1 Ref
Lane 3	PNA-Fur3 + DNA-1 Ref
Lane 4	PNA-Hy1 + DNA-1 Ref
Lane 5	PNA-Hy1 + PNA-Fur3 Ref
Lane 6	PNA-Hy1 + PNA-Fur3 + DNA-1, 0’
Lane 7	PNA-Hy1 + PNA-Fur3 + DNA-1, 15’
Lane 8	PNA-Hy1 + PNA-Fur3 + DNA-1, 30’
Lane 9	PNA-Hy1 + PNA-Fur3 + DNA-1, 60’
Lane 10	PNA-Hy1 + PNA-Fur3 + DNA-2, 0’
Lane 11	PNA-Hy1 + PNA-Fur3 + DNA-2, 15’
Lane 12	PNA-Hy1 + PNA-Fur3 + DNA-2, 30’
Lane 13	PNA-Hy1 + PNA-Fur3 + DNA-2, 60’

Figure S29: sequence selectivity of **PNA-Hy1** and **PNA-Fur3** in a DNA templated setup performed at 5μM (a-c) and 1 μM (d-f) probe concentration. a,d) USDS-PAGE experiments and table with lane loading; b,e) HPLC3 trace of ligation experiment in presence of **DNA-1**; c,f) HPLC3 trace of ligation experiment in presence of **DNA-2**.

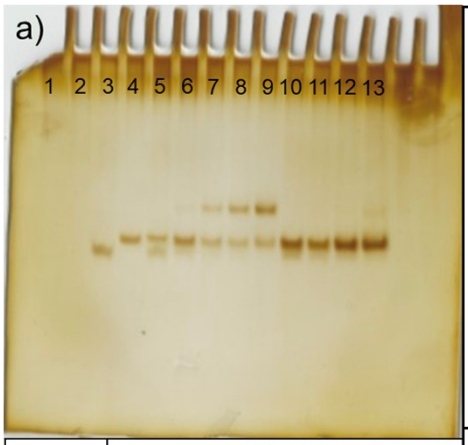

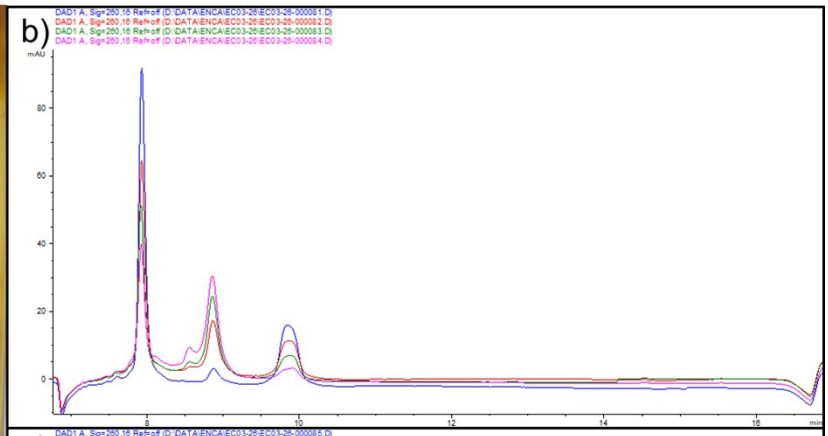

Lane 2	RNA-1 Ref
Lane 3	PNA-Fur3 + RNA-1Ref
Lane 4	PNA-Am1 + RNA-1 Ref
Lane 5	PNA-Am1 + PNA-Fur2 Ref
Lane 6	PNA-Am1 + PNA-Fur3 + RNA-1, 0’
Lane 7	PNA-Am1 + PNA-Fur3 + RNA-1, 15’
Lane 8	PNA-Am1 + PNA-Fur3 + RNA-1, 30’
Lane 9	PNA-Am1 + PNA-Fur3 + RNA-1, 60’
Lane 10	PNA-Am1 + PNA-Fur3 + RNA-2, 0’
Lane 11	PNA-Am1 + PNA-Fur3 + RNA-2, 15’
Lane 12	PNA-Am1 + PNA-Fur3 + RNA-2, 30’
Lane 13	PNA-Am1 + PNA-Fur3 + RNA-2, 60’

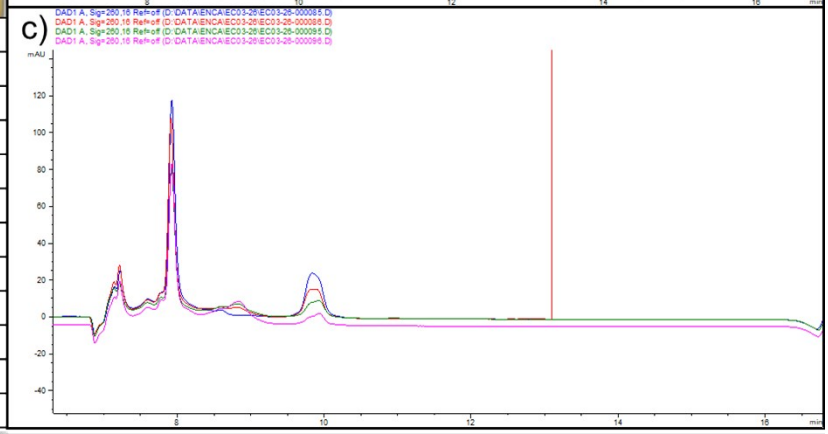

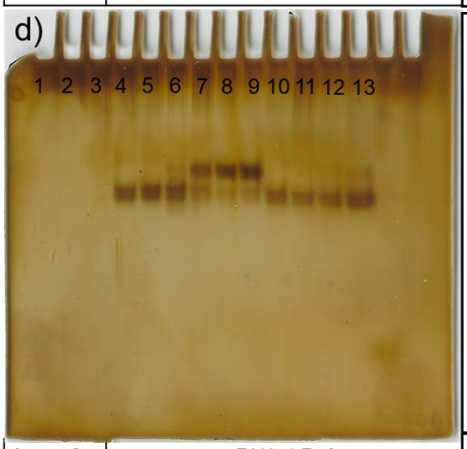

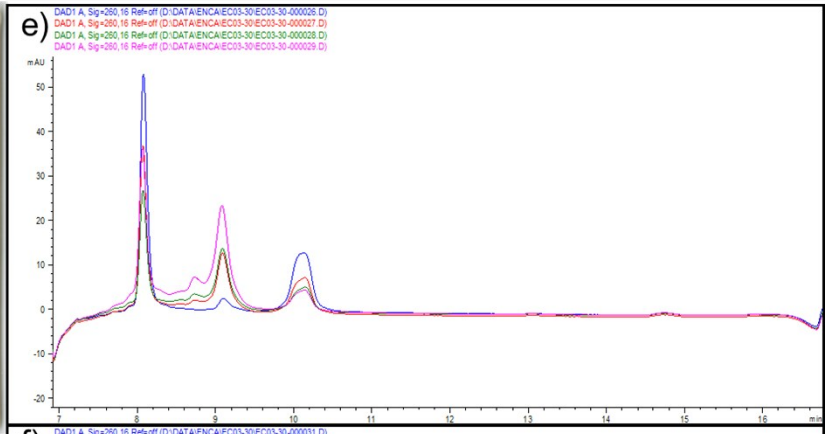

Lane 2	RNA-1 Ref
Lane 3	PNA-Fur3 + RNA-1Ref
Lane 4	PNA-Am1 + RNA-1 Ref
Lane 5	PNA-Am1 + PNA-Fur3 Ref
Lane 6	PNA-Am1 + PNA-Fur3 + RNA-1, 0’
Lane 7	PNA-Am1 + PNA-Fur3 + RNA-1, 15’
Lane 8	PNA-Am1 + PNA-Fur3 + RNA-1, 30’
Lane 9	PNA-Am1 + PNA-Fur3 + RNA-1, 60’
Lane 10	PNA-Am1 + PNA-Fur3 + RNA-2, 0’
Lane 11	PNA-Am1 + PNA-Fur3 + RNA-2, 15’
Lane 12	PNA-Am1 + PNA-Fur3 + RNA-2, 30’
Lane 13	PNA-Am1 + PNA-Fur3 + RNA-2, 60’

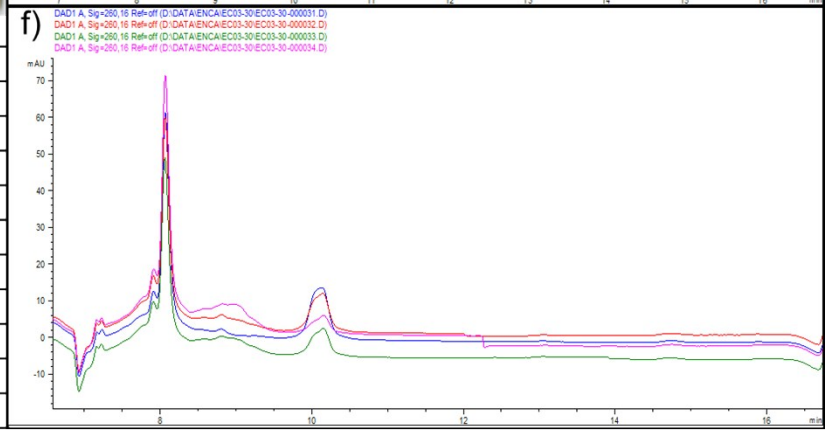

Figure S30: sequence selectivity of **PNA-Am1** and **PNA-Fur3** in a RNA templated setup performed at 5µM (a-c) and 1 µM (d-f) probe concentration. a,d) USDS-PAGE experiments and table with lane loading; b,e) HPLC3 trace of ligation experiment in presence of **RNA-1**; c,f) HPLC3 trace of ligation experiment in presence of **RNA-2**.

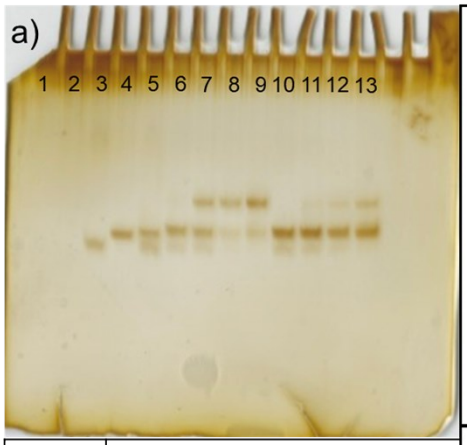

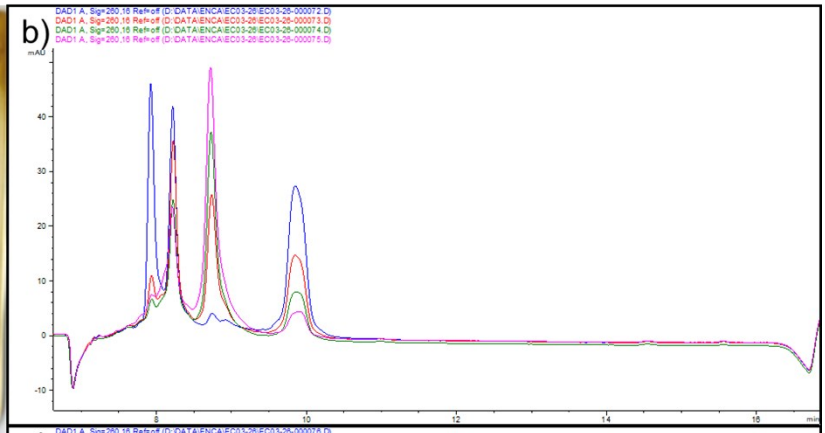

Lane 2	RNA-1 Ref
Lane 3	PNA-Fur3 + RNA-1 Ref
Lane 4	PNA-Hy1 + RNA-1 Ref
Lane 5	PNA-Hy1 + PNA-Fur2 Ref
Lane 6	PNA-Hy1 + PNA-Fur3 + RNA-1, 0’
Lane 7	PNA-Hy1 + PNA-Fur3 + RNA-1, 15’
Lane 8	PNA-Hy1 + PNA-Fur3 + RNA-1, 30’
Lane 9	PNA-Hy1 + PNA-Fur3 + RNA-1, 60’
Lane 10	PNA-Hy1 + PNA-Fur3 + RNA-2, 0’
Lane 11	PNA-Hy1 + PNA-Fur3 + RNA-2, 15’
Lane 12	PNA-Hy1 + PNA-Fur3 + RNA-2, 30’
Lane 13	PNA-Hy1 + PNA-Fur3 + RNA-2, 60’

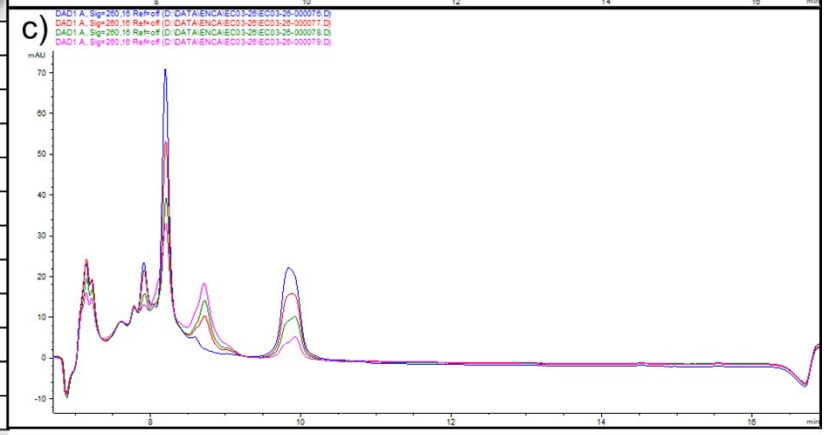

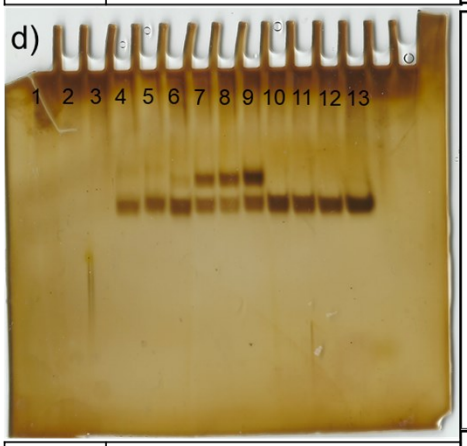

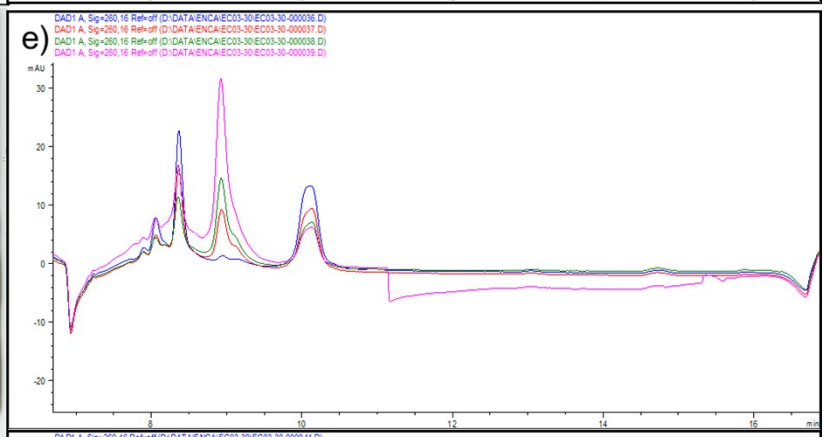

Lane 2	RNA-1 Ref
Lane 3	PNA-Fur3 + RNA-1 Ref
Lane 4	PNA-Hy1 + RNA-1 Ref
Lane 5	PNA-Hy1 + PNA-Fur3 Ref
Lane 6	PNA-Hy1 + PNA-Fur3 + RNA-1, 0’
Lane 7	PNA-Hy1 + PNA-Fur3 + RNA-1, 15’
Lane 8	PNA-Hy1 + PNA-Fur3 + RNA-1, 30’
Lane 9	PNA-Hy1 + PNA-Fur3 + RNA-1, 60’
Lane 10	PNA-Hy1 + PNA-Fur3 + RNA-2, 0 min
Lane 11	PNA-Hy1 + PNA-Fur3 + RNA-2, 15’
Lane 12	PNA-Hy1 + PNA-Fur3 + RNA-2, 30’
Lane 13	PNA-Hy1 + PNA-Fur3 + RNA-2, 60’

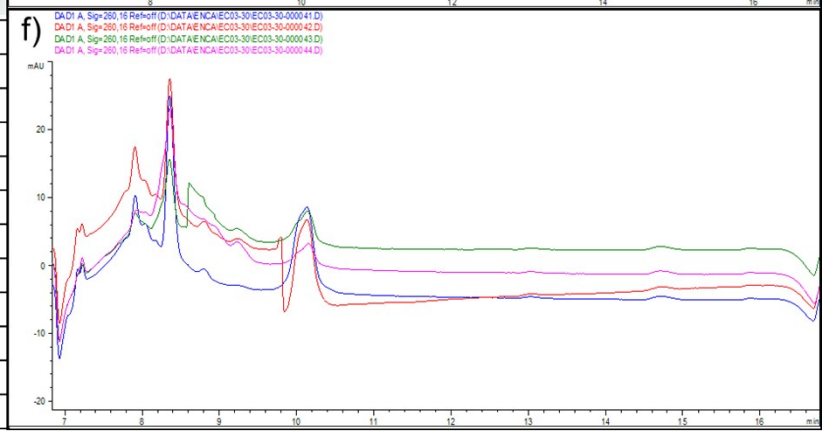

Figure S31: sequence selectivity of **PNA-Hy1** and **PNA-Fur3** in a RNA templated setup performed at 5μM (a-c) and 1 μM (d-f) probe concentration. a,d) USDS-PAGE experiments and table with lane loading; b,e) HPLC3 trace of ligation experiment in presence of **RNA-1**; c,f) HPLC3 trace of ligation experiment in presence of **RNA-2**.

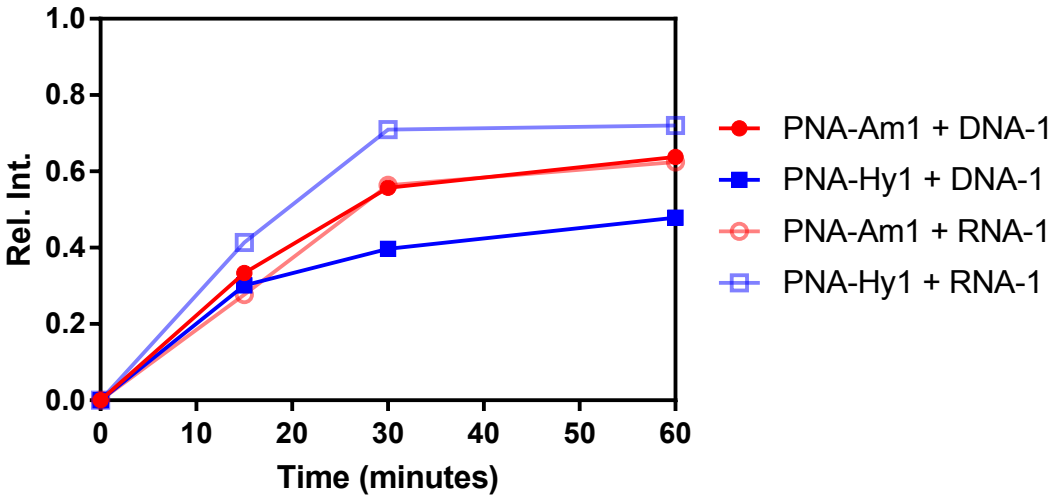

Figure S32: densitometric analysis of ligation product bands of the different nucleophilic PNAs in presence of **PNA-Fur3** and DNA or RNA templates. Densitometric analysis was performed on the USDS-PAGE presented in Figure S28-S31; values are expressed as relative intensity of the product band as compared to the sum of starting materials and product band intensities of each lane.

10. Oxidation studies

Quantum yield calculation

In a typical experiment a 100 µM working solution of PS was freshly prepared from a 1 mM stock solution. Additionally, a 200 µM ABDA working solution was freshly prepared from a 500 µM stock solution. 300 µL of an air saturated buffered solution (PBS, pH 7.4) containing 100 µM ABDA and 5 µM of PS were added to a 1.5 mL Eppendorf vial. The lamp (*vide supra*, general) is placed on top of the Eppendorf and the sample irradiated for the entire duration of the experiment. 20 µL aliquots were taken at different time intervals and protected from light. Absorbance at 380 nm was recorded via UV-Vis spectrophotometry.
Singlet oxygen quantum yields (φ) of PSs were calculated comparing the ABDA oxidation induced by the dye of interest to the oxidation induced by Rose Bengal ($\varphi_{RB} = 0.75$[8]) adapting the methods described in literature:[13,14]

$$\varphi_{(x)} = \varphi_{RB} \frac{m_x}{I_{RB}} \frac{I_x}{m_{RB}} \qquad (5)$$

where m_x, m_{RB} are the slopes of the logarithmic degradation curves in presence of the dye of interest and Rose Bengal, and I_x are defined as:

$$I_x = \int_{400}^{760} P_{(\lambda)} \cdot (1 - 10^{-A_{(\lambda)x}}) d\lambda \qquad (6)$$

where $P_{(\lambda)}$ is the power of the lamp expressed in W/m² (lamp is considered as a black body with a color temperature of 3000 K as specified by the producer) and $A_{(\lambda)}$ is the absorbance of the dye of interest in the experimental conditions.

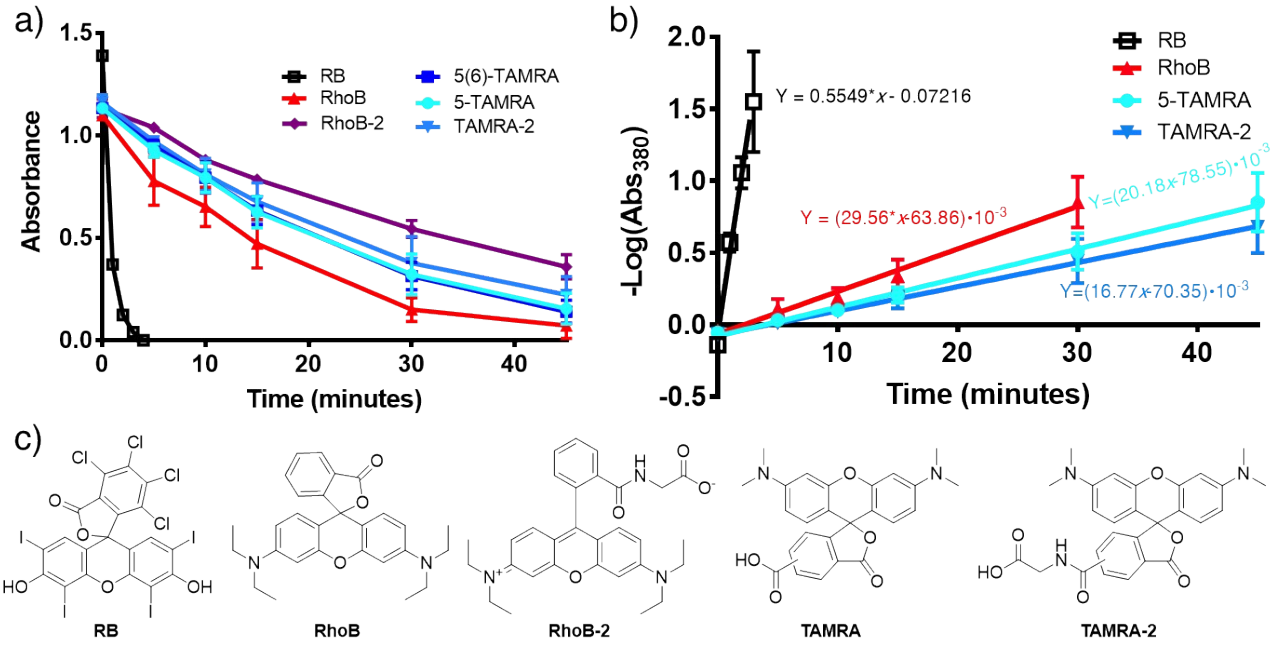

Figure S33: ABDA degradation experiments. a) profile of the 380 nm absorption during light irradiation in presence of different PSs; b) logaritmic plot of the degradation profiles and linear regression of the data points; c) structure of tested PS. Experiment performed at 100 µM ABDA concentration, 5 µM PS concentration in PBS pH 7.4.

Table S7: pH influence on $^1O_2$ production.

PS	***m* (·10⁻³)**		
	pH= 4.7	pH= 6.0	pH= 7.4
RB, 1 µM	22 ± 1	32 ± 2	29 ± 3

RhoB, 5 µM	25.3 ± 0.8	20 ± 1	30 ± 2

Table S8: relative singlet oxygen production and quantum yield of the different PSs employed in this study. Calculations based on experiments shown in Figure S33a.

PS	*m* ($\cdot 10^{-3}$)	Relative $^1O_2$ production (m_x / m_{RB})	φ
RB	555 ± 38	1	0.75[8]
RhoB	30 ± 2	0.0541 ± 0.005	0.0273 ± 0.003
RhoB+DNA	19.6 ± 0.6	0.0353 ± 0.003	0.0178 ± 0.002
Rhob-2	11.2 ± 0.2	0.0203 ± 0.001	0.0396 ± 0.003
5-TAMRA	20.2 ± 0.6	0.0364 ± 0.003	0.0251 ± 0.002
5(6)-TAMRA	21.0 ± 0.8	0.0378 ± 0.003	0.0266 ± 0.002
TAMRA-2	16.8 ± 0.2	0.0303± 0.002	0.0230 ± 0.002

Extended discussion on photosensitizer selection: it can be noted that the introduction of an extra carboxylic function (5(6)-TAMRA versus RhoB) does not affect the singlet oxygen quantum yield production, but results in a lower singlet oxygen generation due to the lower molar extinction factor. No significant differences were found between a single TAMRA isomer and the mixture of the two, suggesting similar oxygen excitation behaviors for the two isomers. Conversion of the carboxylate to a secondary amide (as it will be after PNA conjugation) also results in a lower singlet oxygen production, as a consequence of a reduced quantum yield. This effect is less dramatic for **TAMRA-2** (as compared to **Rhob-2)**, as a consequence of the possibility to still form the spirolactone under neutral conditions.[15] For this reasons we selected TAMRA as photosensitizer for the realization of the third generation of the nucleophilic probes.

Furan probes oxidation evaluation

In a typical experiment a 100 µM stock solution of PS was freshly prepared from a 1 mM stock solution. In a 1.5 mL Eppendorf vial, 300 µL of an air saturated buffered solution (PBS, pH 7.4) containing all probes at 5 µM concentration was prepared and allowed to equilibrate for 10 minutes at 25 °C, before the addition of the PS at 5 µM final concentration (when needed). When reported, glutathione (GSH) is added to a final concentration of 2 mM. The lamp (*vide supra*, general) is then placed on top of the Eppendorf vial for the entire duration of the experiment. 50 µL of solution were sampled at different irradiation times and analyzed under HPLC3 conditions. Furan oxidation was followed through integration of the 260 nm absorbance of **PNA-Fur1** or **PNA-Fur3** peaks. Integration was performed using Agilent ChemStation for LC 3D systems software (Rev.B.04.01[481]). Data reported are normalized to 0 minutes irradiation integral.

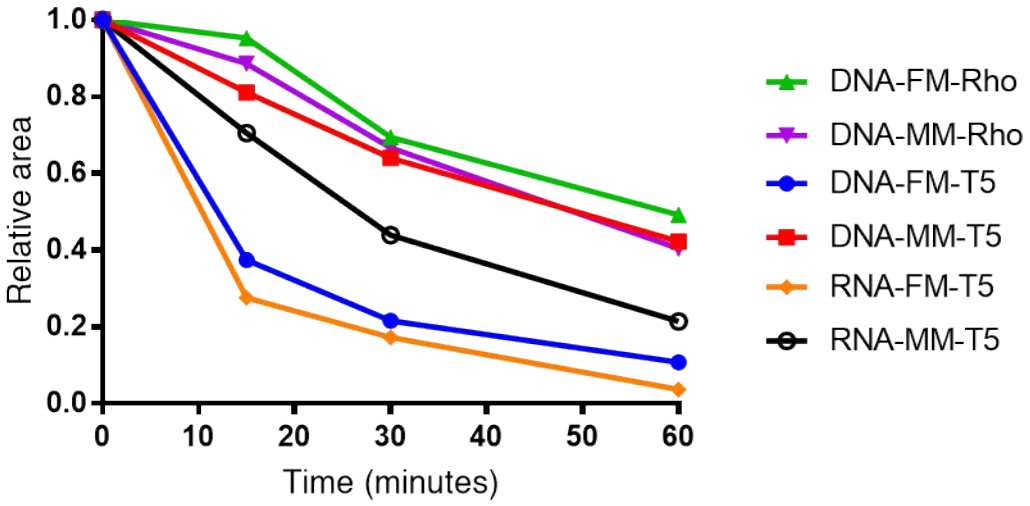

Figure S34: furan oxidation experiments performed at 5 µM probe and photosensitizer concentration using capped nucleophiles, in PBS pH 7.4, at 25°C. PNA-Fur3 and PNA-Ac1 in presence of DNA-1 (DNA-FM-Rho), DNA-2 (DNA-MM-Rho), or PNA-Fur3 and

PNA-Ac2(5-TAMRA) in presence of DNA-1 (DNA-FM-T5), and DNA-2 (DNA-MM-T5), RNA-1 (RNA-FM-T5), and RNA-2 (RNA-MM-T5).

Extended discussion on the oxidation behavior in presence of RNA: when fully matched **RNA-1** is used as template, no significant differences in the oxidation rate were observed as compared to the DNA case. The mentioned higher PNA:RNA complex stability that allows partial formation of the perturbed MM complex (under experimental conditions) here resulted in a faster oxidation in presence of **RNA-2** as compared to the experiment performed with **DNA-2**. The oxidation rate in this case is, however, less pronounced if compared with the FM **RNA-1**.

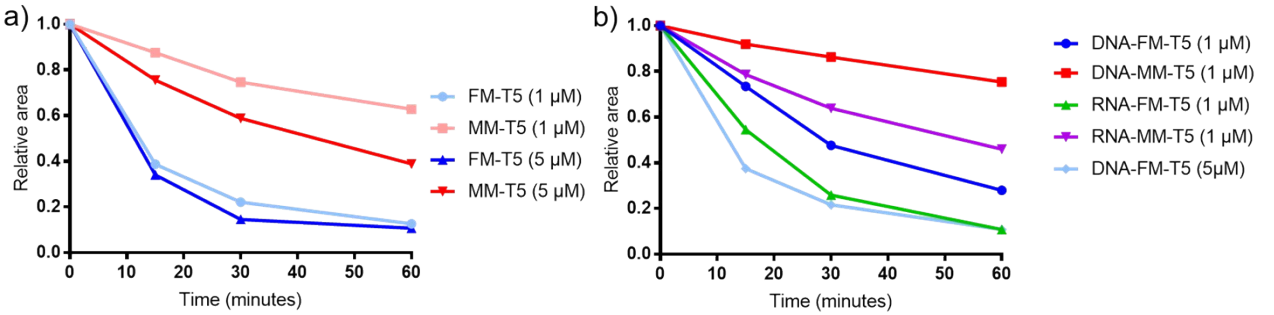

Figure S35: furan oxidation experiments performed at 1 μM probes and photosensitizer concentration using PNA-Ac2(5-TAMRA) probe, in PBS pH 7.4, at 25°C. (a) PNA:PNA setup: (FM-T5) PNA-Fur1; (MM-T5) PNA-Fur3. (b) DNA Templated setup: (DNA-FM-T5) PNA-Fur3 and DNA-1; (DNA-MM-T5) PNA-Fur3 and DNA-2; (RNA-FM-T5) PNA-Fur3 and RNA-1; (RNA-MM-T5) PNA-Fur3 and RNA-2. PNA-Fur3 and PNA-Ac1 in presence of DNA-1 (DNA-FM-Rho), DNA-2 (DNA-MM-Rho), or PNA-Fur3 and PNA-Ac2(5-TAMRA) in presence of DNA-1 (DNA-FM-T5), and DNA-2 (DNA-MM-T5), RNA-1 (RNA-FM-T5), and RNA-2 (RNA-MM-T5). Experiments at 5 μM probe concentration are reported in both panels for comparison.

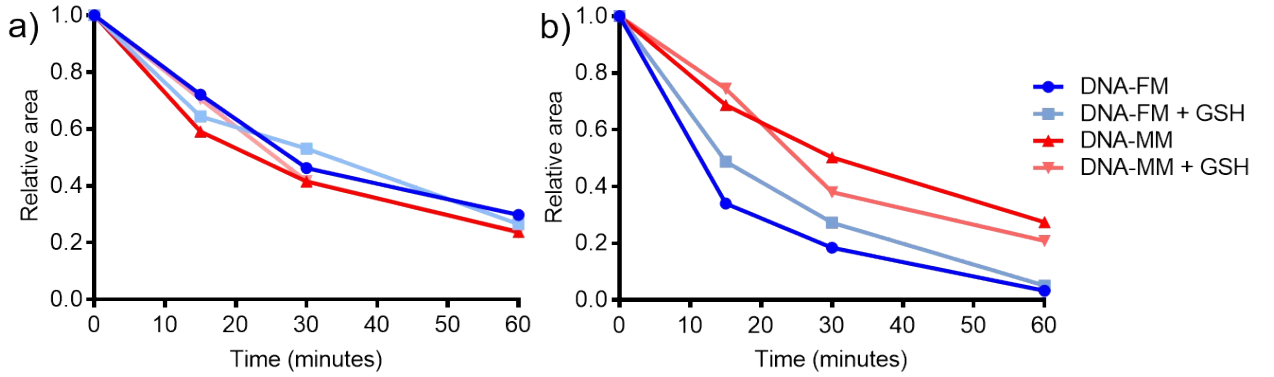

Figure S36: furan oxidation experiments in DNA templated setup, performed at 5 μM probe concentration in presence of at 2 mM glutathione in PBS pH 7.4, at 25°C in presence of DNA-1 (DNA-FM) or DNA-2 (DNA-MM). (a) PNA-Ac1 + PNA-Fur3 + RhoB. (b) PNA-Ac2 + PNA-Fur3.

11. Fully integrated probe ligation

In a typical experiment a 100 µM stock solution of PS was freshly prepared from a 1 mM stock solution. In a 1.5 mL Eppendorf vial, 300 µL of an air saturated buffered solution (PBS, pH 7.4) containing all probes at 5 µM concentration was prepared and allowed to equilibrate for 10 minutes at 25 °C, before the addition of the PS at 5 µM final concentration (when needed). The lamp (*vide supra*, general) is then placed on top of the Eppendorf vial for the entire duration of the experiment. 50 µL of solution were sampled at different irradiation times and left to react overnight at 25°C. Results were analyzed via USDS-PAGE and HPLC-UV experiments.

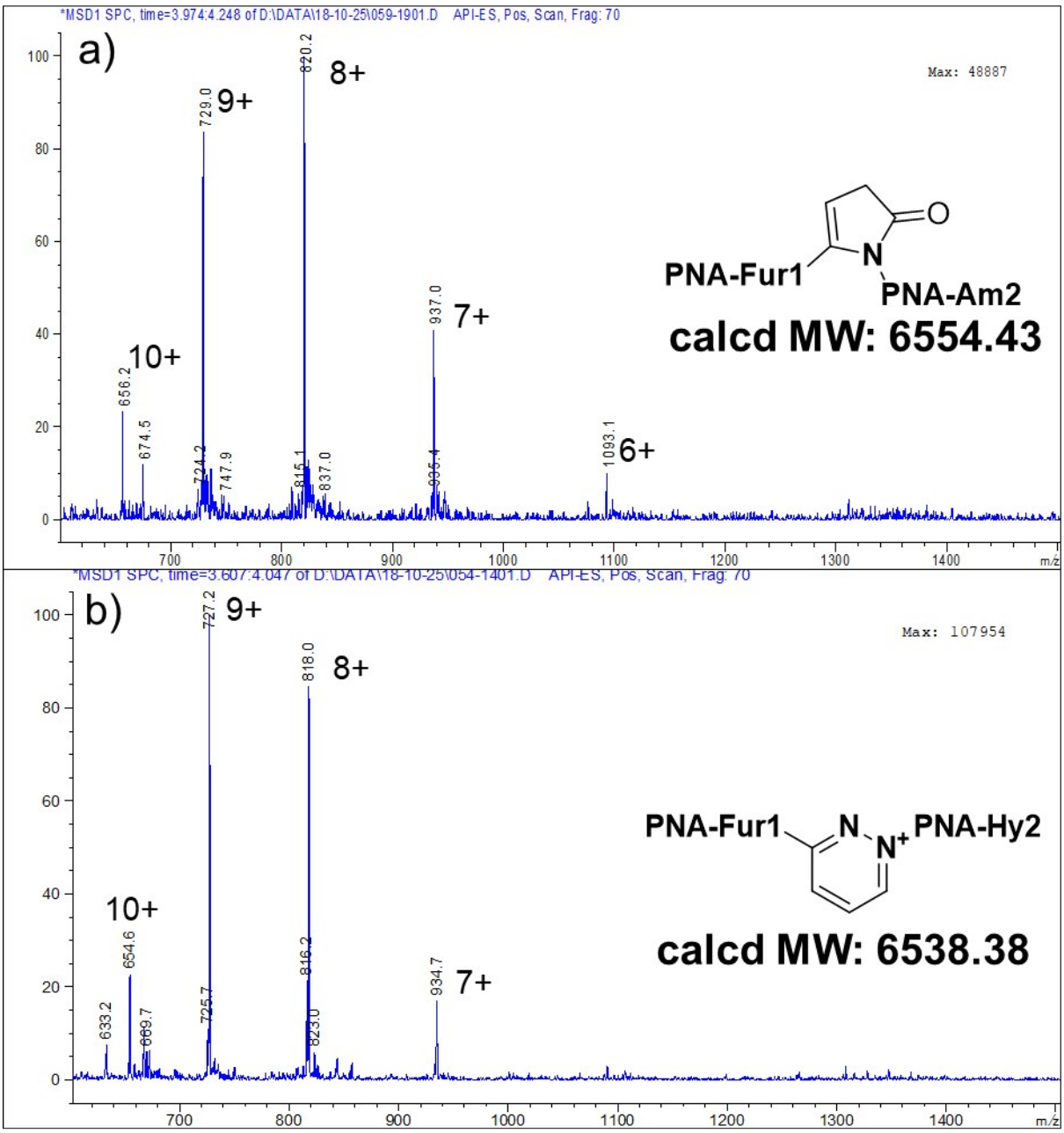

Figure S37: ESI-MS spectra of the peak corresponding to product formed in presence of the second generation probes. a) **PNA-Fur1** + **PNA-Am2** calcd MW 6554.43: 1093.1 $[M+6H]^{6+}$, 937.0 $[M+7H]^{7+}$, 820.2 $[M+8H]^{8+}$, 729.0 $[M+9H]^{9+}$, 656.2 $[M+10H]^{10+}$; b) **PNA-Fur3** + **PNA-Hy2** calcd MW 6554.43: 934.7 $[M+7H]^{7+}$, 818.0 $[M+8H]^{8+}$, 727.2 $[M+9H]^{9+}$, 654.6 $[M+10H]^{10+}$.

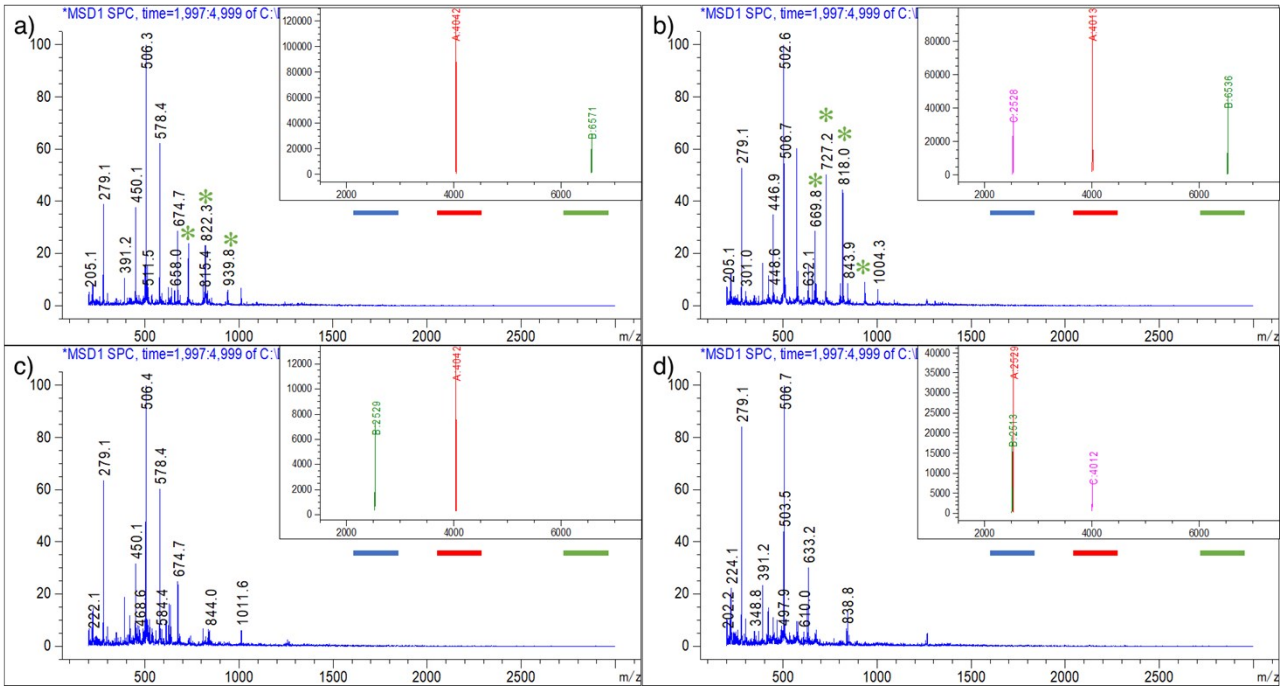

Figure S38: ESI-MS spectra of the reaction crude between PNA-Am2 (a,c) or PNA-Hy2 (b,d), in presence of PNA-Fur1 (a,b) or PNA-Fur2 (c,d), and their deconvolution (insert). For clarity, the MW regions of the different probes are highlighted in blue (furan or oxidation products), red (nucleophile) and green (product). Green stars in the ESI-MS sprectra indicate product peaks.

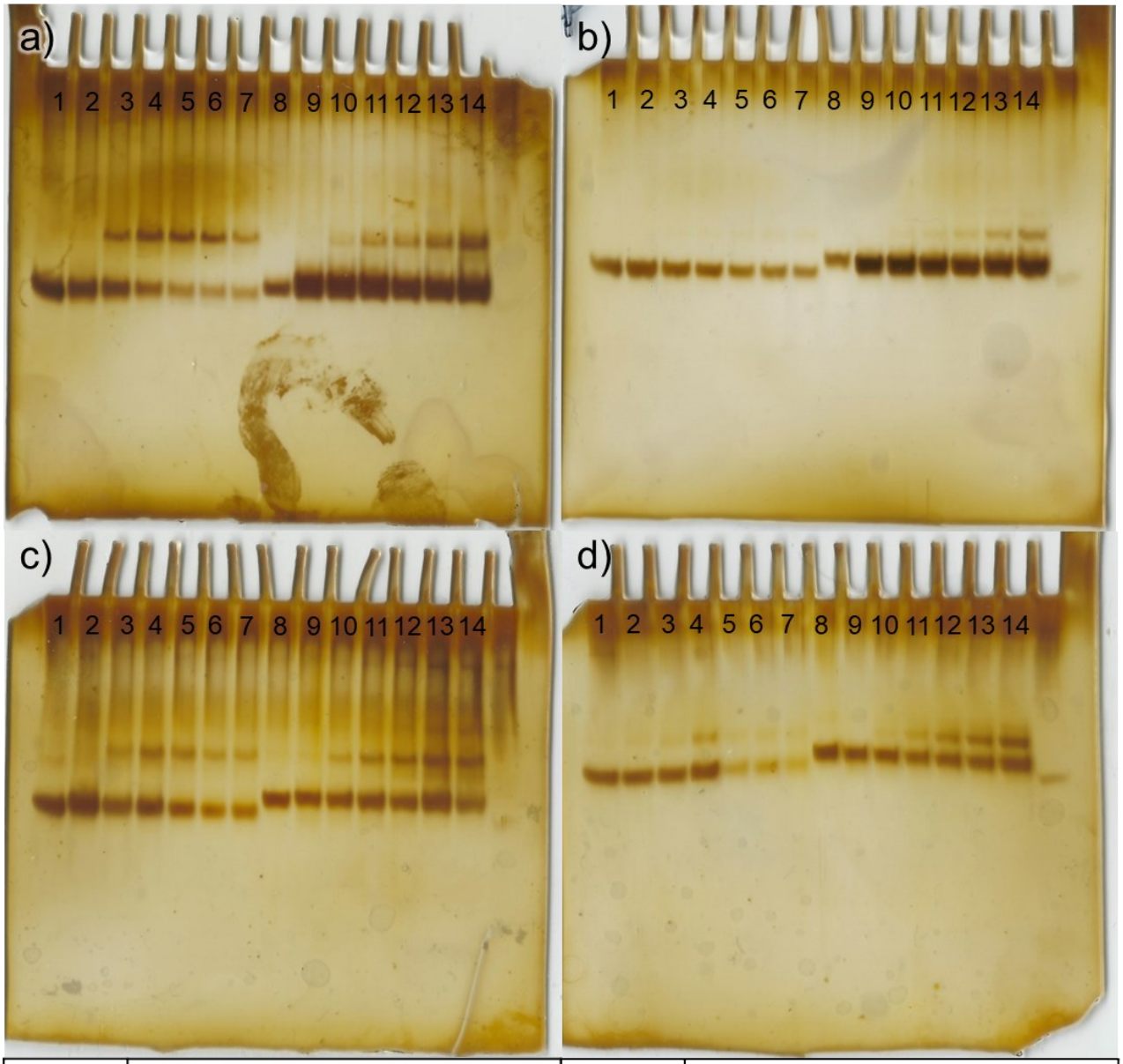

Lane 1	PNA-Am2/Hy2 Ref	**Lane 8**	PNA-Am1/Hy1 Ref
Lane 2	PNA-Fur1/Fur2 + PNA-Am2/Hy2, 0’	**Lane 9**	PNA-Fur1/Fur2 + PNA-Am1/Hy1, 0’
Lane 3	PNA-Fur1/Fur2+ PNA-Am2/Hy2, 5’	**Lane 10**	PNA-Fur1/Fur2 + PNA-Am1/Hy1, 5’
Lane 4	PNA-Fur1/Fur2 + PNA-Am2/Hy2, 10’	**Lane 11**	PNA-Fur1/Fur2 + PNA-Am1/Hy1, 10’
Lane 5	PNA-Fur1/Fur2 + PNA-Am2/Hy2, 15’	**Lane 12**	PNA-Fur1/Fur2 + PNA-Am1/Hy1, 15’
Lane 6	PNA-Fur1/Fur2+ PNA-Am2/Hy2, 20’	**Lane 13**	PNA-Fur1/Fur2 + PNA-Am1/Hy1, 20’
Lane 7	PNA-Fur1/Fur2 + PNA-Am2/Hy2, 30’	**Lane 14**	PNA-Fur1/Fur2 + PNA-Am1/Hy1, 30’

Figure S39: ligation comparison between **PNA-Am2** and **PNA-Am1** in presence of **PNA-Fur1** (a) or **PNA-Fur2** (b), and **PNA-Hy2** and **PNA-Hy1** in presence of **PNA-Fur1** (c) or **PNA-Fur2** (d). The table specifies the lane loading. Experiments were performed at 5 μM probe concentration, in the experiments where **PNA-Am1** and **PNA-Hy1** are employed, a 5 μM RhoB is used for singlet oxygen production.

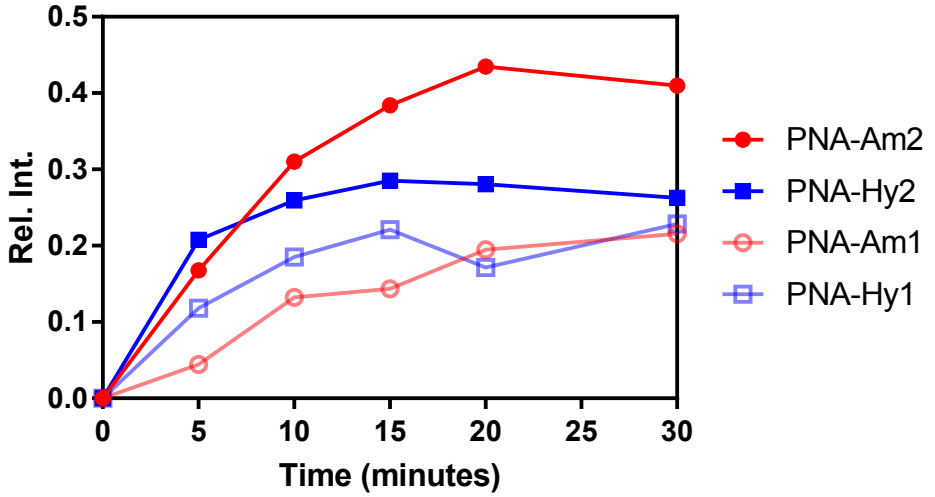

Figure S40: densitometric analysis of the ligation products band of the different nucleophilic PNAs in presence of **PNA-Fur1** and DNA or RNA templates. Densitometric analysis was performed on the USDS-PAGE presented in Figure S39; values are expressed as relative intensity of the product band as compared to the sum of starting materials and product band intensities of each lane.

12. Light triggered templated ligation on surface

Solution ligation in 96well plates

In a typical experiment a 100 μM stock solution of PS was freshly prepared from a 1 mM stock solution. In a 1.5 mL Eppendorf vial, 200 μL of an air saturated buffered solution (PBS, pH 7.4) containing all probes at 5 μM concentration was prepared and allowed to equilibrate for 10 minutes at 25 °C, before the addition of the PS at 5 μM final concentration (when needed) and then 150 μL of that solution were transferred to the 96 well plate. The lamp (*vide supra*, general) was then placed on top of the plate for the entire duration of the experiment. 30 μL aliquots of reaction mixture were sampled at different irradiation times and left to react overnight at 25°C. Results were analyzed via USDS-PAGE.

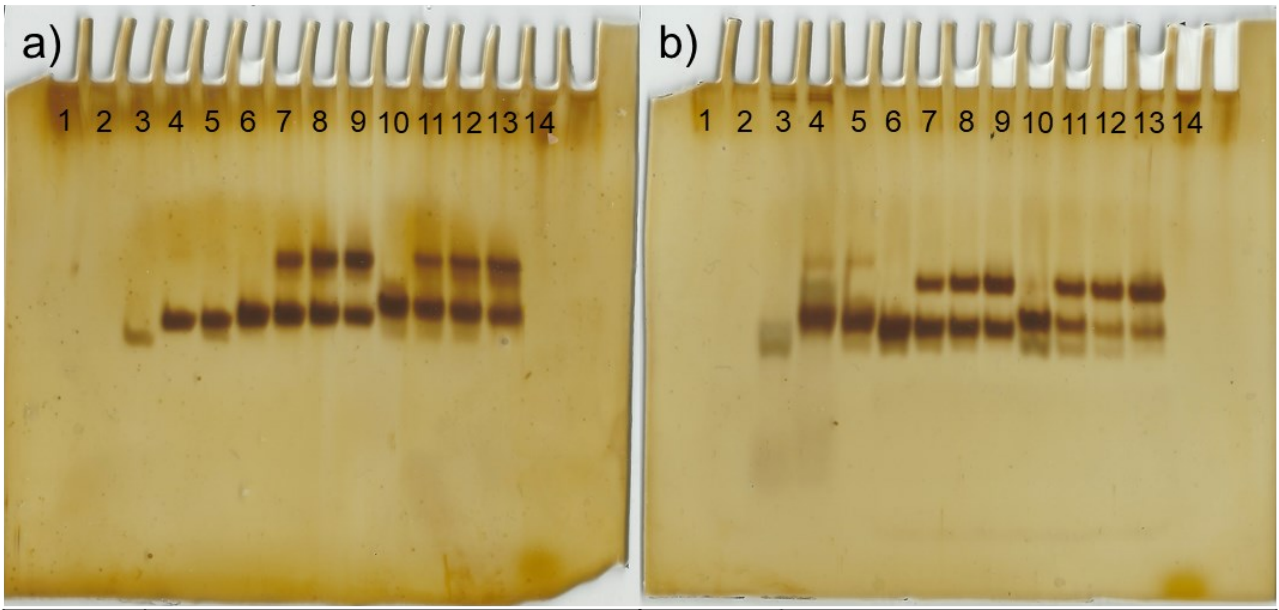

Lane 2	-	**Lane 2**	DNA-1
Lane 3	PNA-Fur1	**Lane 3**	PNA-Fur3
Lane 4	PNA-Am1	**Lane 4**	PNA-Am1
Lane 5	PNA-Am1 + PNA-Fur1	**Lane 5**	PNA-Am1 + PNA-Fur3
Lane 6	PNA-Am1 + PNA-Fur1, 0’	**Lane 6**	PNA-Am1 + PNA-Fur3, 0’
Lane 7	PNA-Am1 + PNA-Fur1, 15’	**Lane 7**	PNA-Am1 + PNA-Fur3, 15’
Lane 8	PNA-Am1 + PNA-Fur1, 30’	**Lane 8**	PNA-Am1 + PNA-Fur3, 30’
Lane 9	PNA-Am1 + PNA-Fur1, 60’	**Lane 9**	PNA-Am1 + PNA-Fur3, 60’
Lane 10	PNA-Hy1 + PNA-Fur1, 0’	**Lane 10**	PNA-Hy1 + PNA-Fur3, 0’
Lane 11	PNA-Hy1 + PNA-Fur1, 15’	**Lane 11**	PNA-Hy1 + PNA-Fur3, 15’
Lane 12	PNA-Hy1 + PNA-Fur1, 30’	**Lane 12**	PNA-Hy1 + PNA-Fur3, 30’
Lane 13	PNA-Hy1 + PNA-Fur1, 60’	**Lane 13**	PNA-Hy1 + PNA-Fur3, 60’

Figure S41: ligation comparison between **PNA-Am1** and **PNA-Hy1** in a 96-well plate set-up in presence of **PNA-Fur1** in a PNA:PNA geometry (a) or in presence of **PNA-Fur3**, using **DNA-1** as template (b). The table specifies the lane loading. Experiments performed at 5 μM probe concentration and 5 μM RhoB is used for singlet oxygen production.

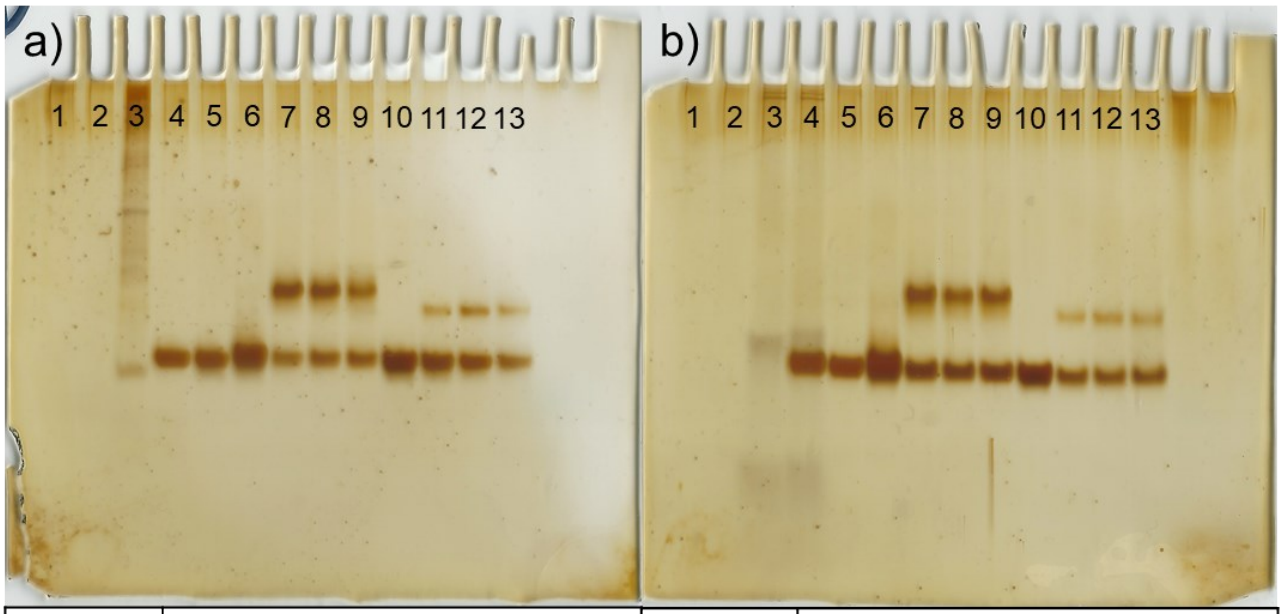

Lane 2	-	**Lane 8**	PNA-Fur1 + PNA-Am2/Hy2, 30’
Lane 3	PNA-Fur1	**Lane 9**	PNA-Fur1 + PNA-Am2/Hy2, 60’
Lane 4	PNA-Am2/Hy2	**Lane 10**	PNA-Fur2 + PNA-Am2/Hy2, 0’
Lane 5	PNA-Fur1 + PNA-Am2/Hy2	**Lane 11**	PNA-Fur2 + PNA-Am2/Hy2, 15’
Lane 6	PNA-Fur1 + PNA-Am2/Hy2, 0’	**Lane 12**	PNA-Fur2 + PNA-Am2/Hy2, 30’
Lane 7	PNA-Fur1 + PNA-Am2/Hy2, 15’	**Lane 13**	PNA-Fur2 + PNA-Am2/Hy2, 60’

Figure S42: ligation comparison between **PNA-Am2** (a) and **PNA-Hy2** (b) in a 96-well plate set-up in presence of **PNA-Fur1** and **PNA-Fur2**. The table specifies the lane loading.. Experiments performed at 5 μM probe concentration.

Evaluation of Biotin stability to oxidation

In a 1.5 mL Eppendorf vial, a 0.5 μM **PNA-Am3** solution was freshly prepared in PBS pH 7.4 from a 10 μM stock solution in mQ. The solution was placed in an Eppendorf thermomixer at 25°C prior to light irradiation. The lamp was placed on top of the vial and light irradiation was performed for 1h. In a parallel experiment the same solution was supplemented with 0.5 μM Rose Bengal and the light irradiation was performed for 2 minutes. The solutions were analyzed via HPLC-UV and MALDI.

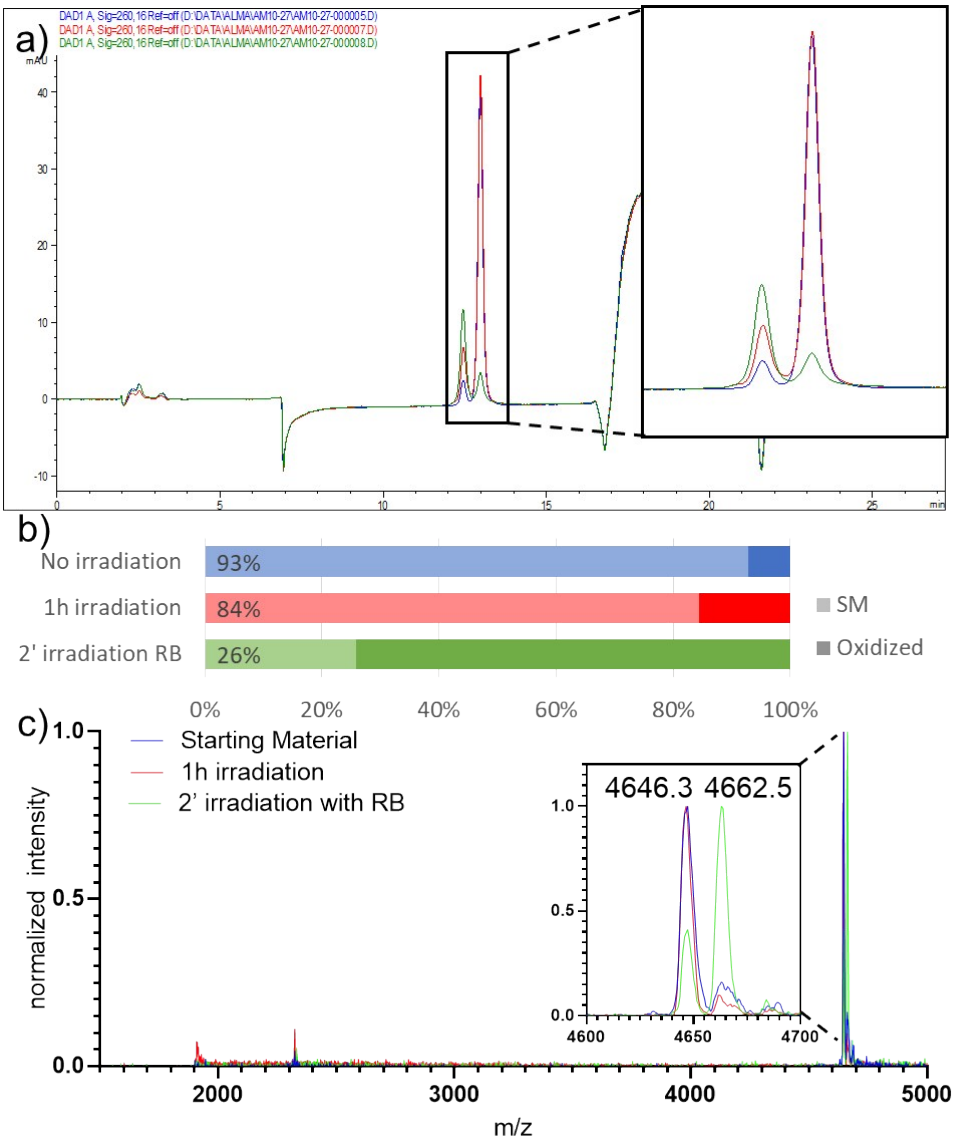

Figure S43: effect on biotin oxidation after light irradiation. (a) HPLC3 traces of the light irradiation experiments. (b) relative amount of starting material based on the integration of the peaks highlighted in panel a. (c) MALDI spectra of the solutions after light irradiation. Blue traces: 0.5 µM **PNA-Am3**, 0 minutes light irradiation; red traces: 0.5 µM **PNA-Am3**, 60 minutes light irradiation; green traces: 0.5 µM **PNA-Am3**, 0.5 µM RB, 2 minutes light irradiation.

96-well plate functionalization

96-well plate functionalization was performed on Pierce 8-well strips, Maleic Anhydride Activated Plates (Thermo). 100 µL of a 500 nM **PNA-Fur5** (or **PNA-Am2** as positive control) solution in 100 mM carbonate buffer pH 9.0 containing 20% acetonitrile and 0.001% SDS were added to each pre-activated well and left to react overnight. The wells were then drained and washed with block solution (50mM ethanolamine in 100 mM carbonate buffer pH 9.0, 2x 2 minutes). The remaining active esters were then quenched by incubation with 300 µL of blocking solution for 2 hours. The wells were then drained and washed with 0.01% SDS (2x 2 minutes), 0.001% SDS (2x 2 minutes) and mQ water. Surfaces were dried and stored in a desiccator until use.

96-well plate ligation

Oligonucleotides and PNA solutions were freshly prepared in PBS pH 7.4 supplemented with 0.001% SDS (PBS-S) from 10 µM stock solutions in mQ. Surfaces where pre-wetted for 30 minutes with a 0.001% SDS solution. Then, 50 µL of oligonucleotides and 50 µL of 1 µM PNA solution were allowed to equilibrate in the well for 1h at 40°C before light irradiation. The strip was placed on top of the light setup and irradiated for 1h. The strip where then left to react overnight before wash and quantification of attached biotin, using 100 µL of 20 ng/mL Pierce High Sensitivity NeutrAvidin-

HRPconjugate (Thermo Scientific) and 1-step Ultra TMB-ELISA (Thermo Scientific) as reagent solution. Final readout of the oxidized TMB was performed monitoring the absorption at 450 nm.

96-well plate – optimization of washing steps

The ligation was performed following the reported protocol using 100 nM **DNA-3**. After probe reaction, the wells were drained and manually washed following different protocols, before the biotin detection.
Protocol A: 4 x 5 minutes with PBS pH 7.4 supplemented with 0.005 % Tween 20 (PBS-T), 45°C;
Protocol B: 4 x 5 minutes with MeCN:mQ 1:1 and final rinse with PBS-T, 45°C;
Protocol C: 2 x 5 minutes with formamide, 2 x 5 minutes with MeCN:mQ 1:1 + 7M Urea, 2x5 minutes MeCN:mQ 1:1, and final rinse with PBS-T, 45°C.

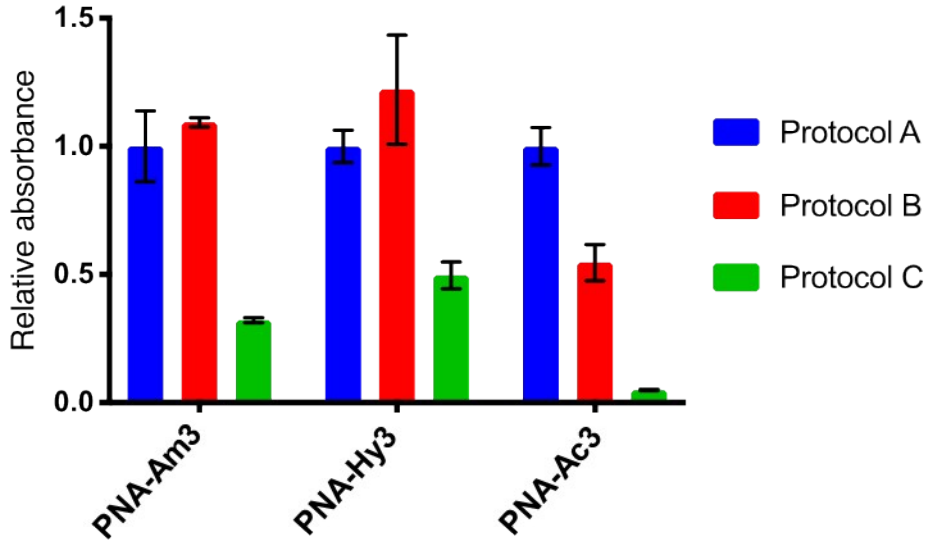

Figure S44: relative biotin detection signals obtained from **DNA-3** templated ligation in presence of **PNA-Am3**, **PNA-Hy3**, and **PNA-Ac3** after the different washing protocols. Each set of data is normalized to the protocol A signal.

96-well plate - sequence selectivity

The ligation was performed following the reported protocol using 200 nM oligonucleotides solutions and washing protocol C.

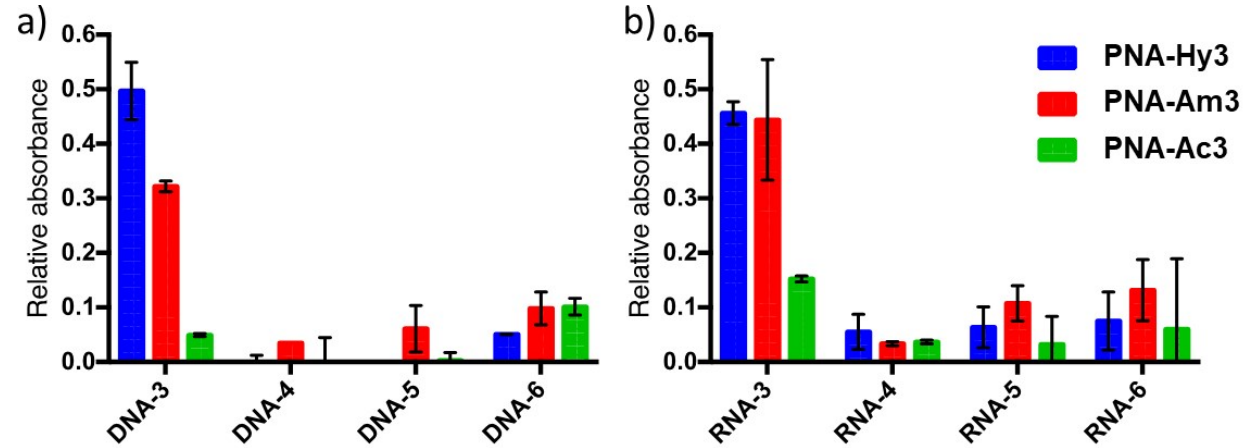

Figure S45: relative TMB_{ox} signal showing sequence selectivity of PNA-Am3, PNA-Hy3 and PNA-Ac3 for different DNA (a) and RNA (b) templates. Each dataset is normalized to the protocol A signal.

LOD calculation

For each nucleophile (Amine and Hydrazine) and probe type (DNA and RNA), a calibration curve was built by plotting the absorbance values at various concentrations (5, 15, 25, 50, 100 nM). Data were fitted by linear regression analysis. LOD for each system was calculated from the calibration curves, using the formula:

$$LOD = 3.3 \times \left(\frac{SD_y}{m}\right) \qquad (7)$$

Where SD_y is the standard deviation of the response (standard deviation of y-intercepts of regression lines) and m is the slope of the calibration curve.

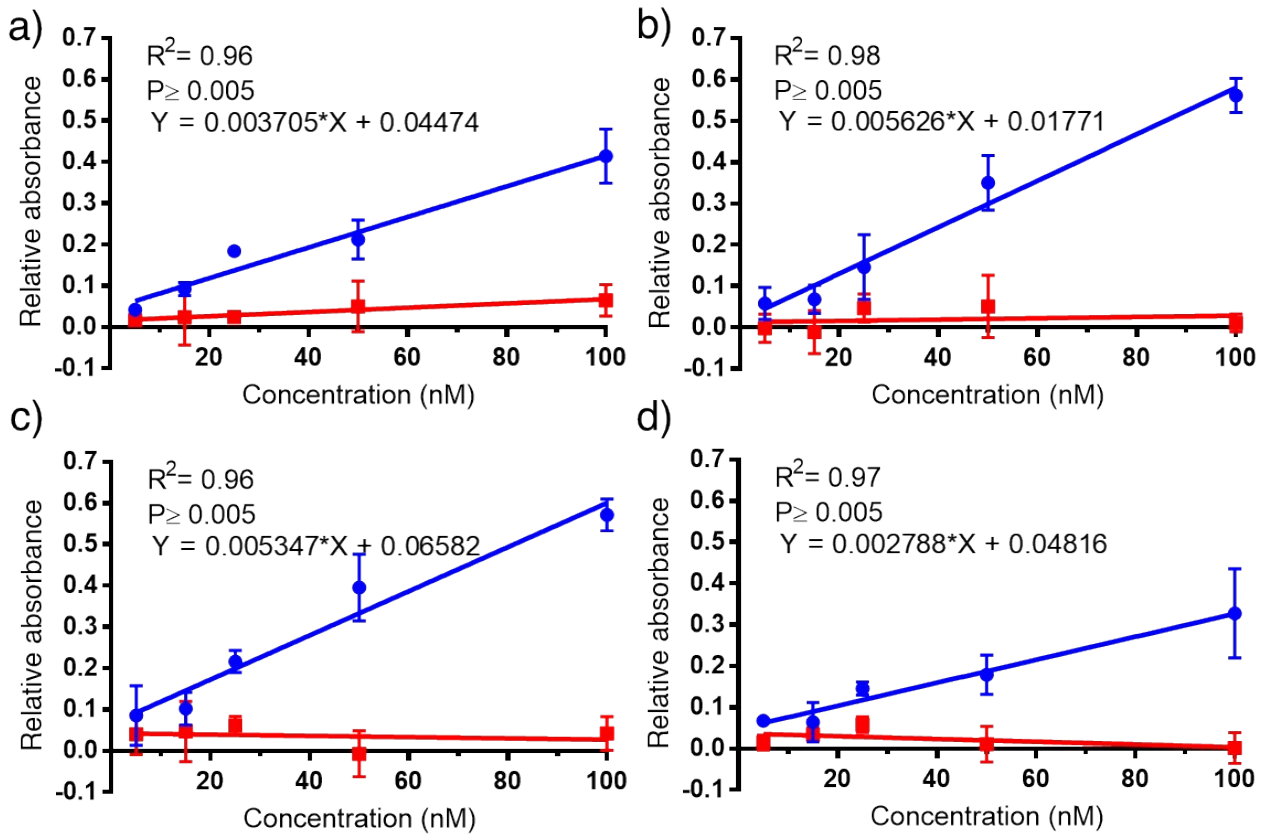

Figure S46: calibration curves for surface templated ligation in presence of fully matching **DNA-3** (blue line in a and b) or **RNA-3** (blue line in c and d) or fully scrambled **DNA-6** (red line in a and b) or **RNA-6** (red line in c and d), in presence of **PNA-Am3** (a and c) or **PNA-Hy3** (b and d). Data are fitted by linear regression analysis.

Table S9: Calculation of LOD of the tested systems. Calculations are based on the experiments shown in Figure S46.

System	SD_y	m ($\cdot 10^{-3}$)	LOD (nM)
DNA-3 + PNA-Am3	0.022	3.705	19.60
DNA-3 + PNA-Hy3	0.027	5.626	15.84
RNA-3 + PNA-Am3	0.033	5.347	20.37
RNA-3 + PNA-Hy3	0.015	2.788	17.75

Preliminary experiment on microarray slides

XL-CX slides (XanTec bioanalytics, Duesseldorf, Germany) were functionalized by spotting of 0.3 µL of a 1 µM (or 200 nM) PNA solution in 100 mM carbonate buffer pH 9.0 containing 30% glycol and 0.001% SDS. Coupling was performed by storing the slides overnight in a humid chamber (75% relative humidity), and the remaining reactive sites where quenched for 2h with a 6% ethanolamine solution. Slides were then washed for 10 minutes with 0.01% SDS, 0.001% SDS and mQ. Surfaces were dried and stored covered from light in a desiccator until use.
For the ligation experiment, oligonucleotide and PNA solutions were freshly prepared in PBS-S from a 10 µM stock solutions in mQ. Surfaces were pre-wetted for 30 minutes with a 0.001% SDS solution. A 16-well hybridization chamber equipped with silicone gasket was then placed on the surface and 50 µL of a solution containing 100 nM DNA and 100

nM PNA was allowed to hybridize for 1h at 40°C before light irradiation. The microarray slide was then place on top of the light setup and irradiated for 30'. The sealed slide was then left to react overnight. Image acquisition was performed using an Agilent G2565CA (green laser only) after weak (2 x 10 minutes with PBS-T) and strong washes (2 x 10 minutes with MeCN:mQ 1:1).

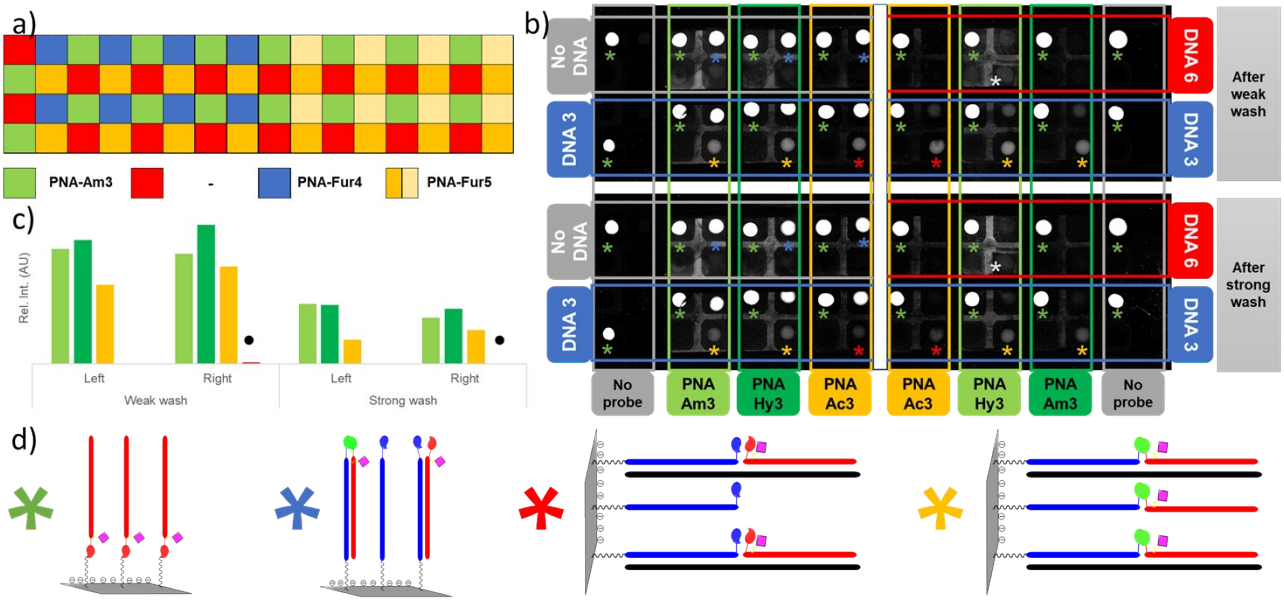

Figure S47: preliminary ligation experiments on glass microarray surfaces. (a) Scheme of the probes spotted on the surface; (b) picture of the microarray slide after weak and strong washes, with indication of the probes loaded before light irradiation; (c) relative signal intensity of spots marked with orange or red stars, red bars (very low, indicated in the graph with a black dot) indicate the signal obtained in the ligation experiment of the hydrazine probe PNA-Hy3 in presence of DNA-6 (white stars in panel b); (d) graphical explanation of the surface architecture for the positive control (green star), strong PNA:PNA hybridization that does not allow to distinguish between non- and ligated probes (blue star), non-ligated PNA_2:DNA complex (red star), and ligated PNA-PNA:DNA complex (orange star). DNA-3: fully matching template; DNA-6: scrambled sequence.

In brief, the microarray slide was divided in two distinct regions (as depicted in Figure S47a). In the left side we tested the possibility to discriminate between the formation of the ligation product from a stable complex in the PNA:PNA format. In the right side we wanted to evaluate the effect of PNA concentration during surface functionalization (light yellow square indicates 200 nM PNA solution for spotting, orange squares indicate 1 μM solution).
In addition, surface images were acquired both after weak as well as strong washes to determine whether part of the signal was attributed to a stable PNA_2:DNA complex rather than true PNA-PNA ligation product. As mentioned in the paper, the washing protocol still needs to be optimized, but the signal of the capped probe **PNA-Ac3** (yellow bars) clearly decreases as compared to the other two after strong washing conditions. This effect is evident in both sides of the slide.

13. Light irradiation setups

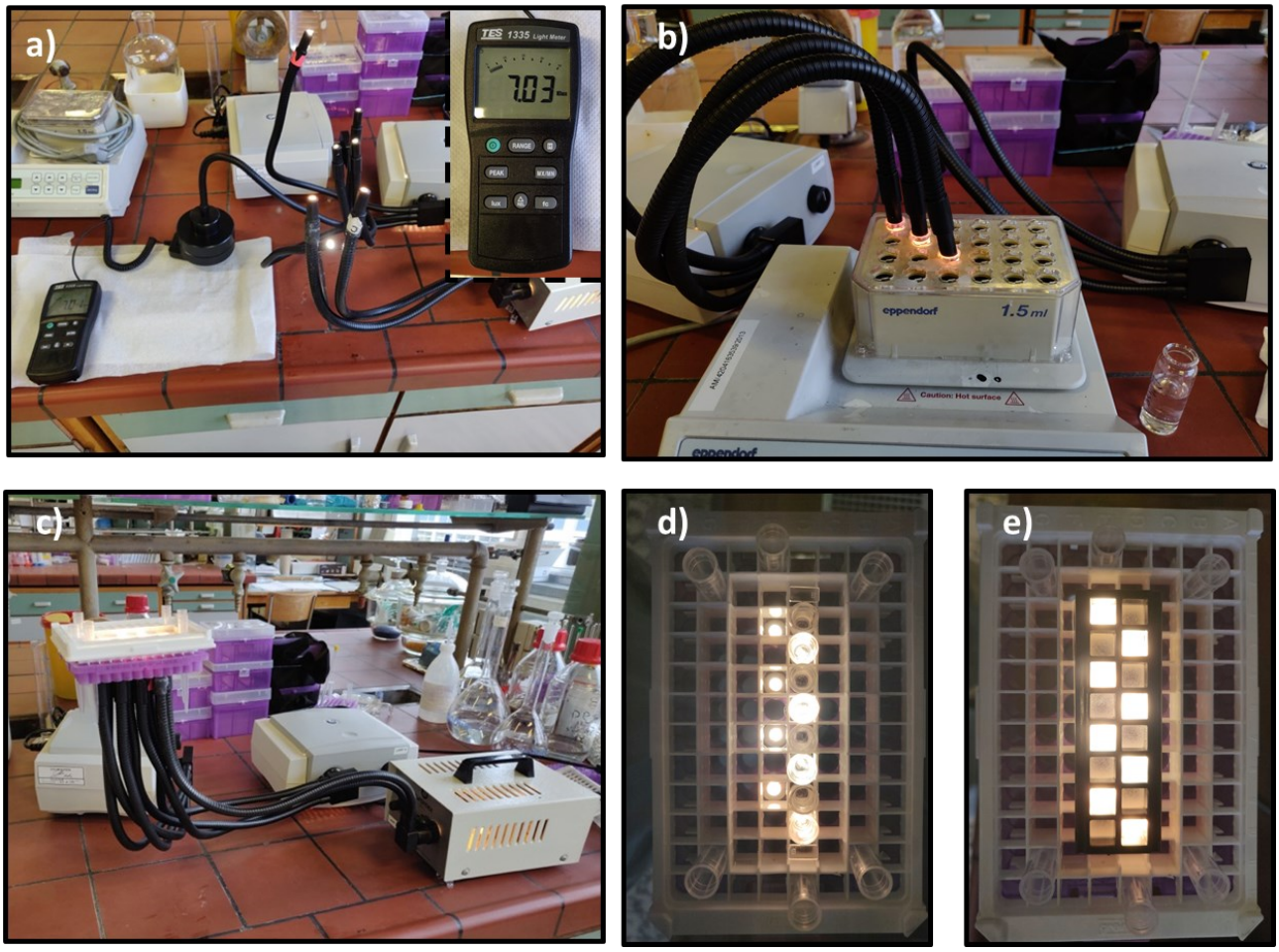

Figure S48: light intensity measurement (a); setup for solution ligation (b); setup for surface ligation (c); example of light irradiation with a 8-well strip (d); example of light irradiation on microarray slides (e).

14.Supporting References

1. Cadoni, E., Rosa-Gastaldo, D., Manicardi, A., Mancin, F., and Madder, A. (2020). Exploiting Double Exchange Diels-Alder Cycloadditions for Immobilization of Peptide Nucleic Acids on Gold Nanoparticles. Front. Chem. *8*, 1–7.
2. Díaz-Mochón, J.J., Bialy, L., and Bradley, M. (2004). Full orthogonality between Dde and Fmoc: The direct synthesis of PNA-peptide conjugates. Org. Lett. *6*, 1127–1129.
3. Chouikhi, D., Ciobanu, M., Zambaldo, C., Duplan, V., Barluenga, S., and Winssinger, N. (2012). Expanding the Scope of PNA-Encoded Synthesis (PES): Mtt-Protected PNA Fully Orthogonal to Fmoc Chemistry and a Broad Array of Robust Diversity-Generating Reactions. Chem. - A Eur. J. *18*, 12698–12704.
4. Dodd, D.W., and Hudson, R.H.E. (2007). Analysis and purification of peptide nucleic acids by denaturing PAGE. Electrophoresis *28*, 3884–3889.
5. Pavlova, A.S., Dyudeeva, E.S., Kupryushkin, M.S., Amirkhanov, N. V., Pyshnyi, D. V., and Pyshnaya, I.A. (2018). SDS-PAGE procedure: Application for characterization of new entirely uncharged nucleic acids analogs. Electrophoresis *39*, 670–674.
6. Elskens, J., Manicardi, A., Costi, V., Madder, A., and Corradini, R. (2017). Synthesis and Improved Cross-Linking Properties of C5-Modified Furan Bearing PNAs. Molecules *22*, 2010.
7. Manicardi, A., Gyssels, E., Corradini, R., and Madder, A. (2016). Furan-PNA: a mildly inducible irreversible interstrand crosslinking system targeting single and double stranded DNA. Chem. Commun. (Camb). *52*, 6930–3.
8. Gandin, E., Lion, Y., and Van de Vorst, A. (1983). Quantum Yield of Singlet Oxygen Production By Xanthene Derivatives. Photochem. Photobiol. *37*, 271–278.
9. Stracke, F., Heupel, M., and Thiel, E. (1999). Singlet molecular oxygen photosensitized by Rhodamine dyes: correlation with photophysical properties of the sensitizers. J. Photochem. Photobiol. A Chem. *126*, 51–58.
10. Decoene, K., Vannecke, W., Passioura, T., Suga, H., and Madder, A. (2018). Pyrrole-Mediated Peptide Cyclization Identified through Genetically Reprogrammed Peptide Synthesis. Biomedicines *6*, 99.
11. Sen, A., and Nielsen, P.E. (2007). On the stability of peptide nucleic acid duplexes in the presence of organic solvents. Nucleic Acids Res. *35*, 3367–3374.
12. Tomac, S., Sarkar, M., Ratilainen, T., Wittung, P., Nielsen, P.E., Norden, B., and Graslund, A. (1996). Ionic effects on the stability and conformation of peptide nucleic acid complexes. J. Am. Chem. Soc. *118*, 5544–5552.
13. Adarsh, N., Avirah, R.R., and Ramaiah, D. (2010). Tuning photosensitized singlet oxygen generation efficiency of novel Aza-BODIPY dyes. Org. Lett. *12*, 5720–5723.
14. Hoebeke, M., and Damoiseau, X. (2002). Determination of the singlet oxygen quantum yield of bacteriochlorin a: A comparative study in phosphate buffer and aqueous dispersion of dimiristoyl-L-α-phosphatidylcholine liposomes. Photochem. Photobiol. Sci. *1*, 283–287.
15. Birtalan, E., Rudat, B., Kölmel, D.K., Fritz, D., Vollrath, S.B.L., Schepers, U., and Bräse, S. (2011). Investigating rhodamine B-labeled peptoids: scopes and limitations of its applications. Biopolymers *96*, 694–701.

15. Raw surface ligation data

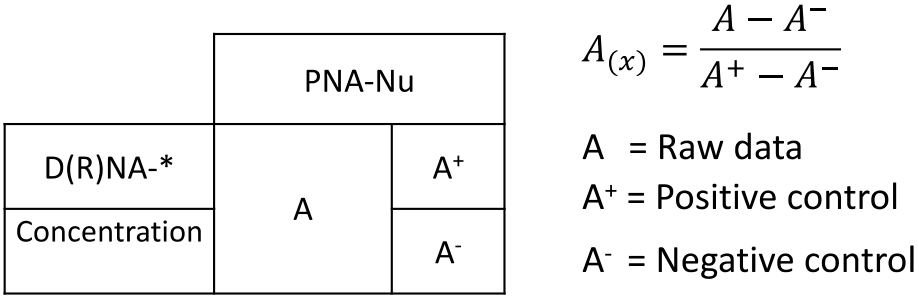

Figure S49: scheme illustrating how data are elaborated, using the reported equation.

Table S10: sequence selectivity test of **PNA-Hy3**, **PNA-Am3** and **PNA-Ac3** in presence of **DNA-3÷6** and **RNA-3÷6** (related to Figure S45: relative TMBox signal showing sequence selectivity of PNA-Am3, PNA-Hy3 and PNA-Ac3 for different DNA (a) and RNA (b) templates. Each dataset is normalized to the protocol A signal.Figure S45 and Figure 9B of the manuscript).

	PNA-Hy3				PNA-Am3				PNA-Ac3			
DNA-3	3.05	5.16	2.94	5.18	3.05	5.16	2.94	5.18	3.05	5.16	2.94	5.18
200		1.17		1.17		1.17		1.17		1.17		1.17
DNA-4	1.48	5.16	1.3	5.18	1.48	5.16	1.3	5.18	1.48	5.16	1.3	5.18
200		1.17		1.17		1.17		1.17		1.17		1.17
DNA-5	1.7	5.16	1.38	5.18	1.31	5.25	1.95	5.03	1.52	5.15	1.35	5.16
200		1.17		1.17		1.12		1.12		1.04		1.04
DNA-6	1.62	5.16	1.32	5.18	1.62	5.16	1.32	5.18	1.62	5.16	1.32	5.18
200		1.17		1.17		1.17		1.17		1.17		1.17
RNA-3	5.25	9.12	5.5	8.59	3.74	8.46	4.02	9.02	2.32	9.99	2.26	9.5
200		1.96		1.96		1.77		1.77		1.72		1.72
RNA-4	2.01	9.12	1.84	8.59	1.81	8.46	1.83	9.02	1.38	9.99	2.1	9.5
200		1.96		1.96		1.77		1.77		1.72		1.72
RNA-5	2.37	9.12	2.25	8.59	2.51	8.46	2.61	9.02	1.93	9.99	2.06	9.5
200		1.96		1.96		1.77		1.77		1.72		1.72
RNA-6	2.32	9.12	2.3	8.59	2.1	8.46	2.46	9.02	2.82	9.99	2.59	9.5
200		1.96		1.96		1.77		1.77		1.72		1.72

Table S11: concentration optimization of **PNA-Am3** in presence **of DNA(RNA)-3** and **DNA(RNA)-6** (related to Figure S46 and Figure 9C of the manuscript).

	PNA-Am3 + DNA						PNA-Am3 + RNA					
*NA-3	1.22	5.15	1.07	5.21	1.16	5.87		8.85	3.03	8.13	1.86	7.79
5		1.01		0.95		0.92	2.19	1.75		2.01		1.69
*NA-6	1.04	5.15	1.09	5.21	0.97	5.87	1.64	8.85	2.35	8.13	2.18	7.79
5		1.01		0.95		0.92		1.75		2.01		1.69
*NA-3	1.34	5.15	1.42	5.21	1.54	5.87	2.58	8.85	2.82	8.13	2.88	7.79
15		1.01		0.95		0.92		1.75		2.01		1.69
*NA-6	0.81	5.15	1.1	5.21	1.35	5.87	2.56	8.85	1.82	8.13	2.04	7.79
15		1.01		0.95		0.92		1.75		2.01		1.69
*NA-3	1.77	5.15	1.7	5.21	1.88	5.87	3.5	8.85	3.2	8.13	2.96	7.79
25		1.01		0.95		0.92		1.75		2.01		1.69
*NA-6	1.09	5.15	1.05	5.21	1.08	5.87	2.35	8.85	2.26	8.13	2.05	7.79
25		1.01		0.95		0.92		1.75		2.01		1.69
*NA-3	1.54	4.98	1.71	5.76	1.87	4.79	4.72	8.28	3.75	7.74	3.85	6.73
50		1.01		0.95		0.92		1.75		2.01		1.69
*NA-6	1.08	4.98	1.01	5.76	1.39	4.79	2.03	8.28	1.62	7.74	1.71	6.73
50		1.01		0.95		0.92		1.75		2.01		1.69
*NA-3	2.67	4.98	2.62	5.76	2.77	4.79	5.23	8.28	4.14	7.74	4.77	6.73
100		1.01		0.95		0.92		1.75		2.01		1.69
*NA-6	1.16	4.98	1.18	5.76	1.34	4.79	2.18	8.28	1.98	7.74	2.02	6.73
100		1.01		0.95		0.92		1.75		2.01		1.69
*NA-3	2.45	4.98	2.39	5.76	2.47	4.79	4.51	8.28	4.39	7.74	4.5	6.73
200		1.01		0.95		0.92		1.75		2.01		1.69
*NA-6	1.02	4.98	1.07	5.76	0.92	4.79	2.21	8.28	2.02	7.74	2.12	6.73
200		1.01		0.95		0.92		1.75		2.01		1.69

Table S12: concentration optimization of **PNA-Hy3** in presence **of DNA(RNA)-3** and **DNA(RNA)-6** (related to Figure S46 and Figure 9C of the manuscript).

	PNA-Hy3 + DNA						PNA-Hy3 + RNA					
*NA-3 5	1.52	8.67 1.52	1.62	7.6 1.1	1.59	7.26 1.09	2.9	10.12 2.31	2.80	10.43 2.25	2.45	10.46 1.94
*NA-6 5	1.62	8.67 1.52	1.3	7.6 1.1	0.86	7.26 1.09	1.48	10.12 2.31	2.48	10.43 2.25	1.89	10.46 1.94
*NA-3 15	1.53	8.67 1.52	1.64	7.6 1.1	1.66	7.26 1.09	2.7	10.12 2.31	3.21	10.43 2.25	2.79	10.46 1.94
*NA-6 15	1.73	8.67 1.52	1.42	7.6 1.1	0.82	7.26 1.09	2.73	10.12 2.31	2.44	10.43 2.25	2.16	10.46 1.94
*NA-3 25	1.24	8.67 1.52	1.97	7.6 1.1	2.51	7.26 1.09	3.5	10.12 2.31	3.29	10.43 2.25	3.28	10.46 1.94
*NA-6 25	2.06	8.67 1.52	1.6	7.6 1.1	1.42	7.26 1.09	2.6	10.12 2.31	2.83	10.43 2.25	2.51	10.46 1.94
*NA-3 50	1.59	8.07 1.52	3.05	5.79 1.1	2.97	7.73 1.09	4.14	10.12 2.25	3.68	10.49 2.25	3.10	10.53 1.94
*NA-6 50	3.83	8.07 1.52	1.47	5.79 1.1	1.81	7.73 1.09	2.12	10.12 2.25	2.23	10.49 2.25	2.45	10.53 1.94
*NA-3 100	5.33	8.07 1.52	3.51	5.79 1.1	5.01	7.73 1.09	5.82	10.12 2.25	4.07	10.49 2.25	4.74	10.53 1.94
*NA-6 100	1.43	8.07 1.52	1.22	5.79 1.1	1.23	7.73 1.09	2.2	10.12 2.25	2.04	10.49 2.25	2.32	10.53 1.94
*NA-3 200	2.7	8.07 1.52	2.24	5.79 1.1	2.54	7.73 1.09	5.05	10.12 2.25	4.00	10.49 2.25	5.64	10.53 1.94
*NA-6 200	1.45	8.07 1.52	1.24	5.79 1.1	1.58	7.73 1.09	2.3	10.12 2.25	2.23	10.49 2.25	2.35	10.53 1.94

Table S13: washing optimization protocols A and B in presence of **DNA-3** and **PNA-Hy3**, **PNA-Am3** and **PNA-Ac3** (related to Figure S44).

	Protocol-A						Protocol-B					
PNA-Hy3	5.49	7.59	6.00	7.59	7.61	7.59	6.07	6.68	4.65	6.68	6.4	6.68
		0.33		0.33		0.33		0.38		0.38		0.38
PNA-Am3	5.73	7.5	7.20	7.5	8.58	7.5	5.74	5.81	5.65	5.81	5.83	5.81
		0.7		0.7		0.7		0.9		0.9		0.9
PNA-Ac3	5.03	7.33	7.27	7.33	8.09	7.33	3.73	6.23	4.03	6.23	4.54	6.23
		0.44		0.44		0.44		0.95		0.95		0.95

16.NMR spectra

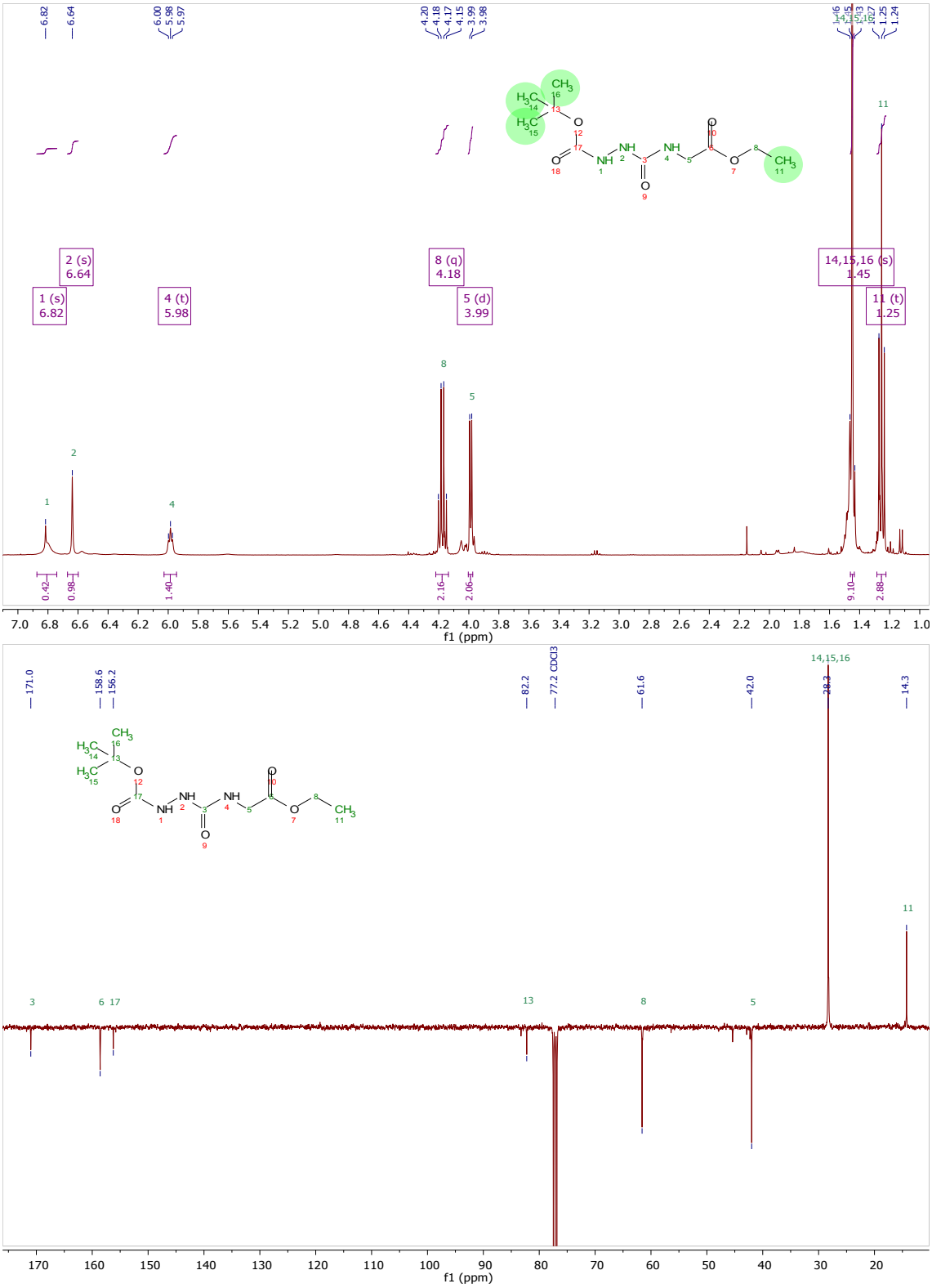

Figure S50: ^{1}H-NMR and ^{13}C-NMR of compound **S2**.

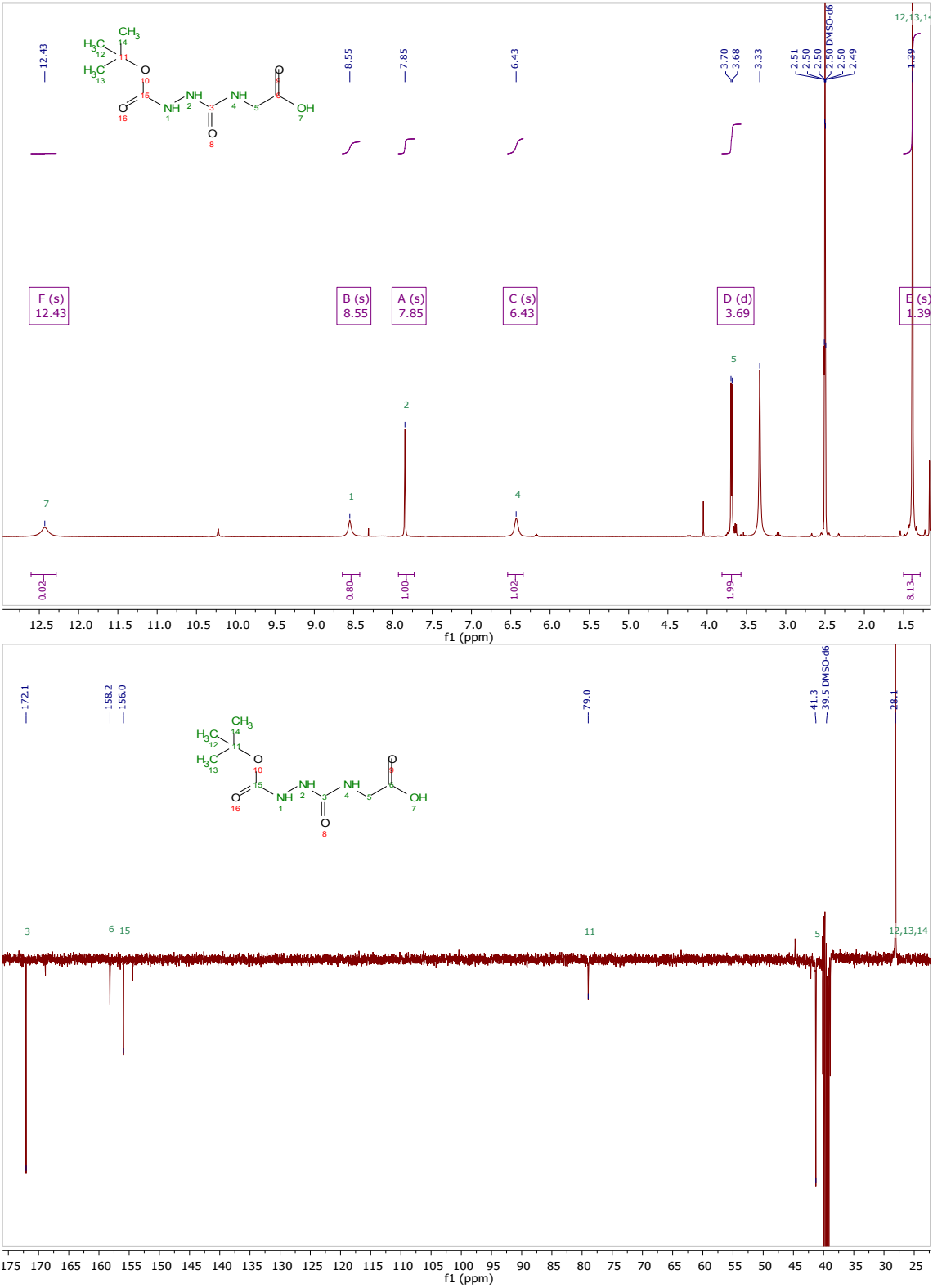

Figure S51: ^{1}H-NMR and ^{13}C-NMR of compound **S3**.

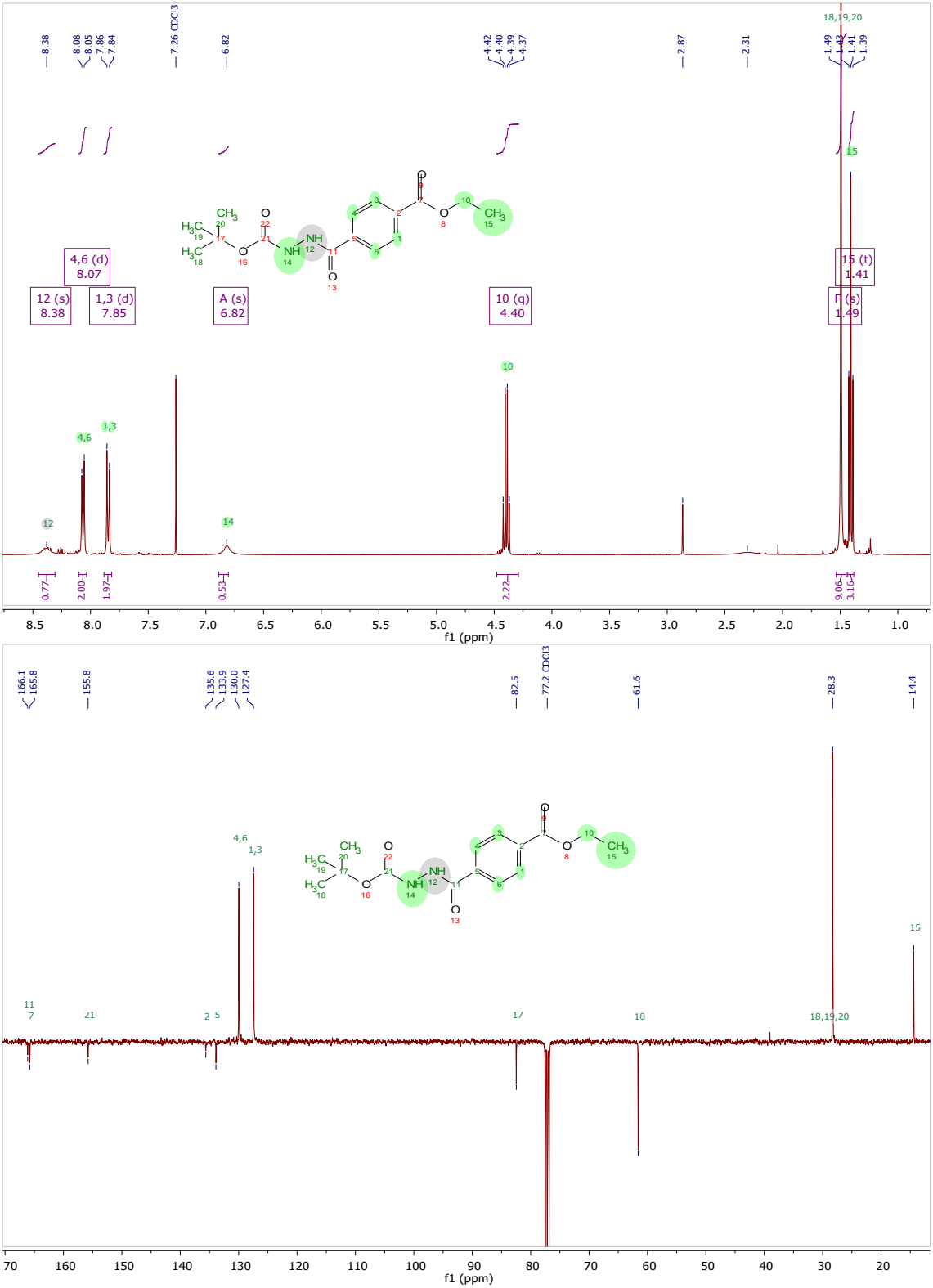

Figure S52: ^{1}H-NMR and ^{13}C-NMR of compound **Z2**.

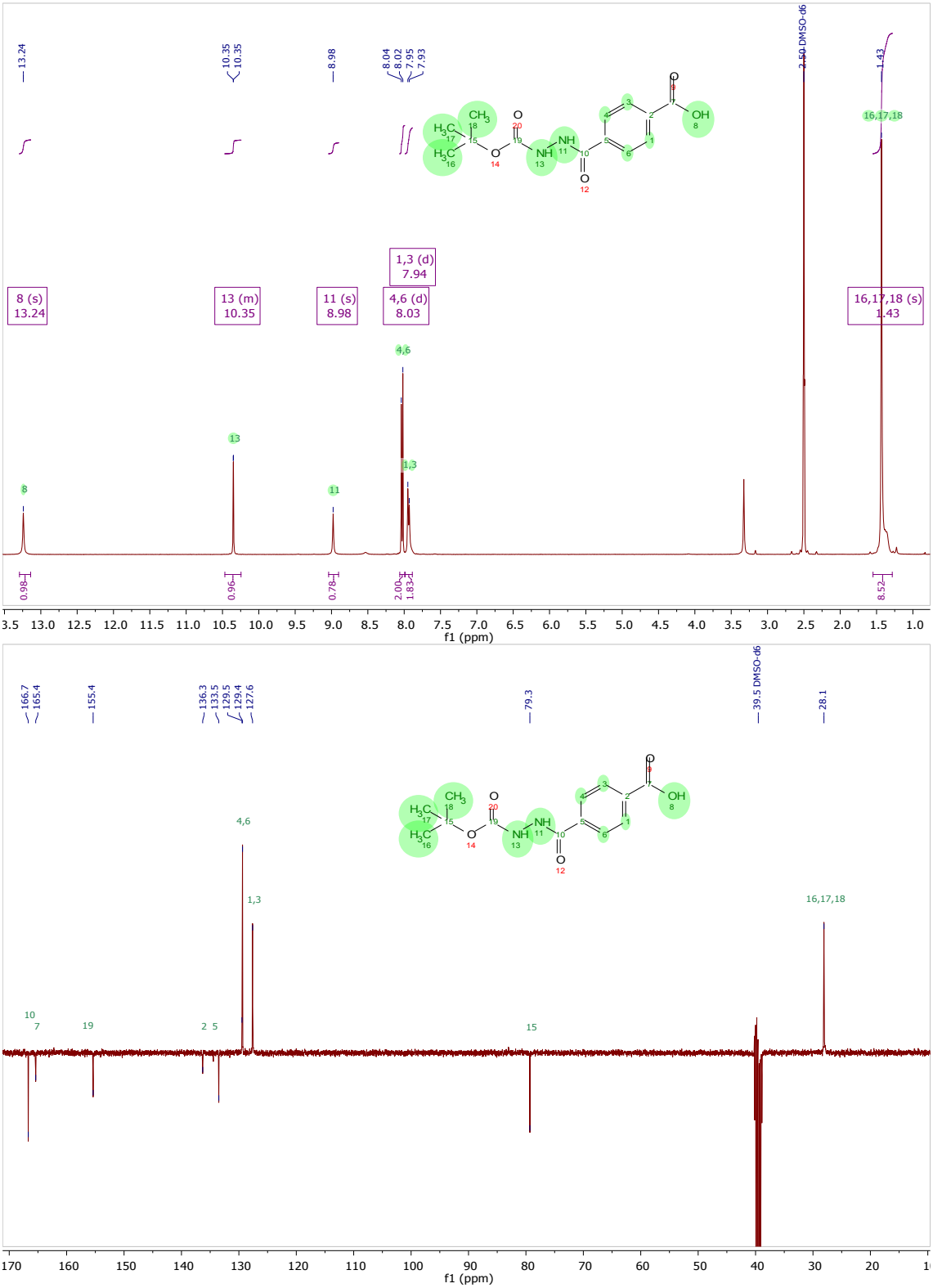

Figure S53: ^{1}H-NMR and ^{13}C-NMR of compound **Z3**.

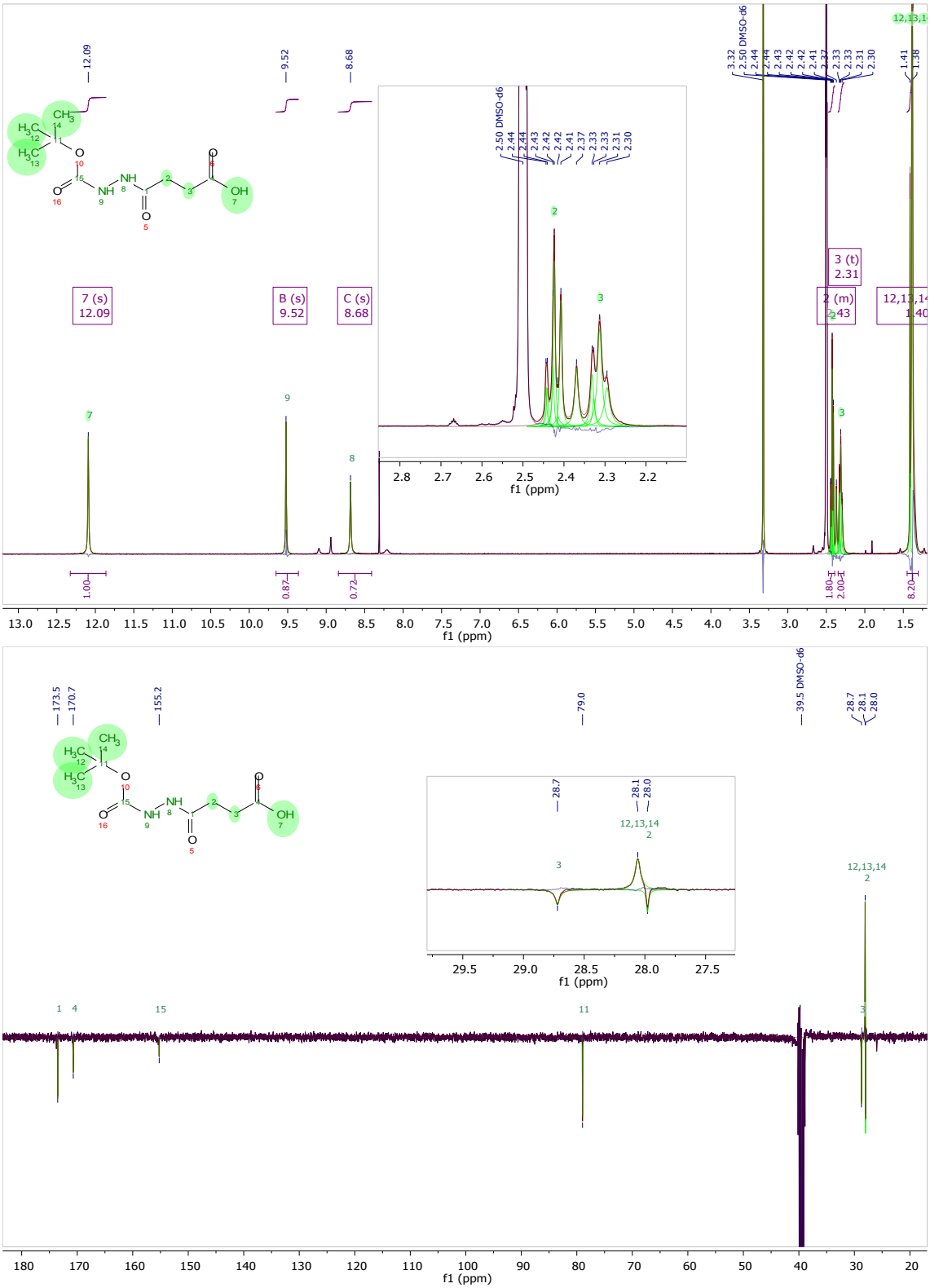

Figure S54: ^{1}H-NMR and ^{13}C-NMR of compound **Z5**.

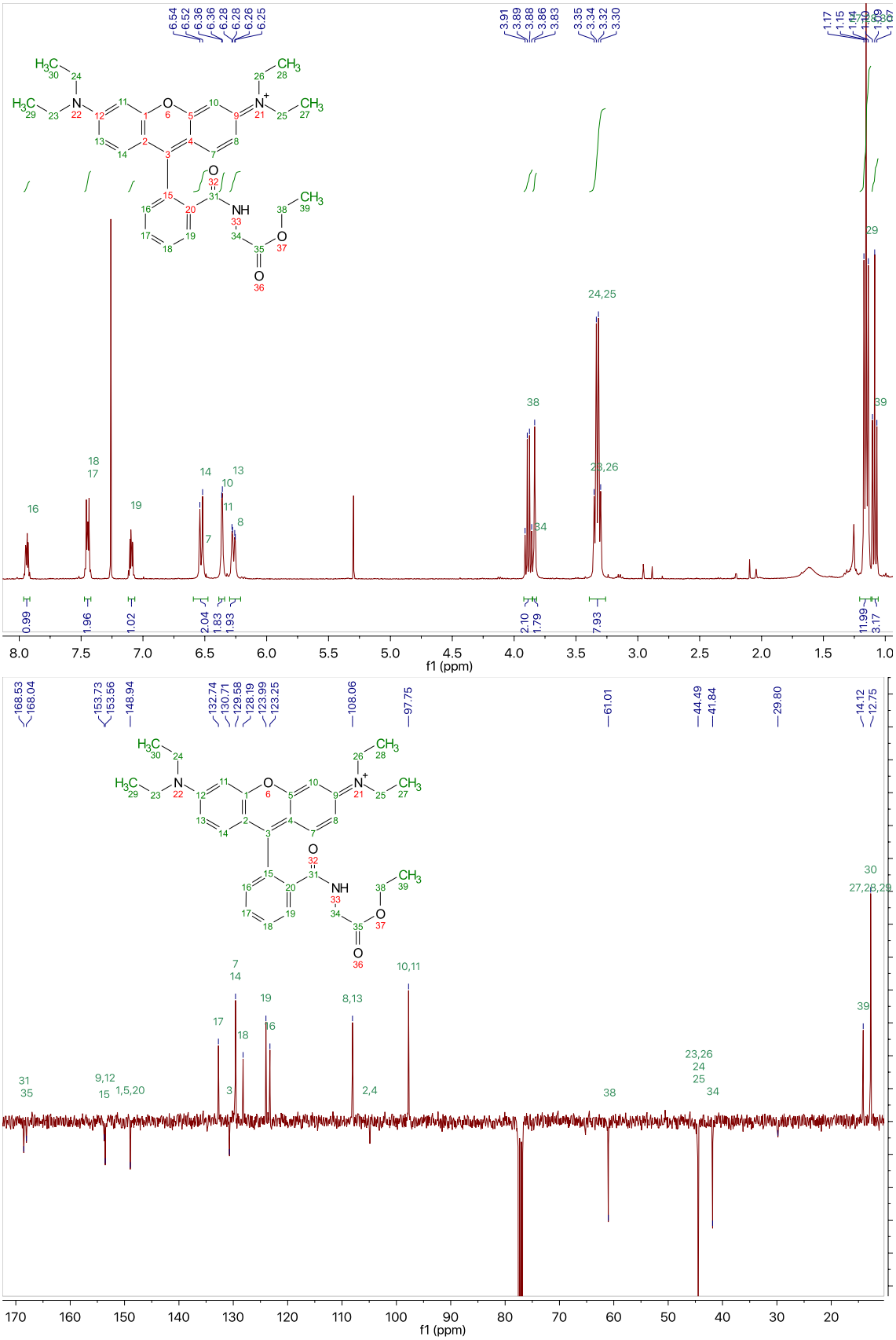

Figure S55: H-NMR and ^{13}C-NMR of compound **Rhob-1**.

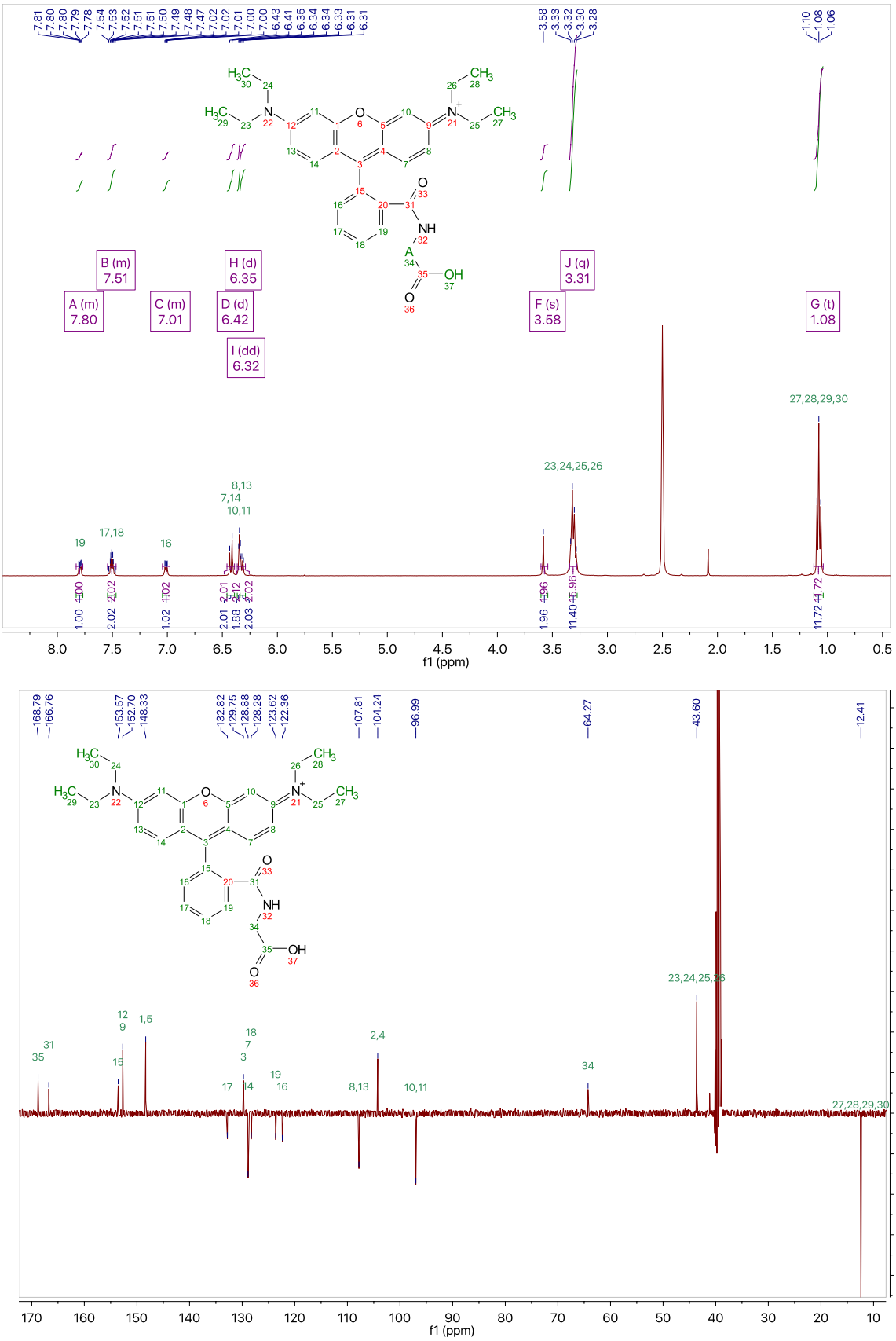

Figure S56: ^{1}H-NMR and ^{13}C-NMR of compound **Rhob-2**.

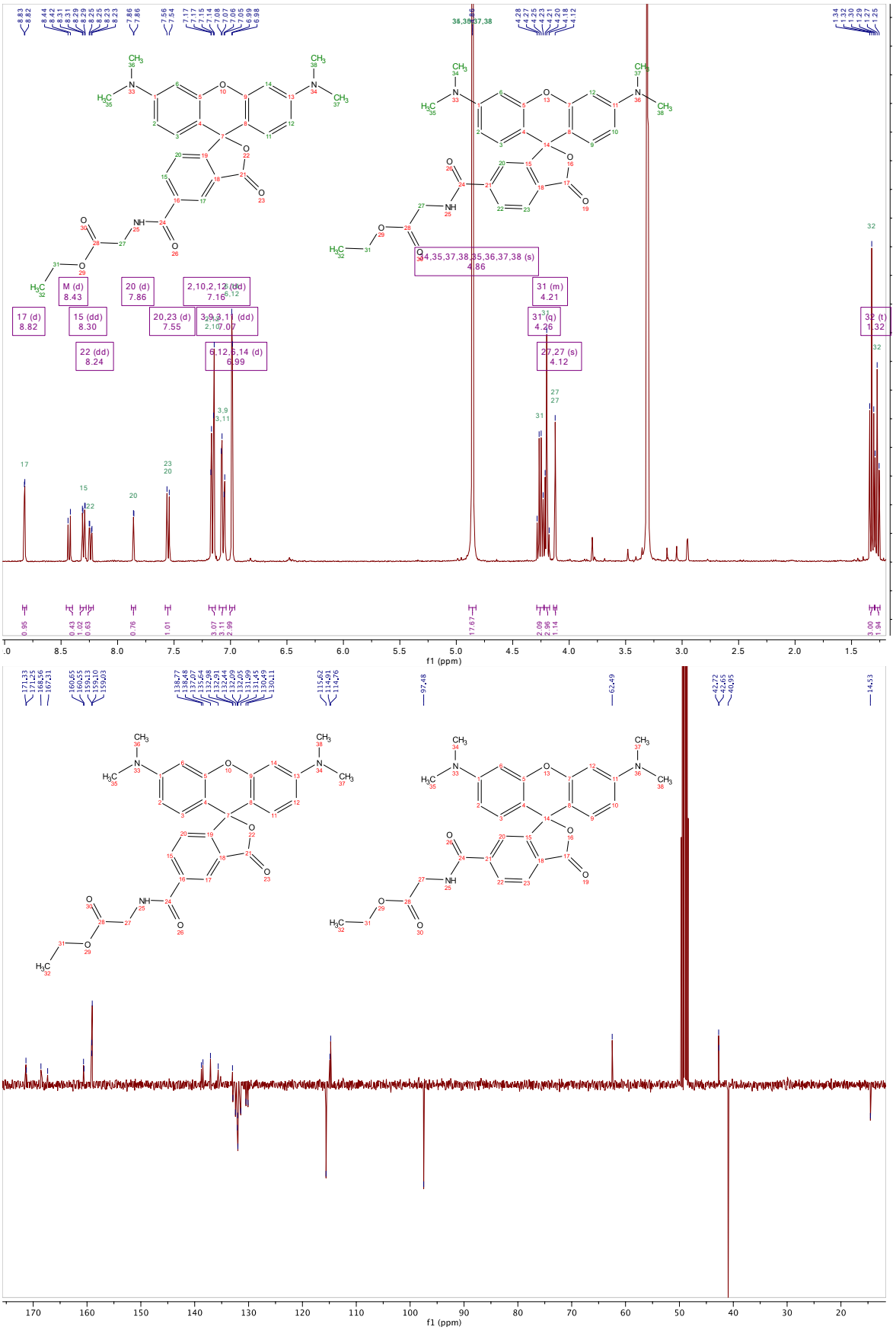

Figure S57: ^{1}H-NMR and ^{13}C-NMR of compound **TAMRA-1.**

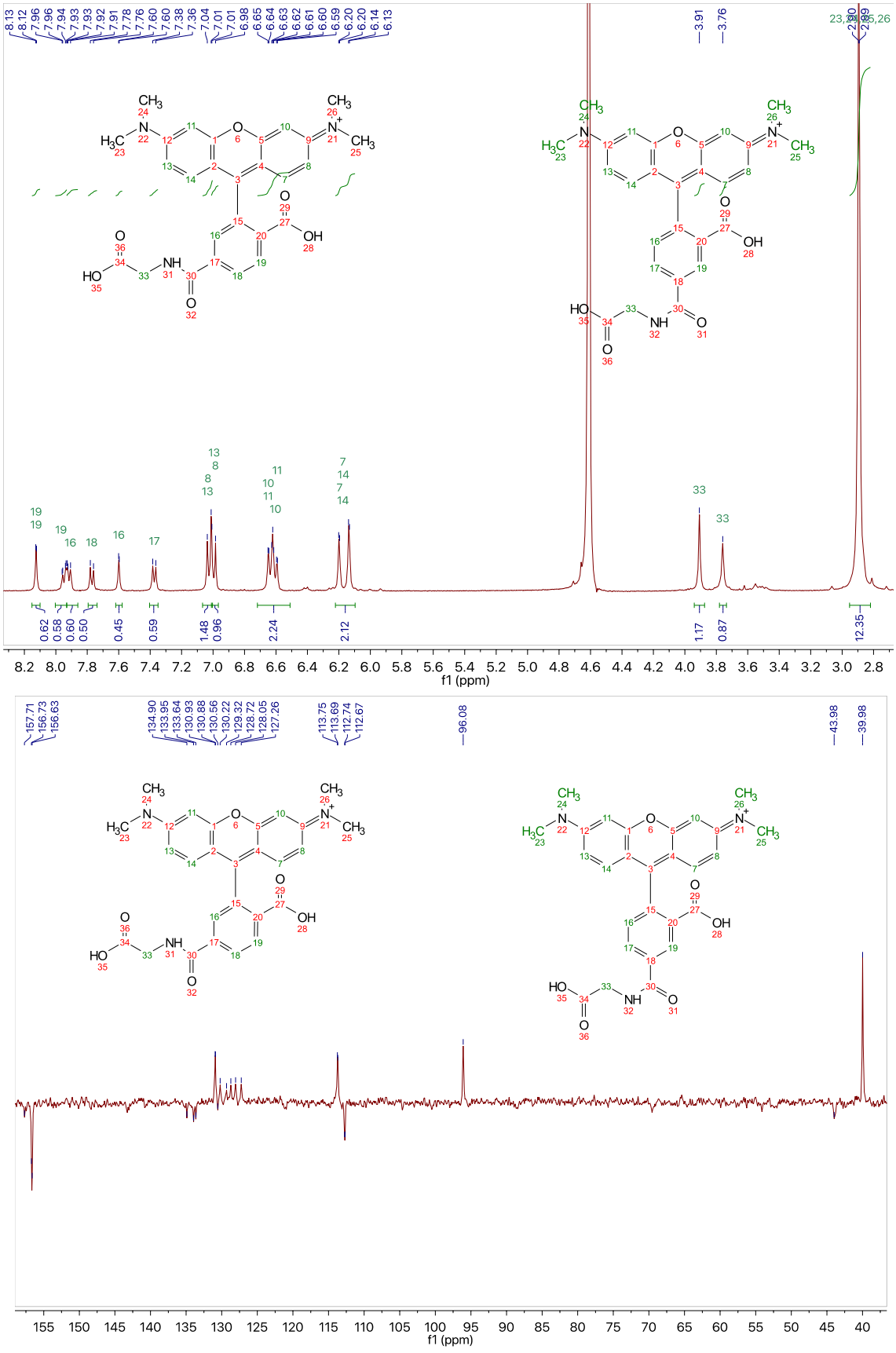

Figure S58: ^{1}H-NMR and ^{13}C-NMR of compound **TAMRA-2**.

17. HPLC-MS chromatograms of pure PNAs

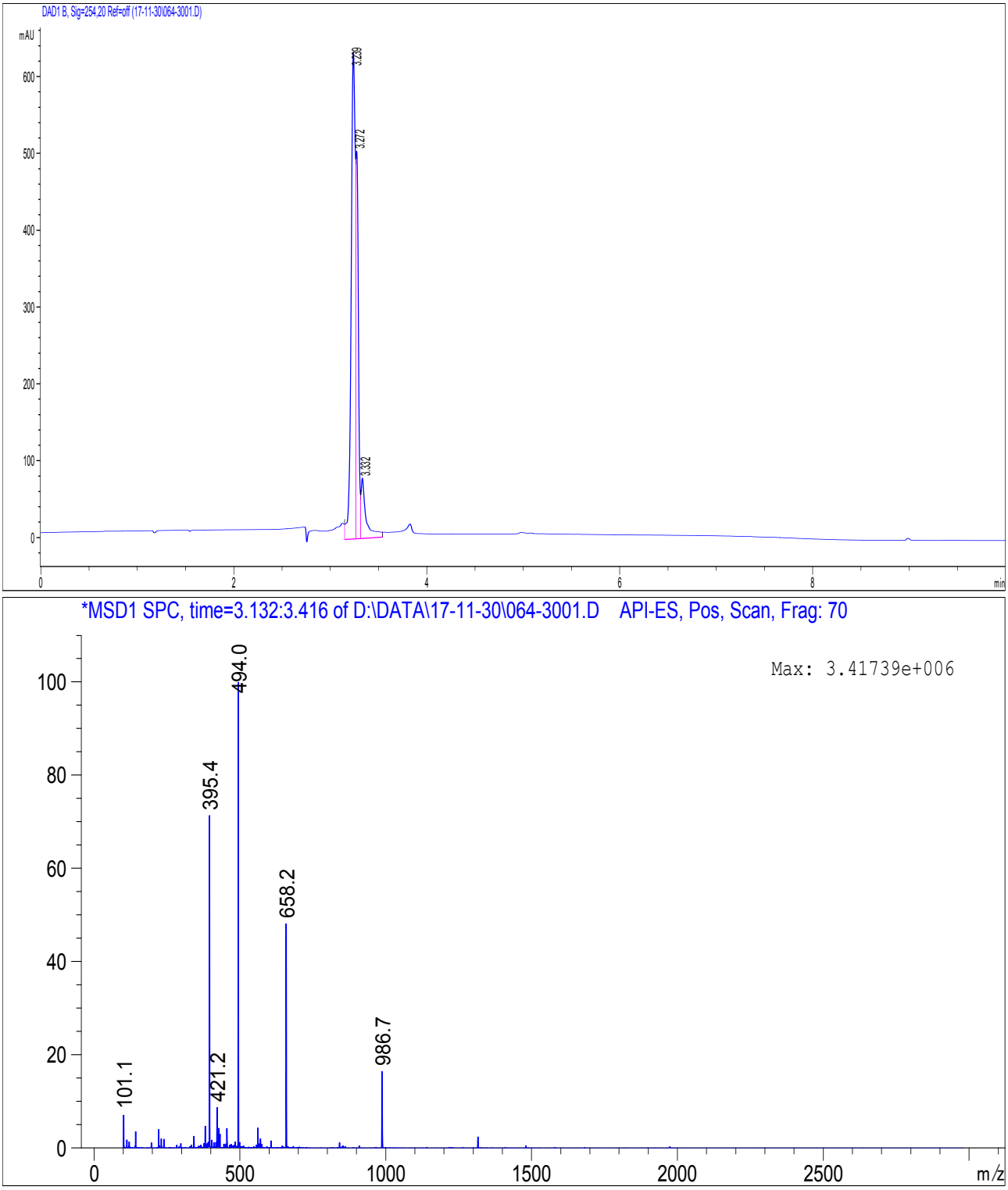

Figure S59: HPLC-MS chromatogram of purified **PNA-Fur0-5mer**. HPLC-UV trace at 254 nm (top) and MS spectrum of the corresponding peak (bottom). Calcd MW: 1972.05.

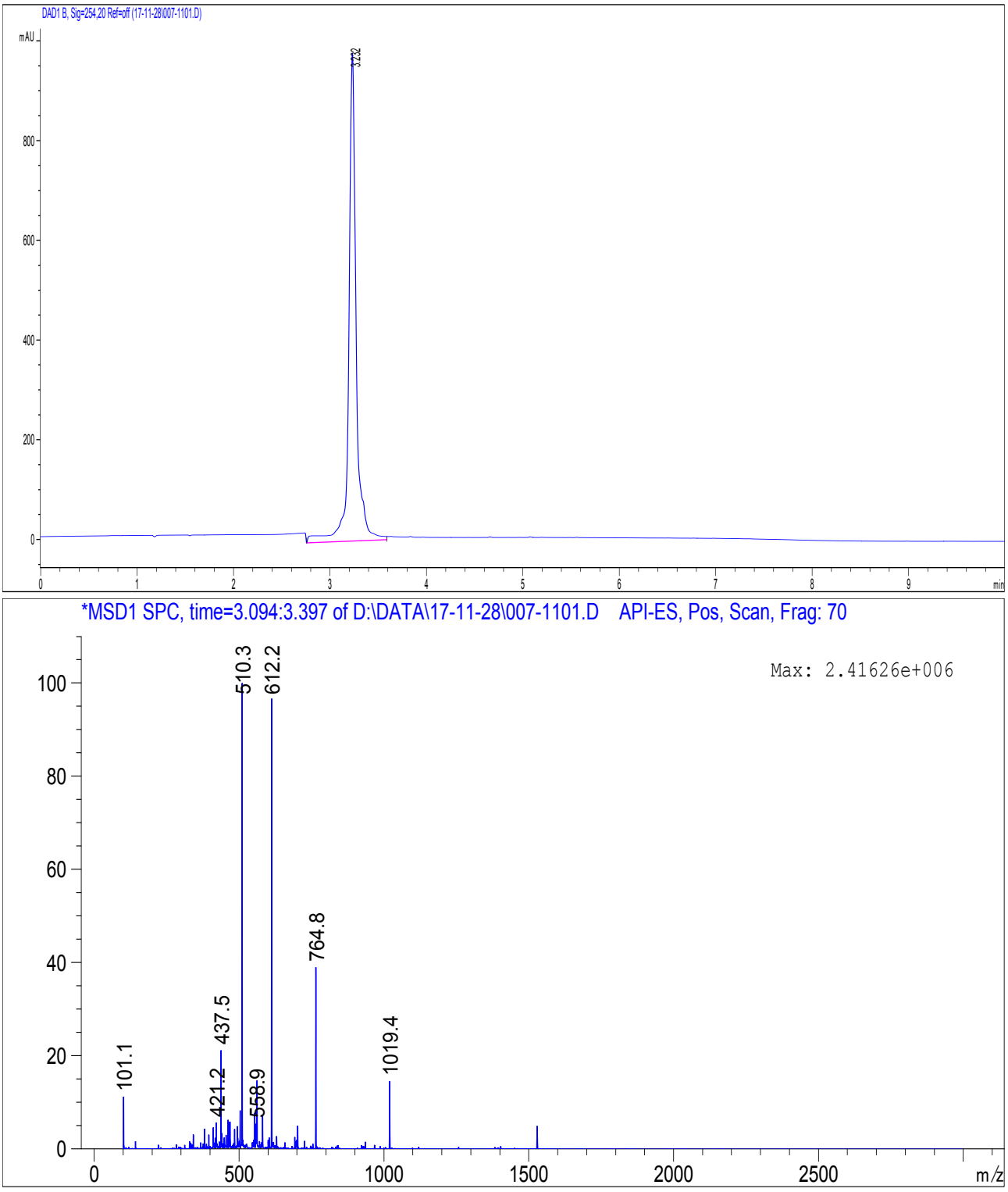

Figure S60: HPLC-MS chromatogram of purified **PNA-Fur0-9mer**. HPLC-UV trace at 254 nm (top) and MS spectrum of the corresponding peak (bottom). Calcd MW: 3056.10.

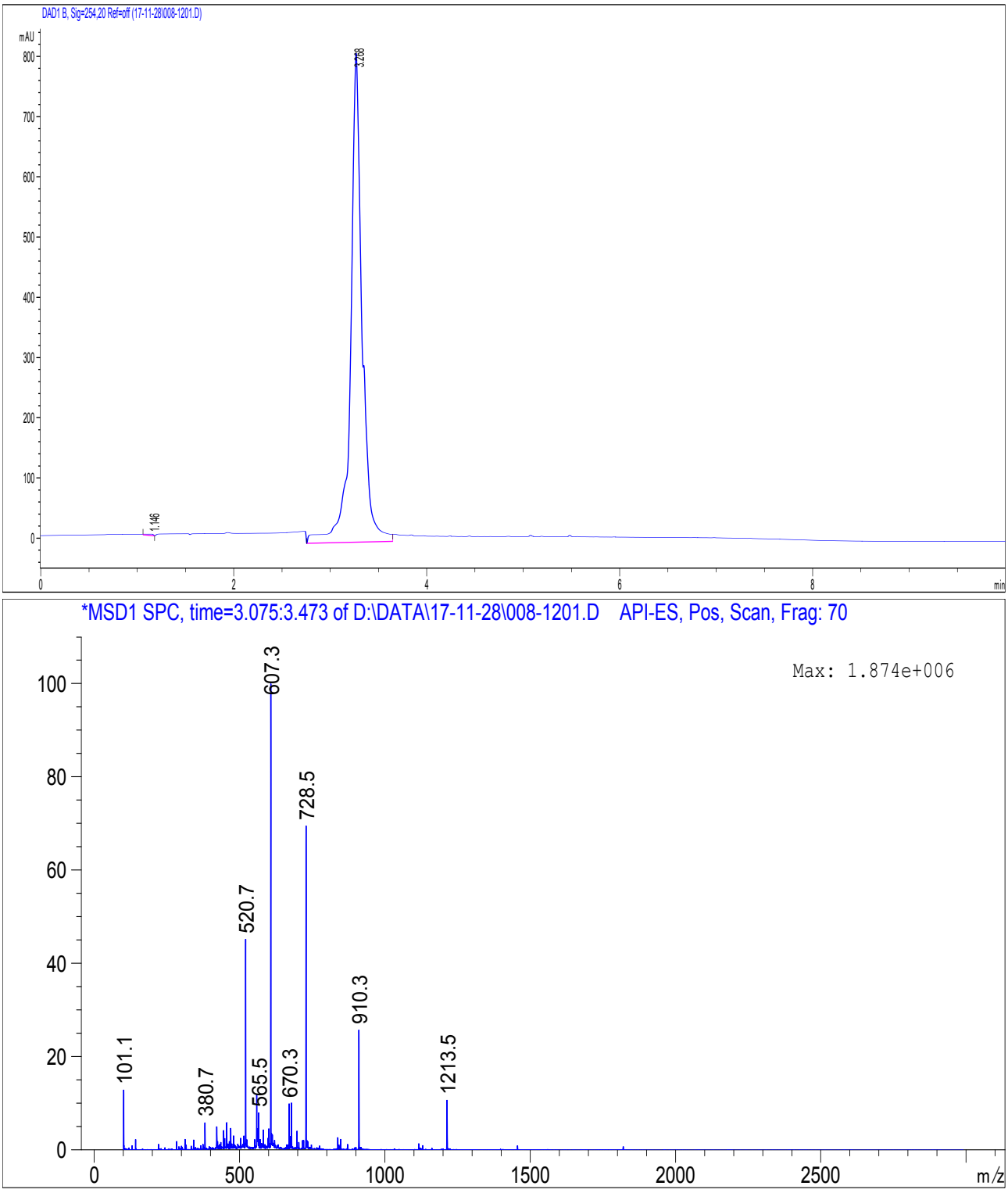

Figure S61: HPLC-MS chromatogram of purified **PNA-Fur0-11mer**. HPLC-UV trace at 254 nm (top) and MS spectrum of the corresponding peak (bottom). Calcd MW:3638.64.

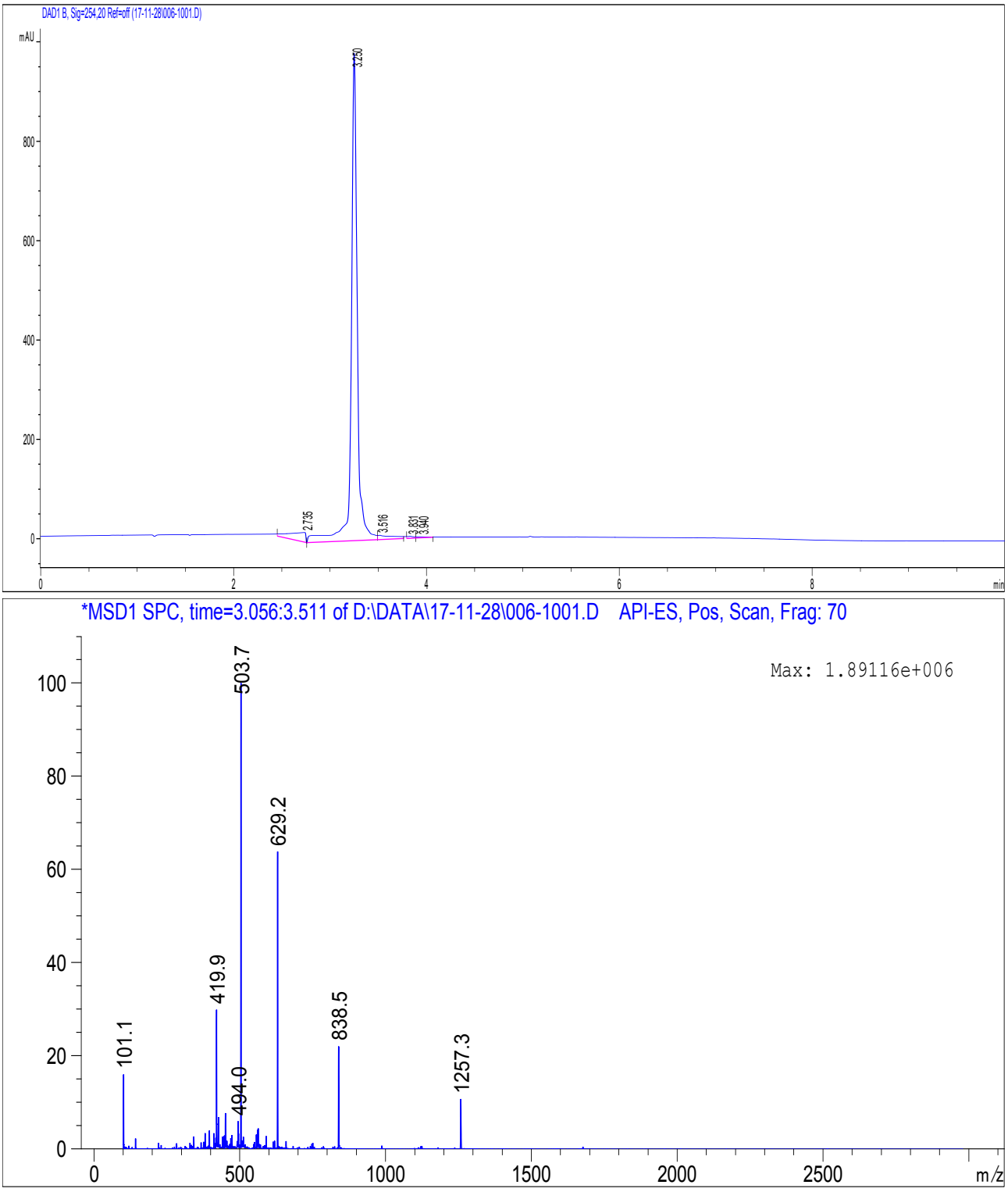

Figure S62: HPLC-MS chromatogram of purified **PNA-Fur1**. HPLC-UV trace at 254 nm (top) and MS spectrum of the corresponding peak (bottom). Calcd MW: 2513.58.

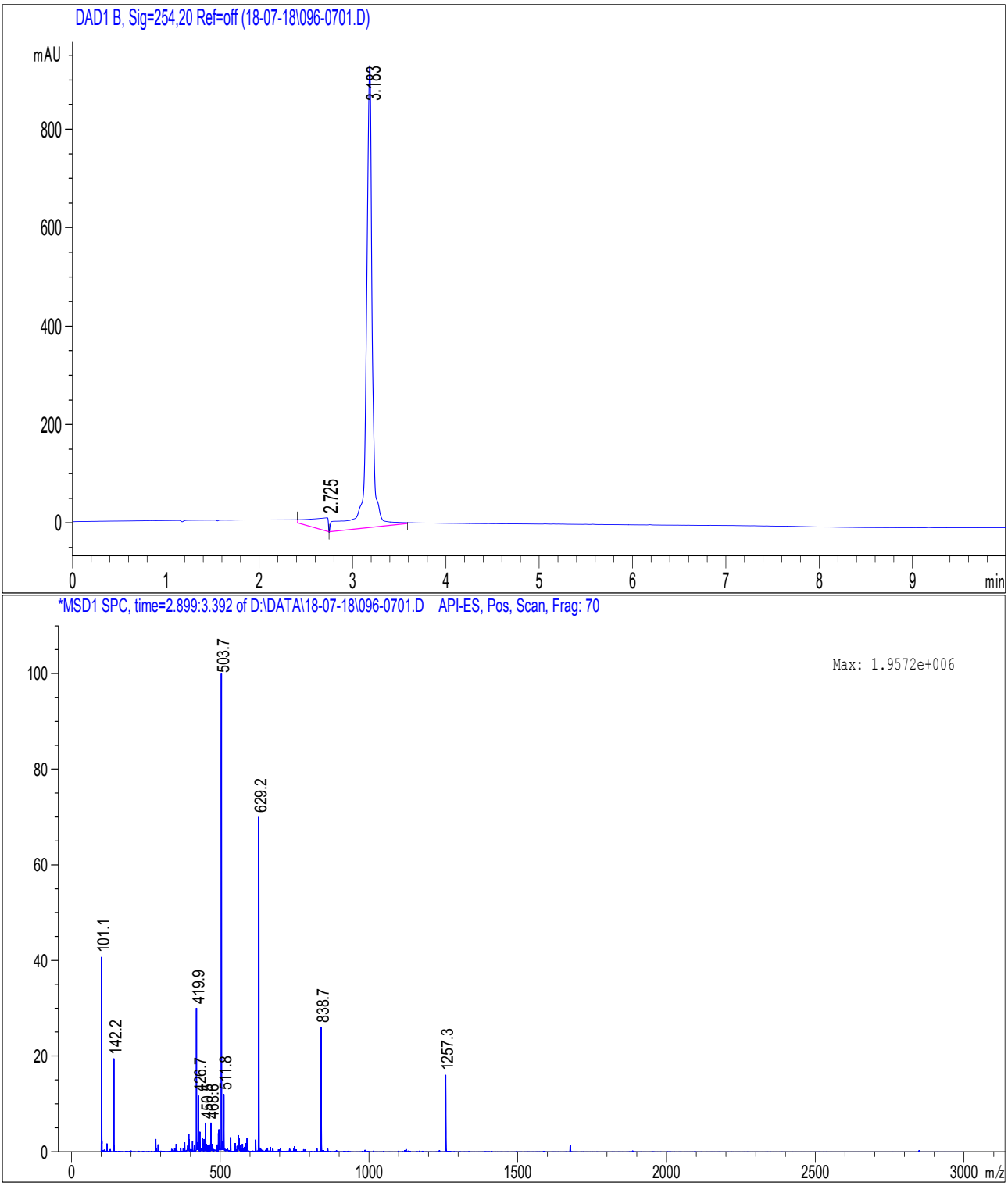

Figure S63: HPLC-MS chromatogram of purified **PNA-Fur2**. HPLC-UV trace at 254 nm (top) and MS spectrum of the corresponding peak (bottom). Calcd MW:2513.6.

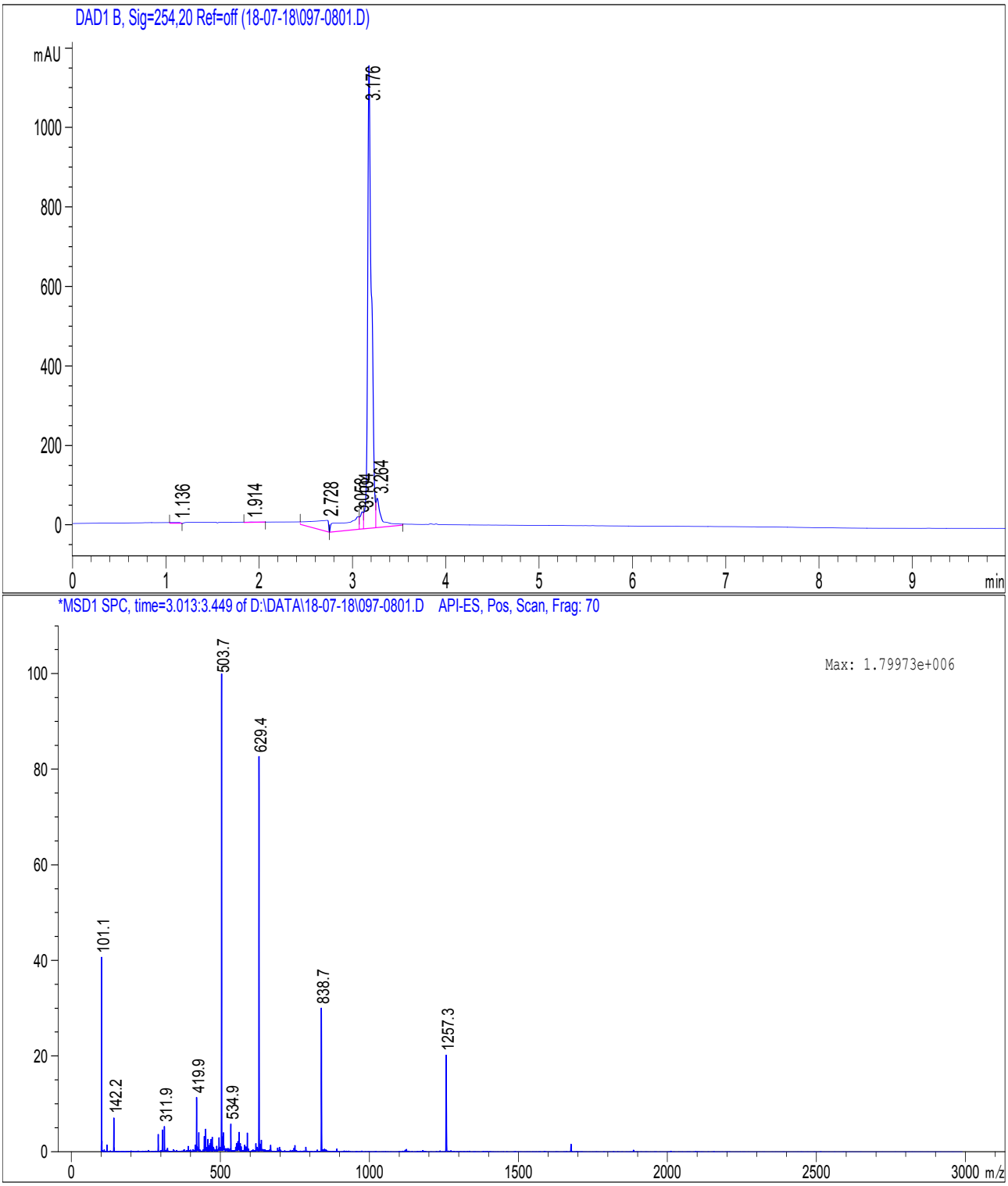

Figure S64: HPLC-MS chromatogram of purified **PNA-Fur3**. HPLC-UV trace at 254 nm (top) and MS spectrum of the corresponding peak (bottom). Calcd MW:2513.6.

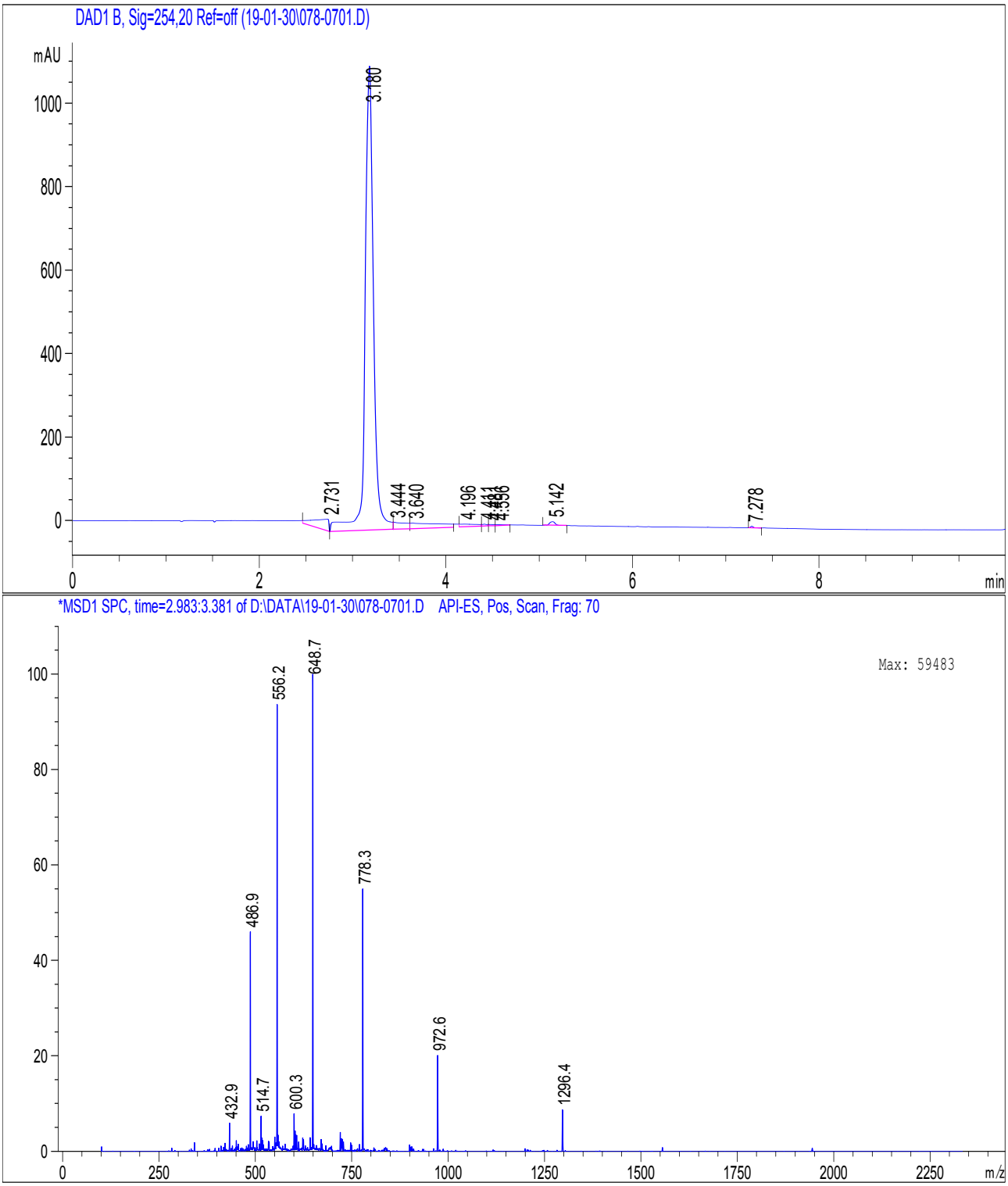

Figure S65: HPLC-MS chromatogram of purified **PNA-Fur4**. HPLC-UV trace at 254 nm (top) and MS spectrum of the corresponding peak (bottom). Calcd MW: 3886.92.

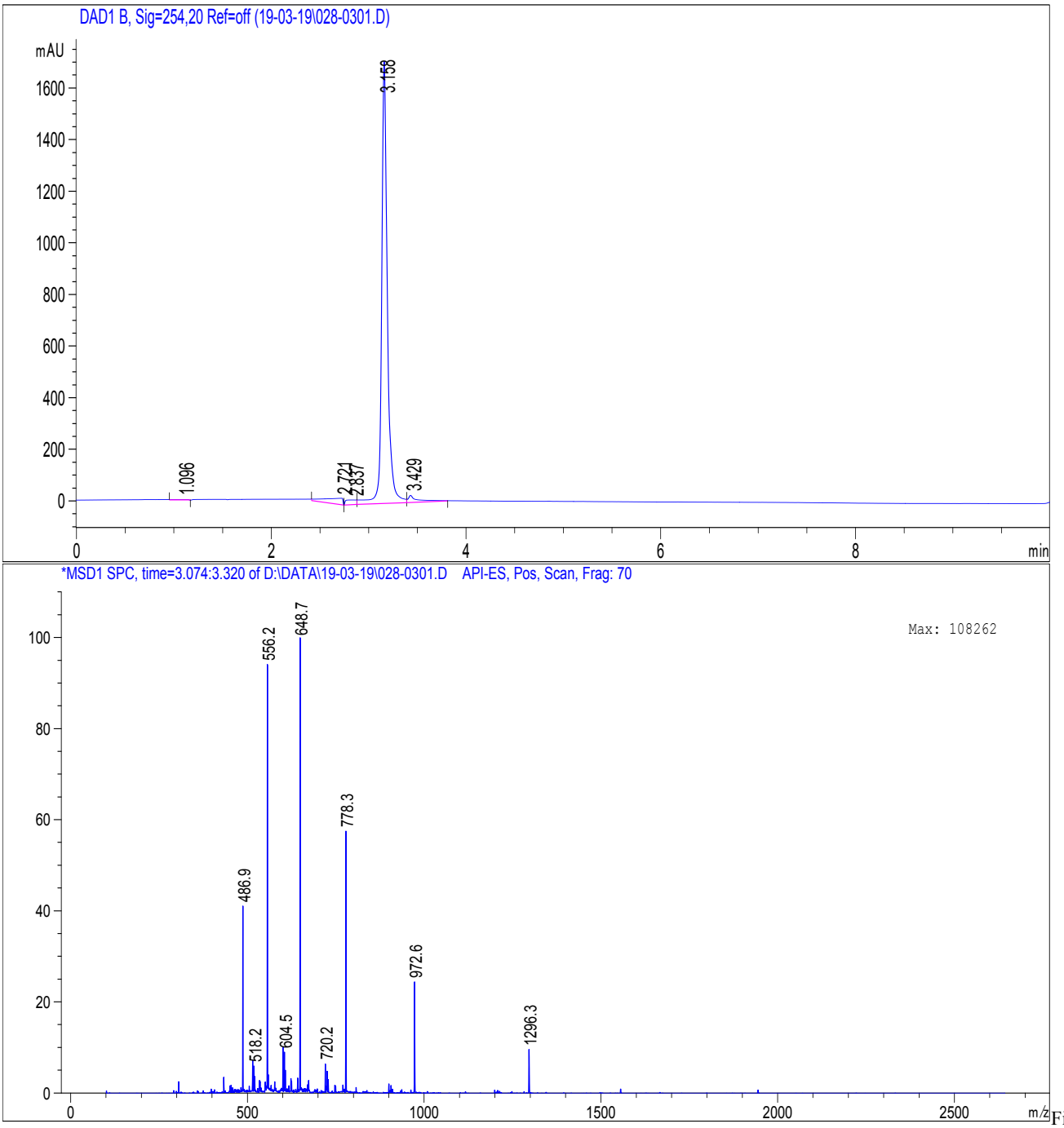

Figure S66: HPLC-MS chromatogram of purified **PNA-Fur5**. HPLC-UV trace at 254 nm (top) and MS spectrum of the corresponding peak (bottom). Calcd MW: 3886.92.

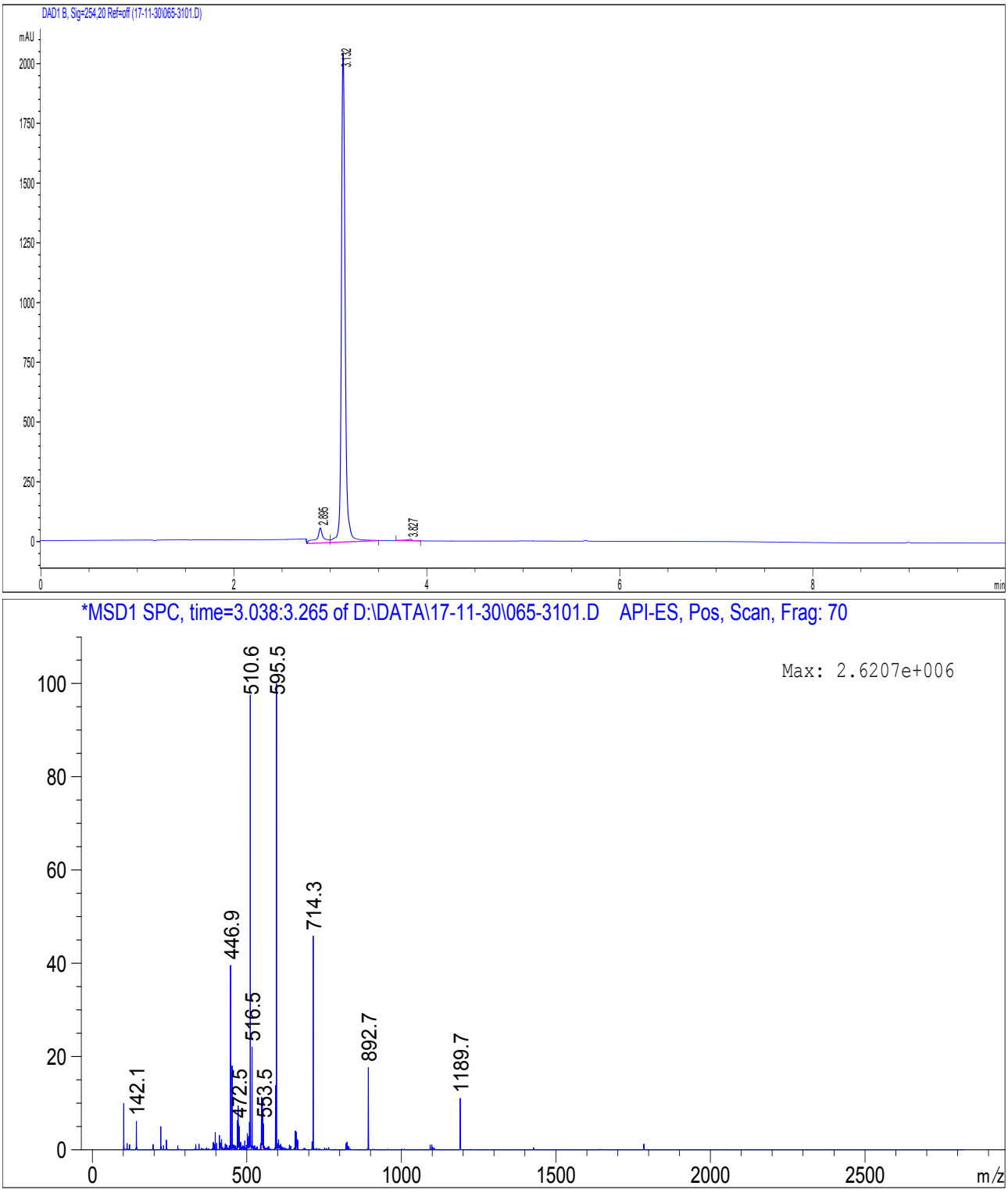

Figure S67: HPLC-MS chromatogram of purified **PNA-Am0**. HPLC-UV trace at 254 nm (top) and MS spectrum of the corresponding peak (bottom). Calcd MW:3567.66.

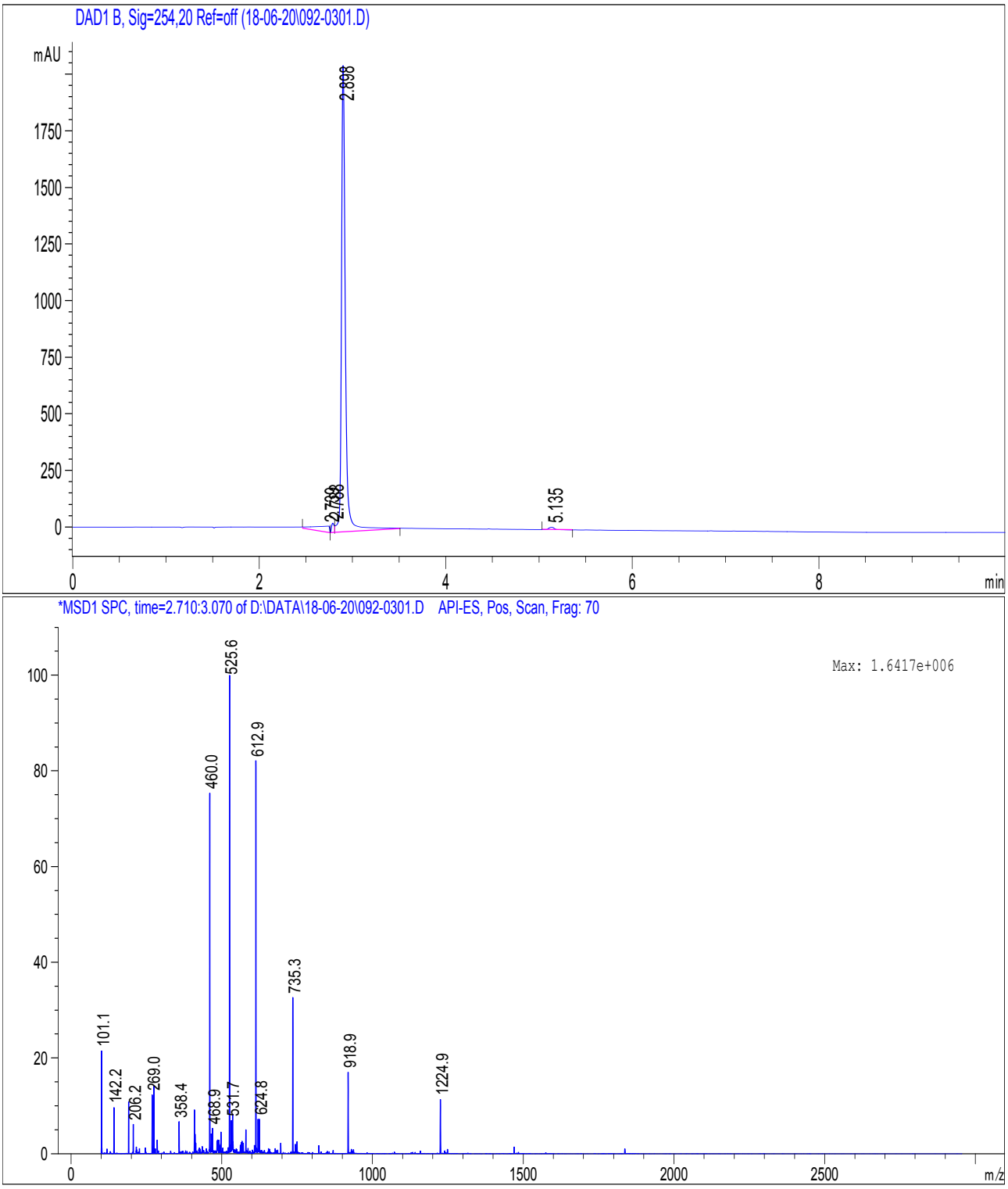

Figure S68: HPLC-MS chromatogram of purified **PNA-Am1**. HPLC-UV trace at 254 nm (top) and MS spectrum of the corresponding peak (bottom). Calcd MW:3672.8.

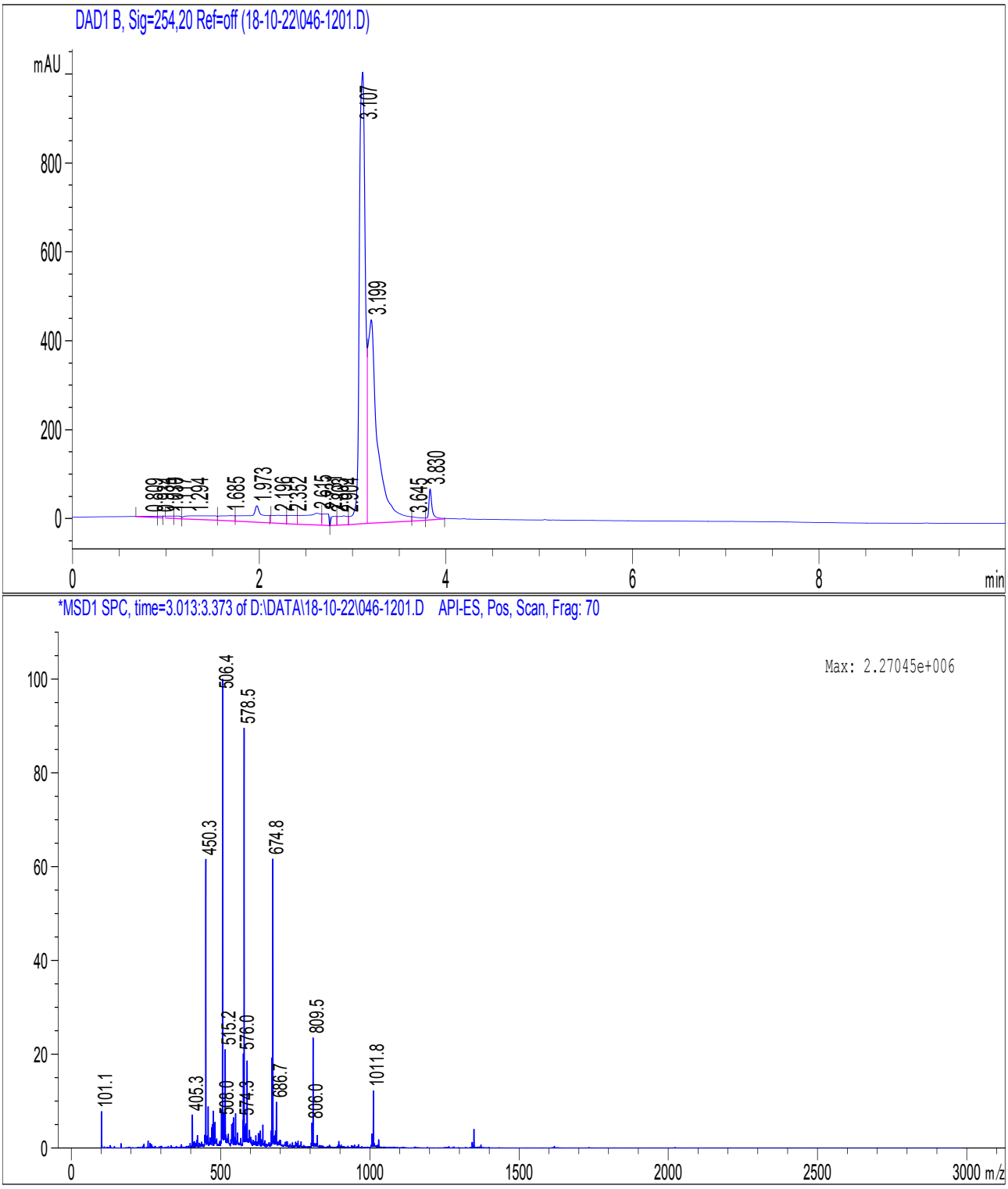

Figure S69: HPLC-MS chromatogram of purified **PNA-Am2(6-TAMRA)**. HPLC-UV trace at 254 nm (top) and MS spectrum of the corresponding peak (bottom). Calcd MW:4042.85.

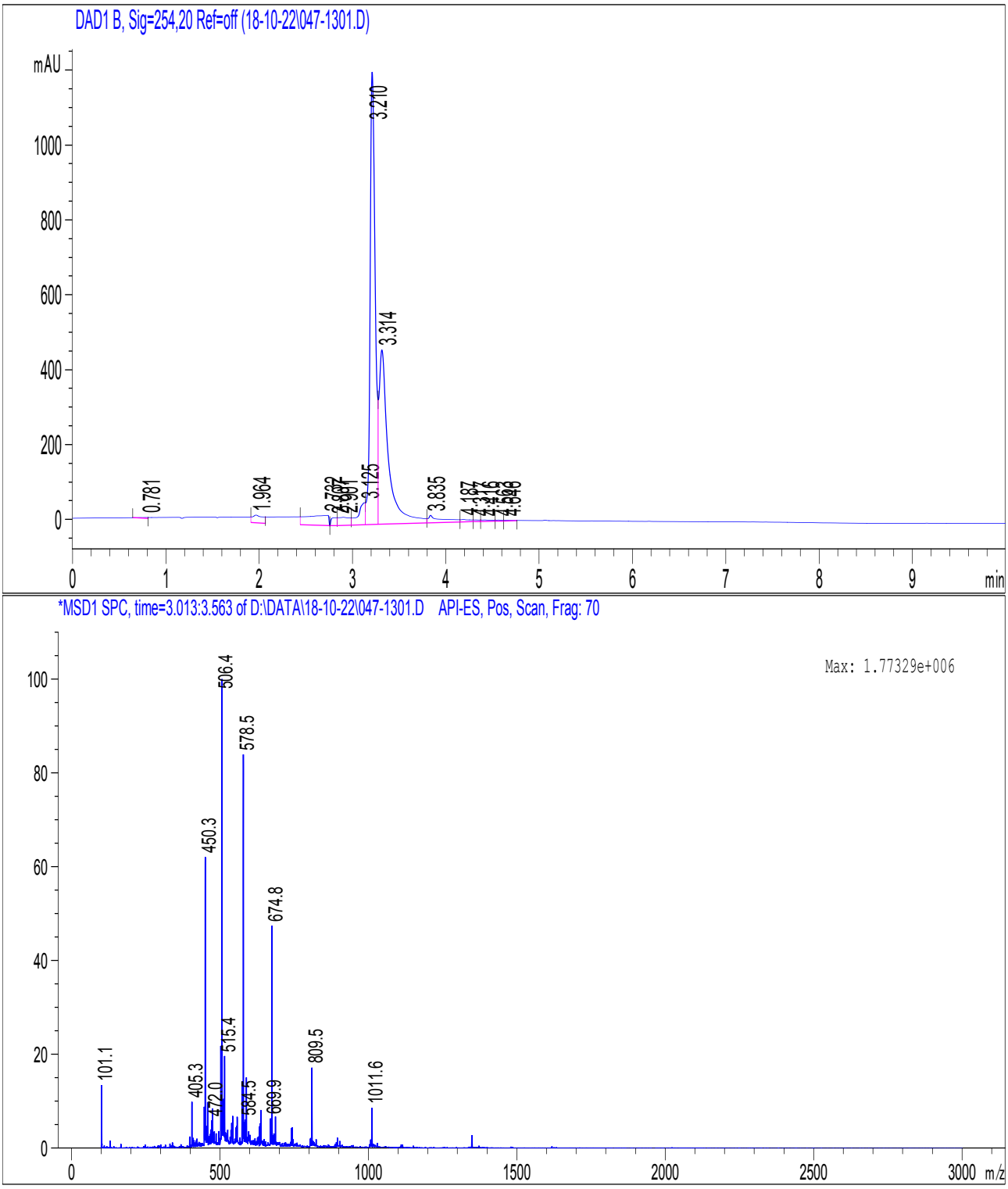

Figure S70: HPLC-MS chromatogram of purified **PNA-Am2(5-TAMRA)**. HPLC-UV trace at 254 nm (top) and MS spectrum of the corresponding peak (bottom). Calcd MW:4042.85.

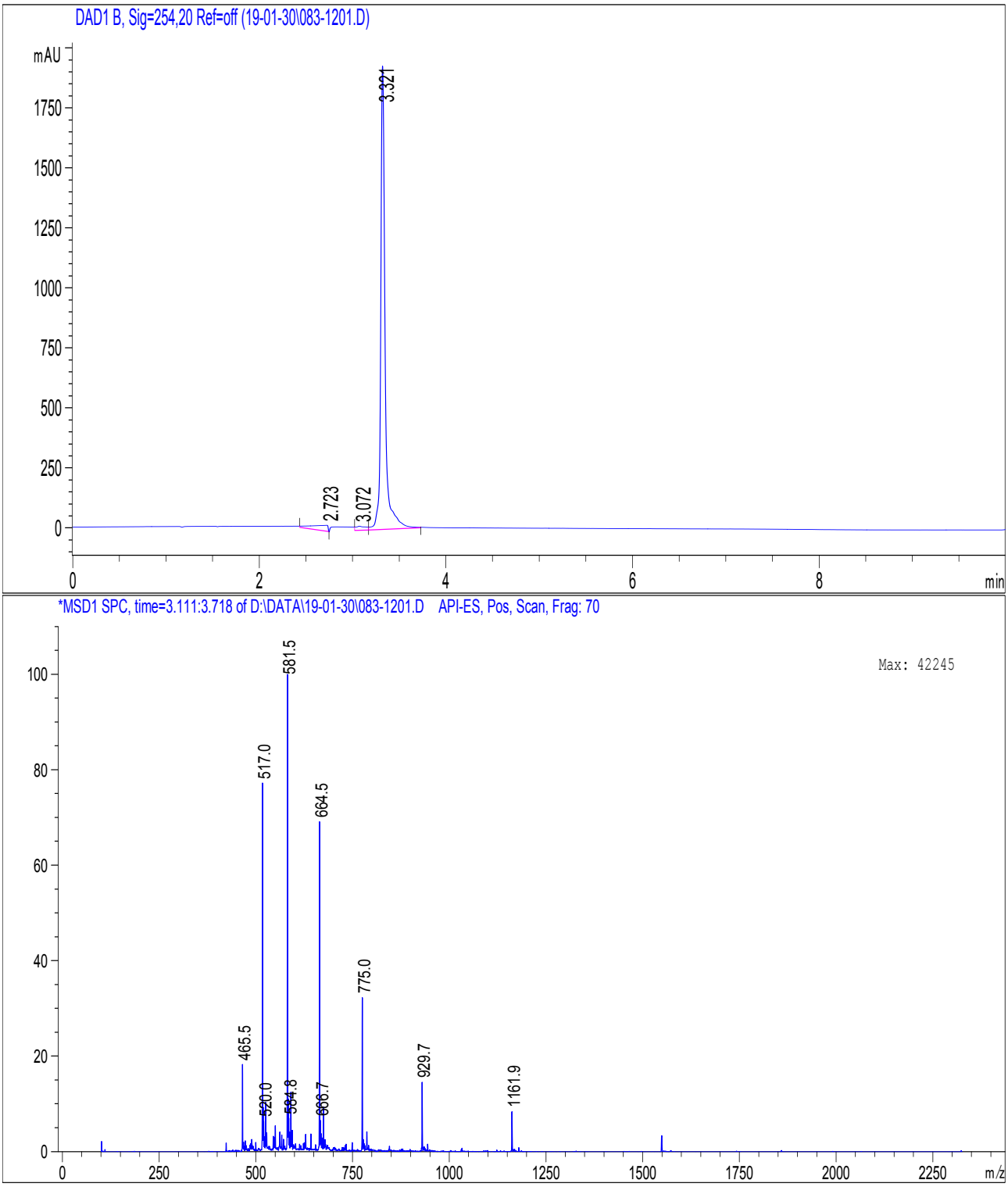

Figure S71: HPLC-MS chromatogram of purified **PNA-Am3**. HPLC-UV trace at 254 nm (top) and MS spectrum of the corresponding peak (bottom). Calcd MW: 4644.9.

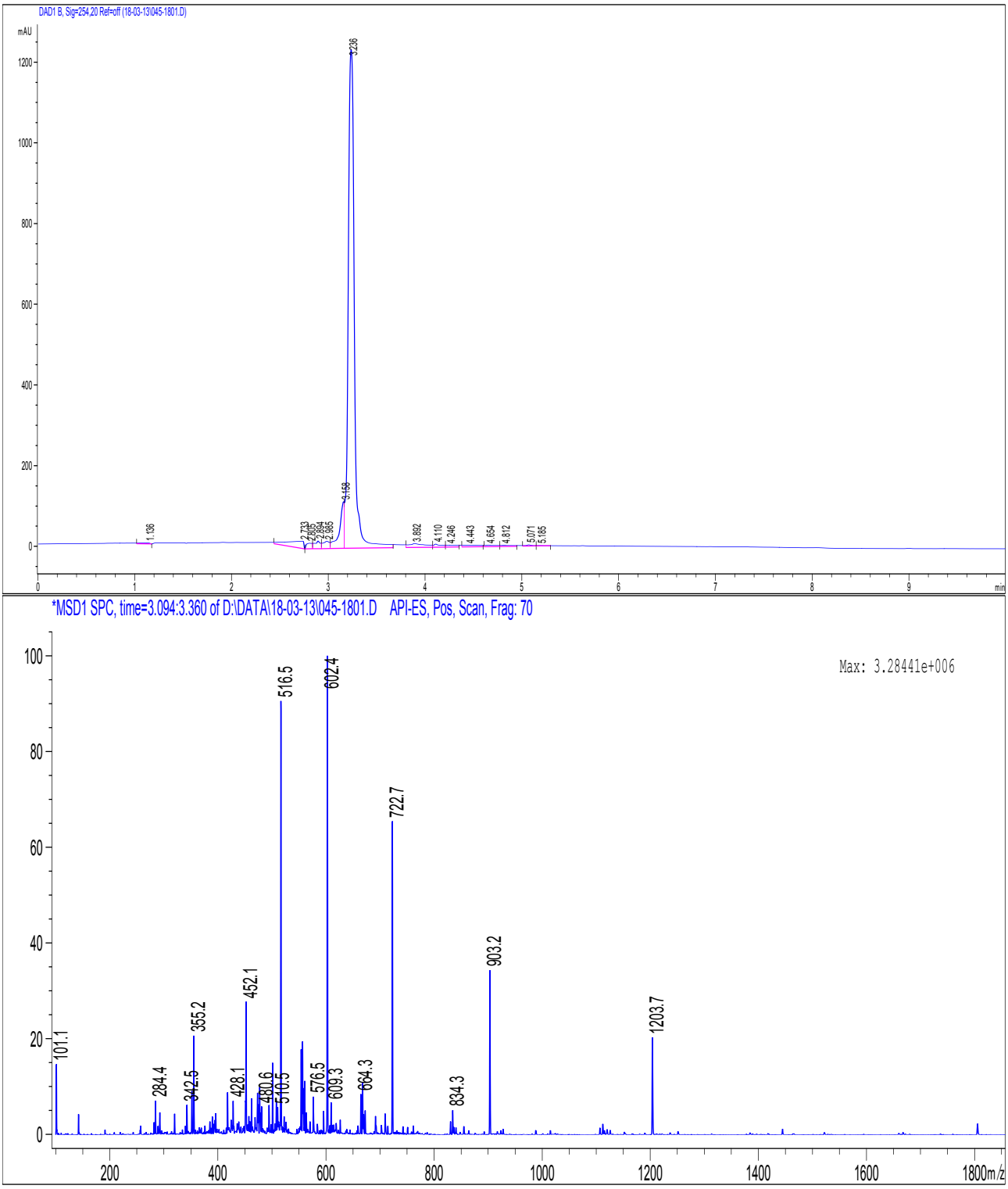

Figure S72: HPLC-MS chromatogram of purified **PNA-Ac0**. HPLC-UV trace at 254 nm (top) and MS spectrum of the corresponding peak (bottom). Calcd MW:3609.70.

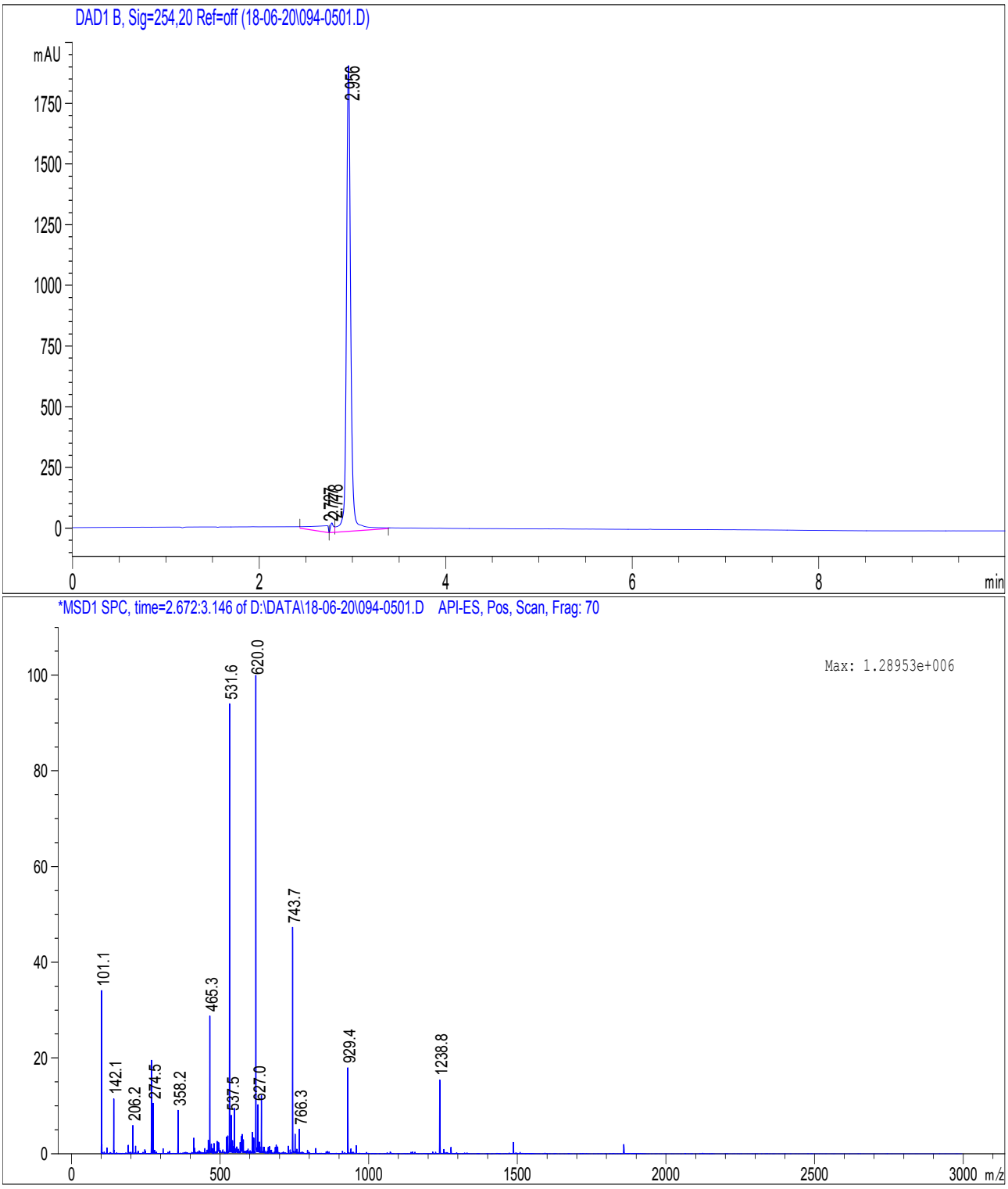

Figure S73: HPLC-MS chromatogram of purified **PNA-Ac1**. HPLC-UV trace at 254 nm (top) and MS spectrum of the corresponding peak (bottom). Calcd MW:3714.8.

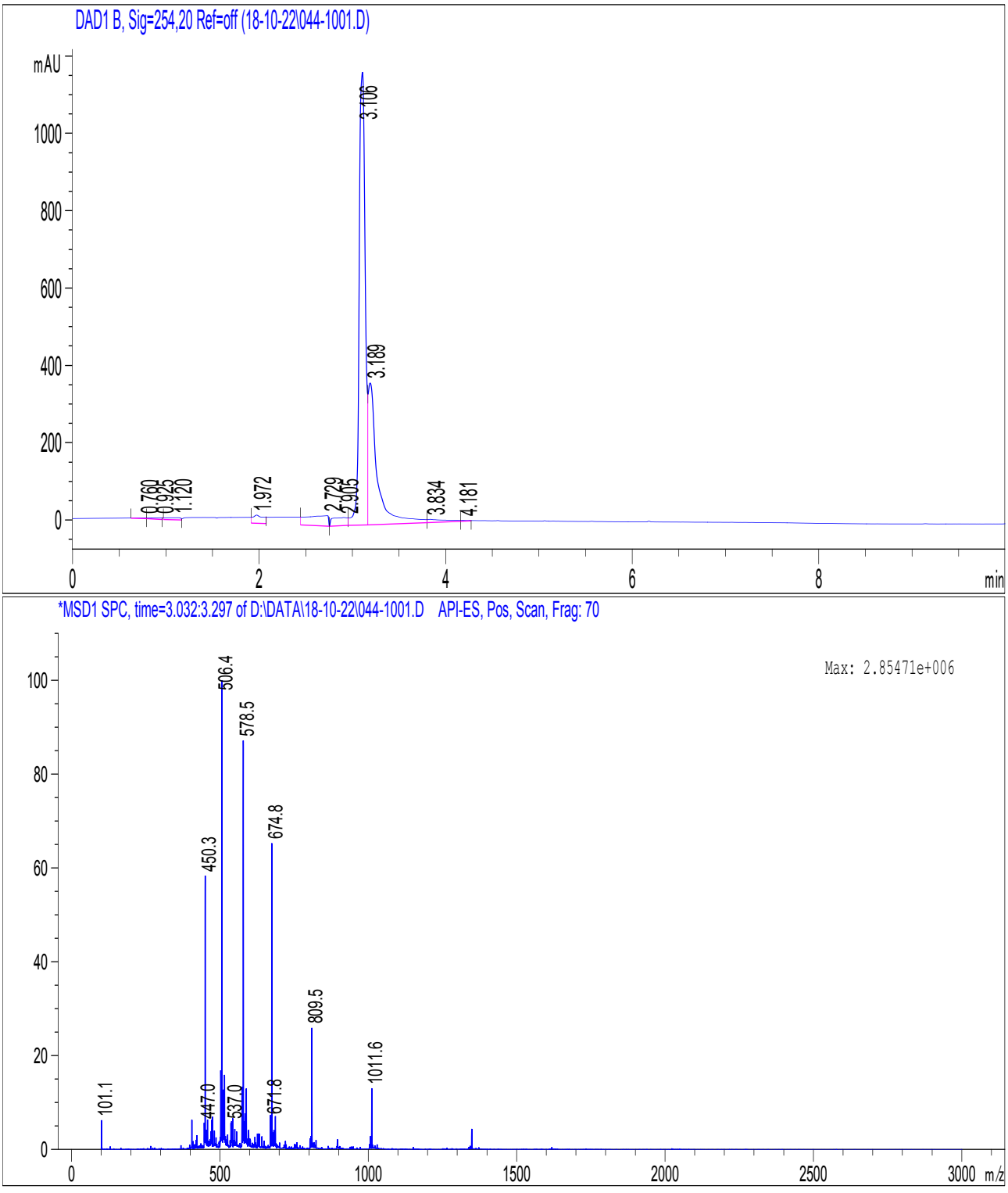

Figure S74: HPLC-MS chromatogram of purified **PNA-Ac2(6-TAMRA)**. HPLC-UV trace at 254 nm (top) and MS spectrum of the corresponding peak (bottom). Calcd MW:4084.89.

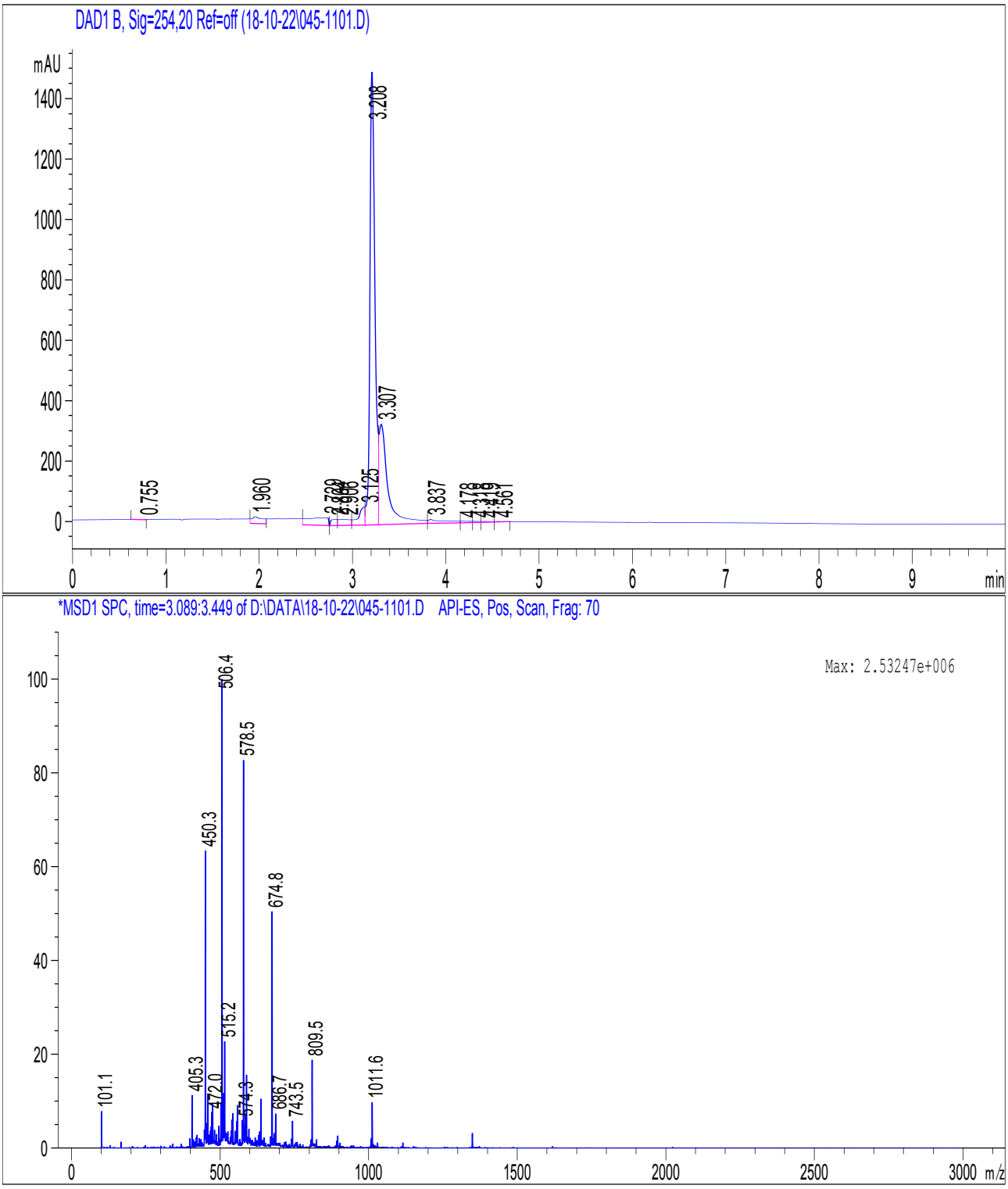

Figure S75: HPLC-MS chromatogram of purified **PNA-Ac2(5-TAMRA)**. HPLC-UV trace at 254 nm (top) and MS spectrum of the corresponding peak (bottom). Calcd MW:4084.89.

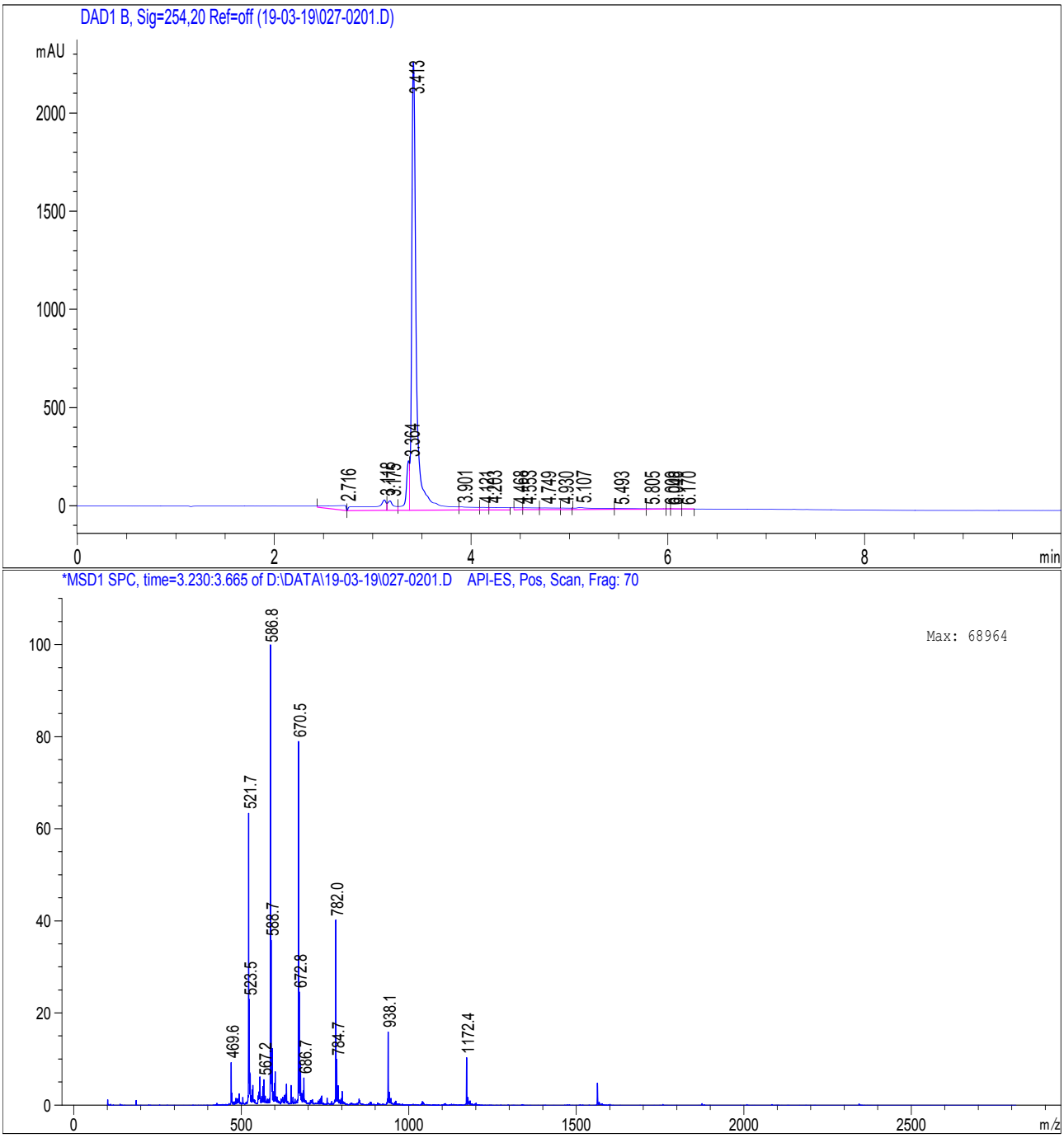

Figure S76: HPLC-MS chromatogram of purified **PNA-Ac3**. HPLC-UV trace at 254 nm (top) and MS spectrum of the corresponding peak (bottom). Calcd MW:4687.0.

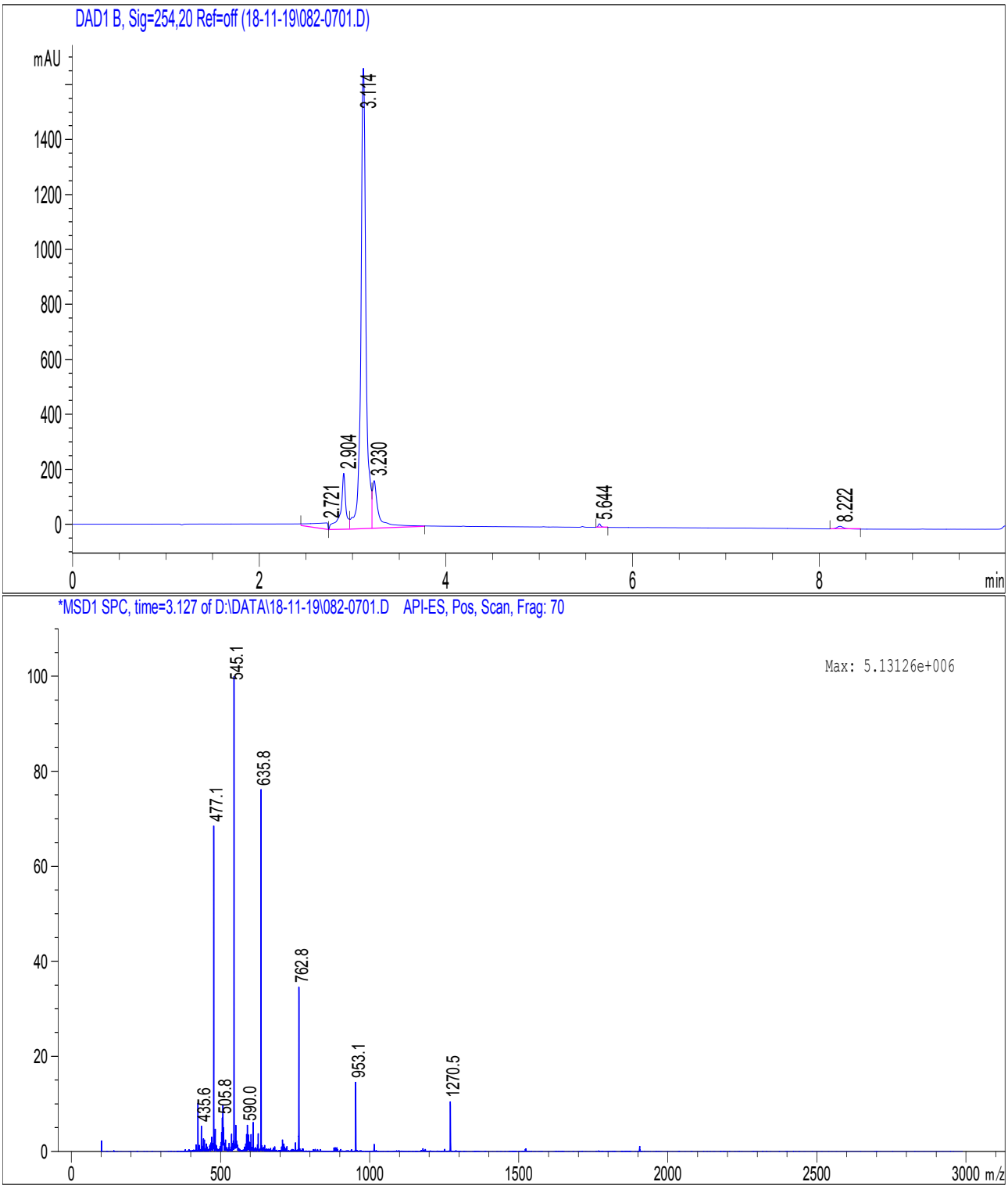

Figure S77: HPLC-MS chromatogram of purified **PNA-Hy0**. HPLC-UV trace at 254 nm (top) and MS spectrum of the corresponding peak (bottom). Calcd MW:3809.94.

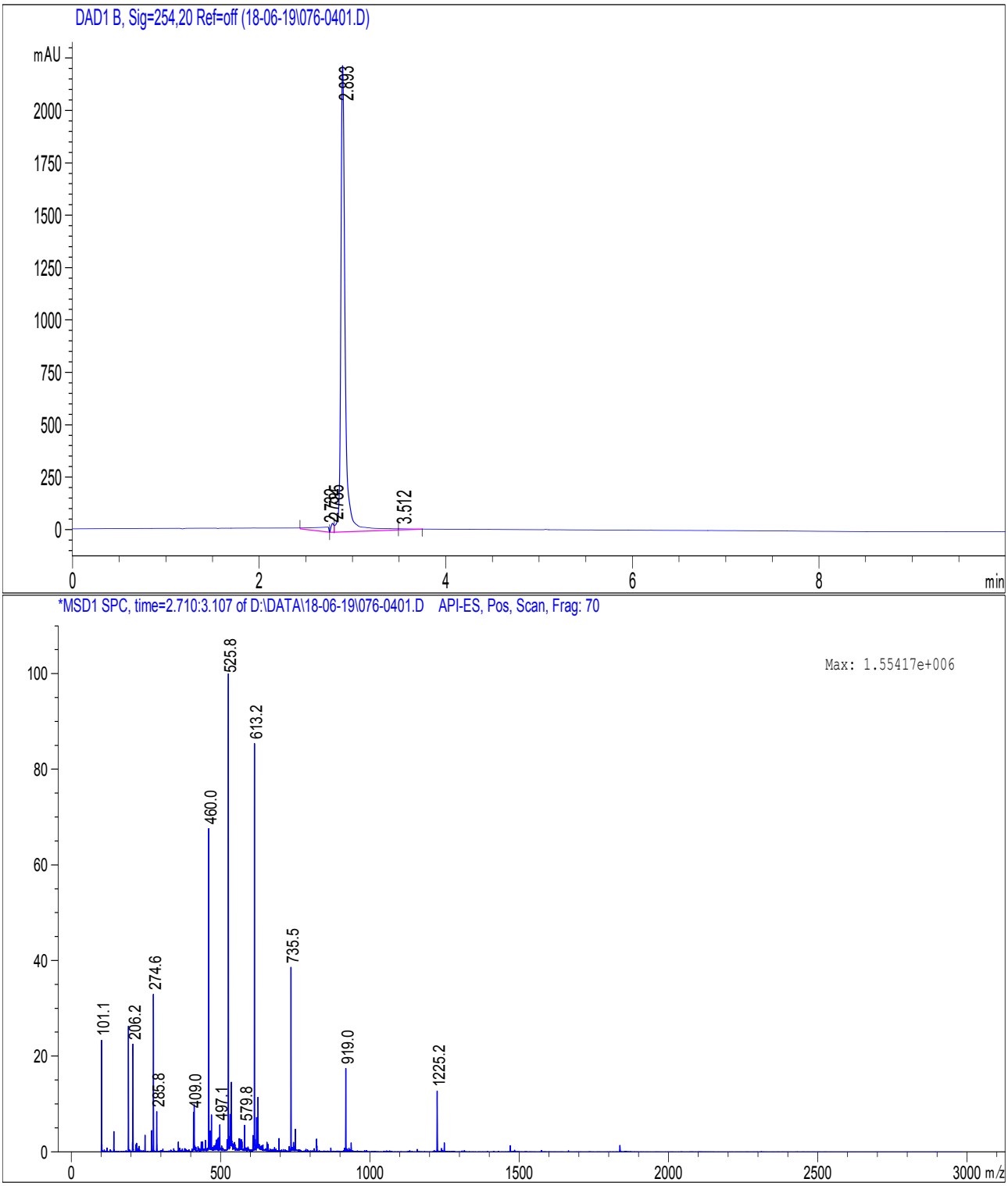

Figure S78: HPLC-MS chromatogram of purified **PNA-Hy1**. HPLC-UV trace at 254 nm (top) and MS spectrum of the corresponding peak (bottom). Calcd MW:3673.8.

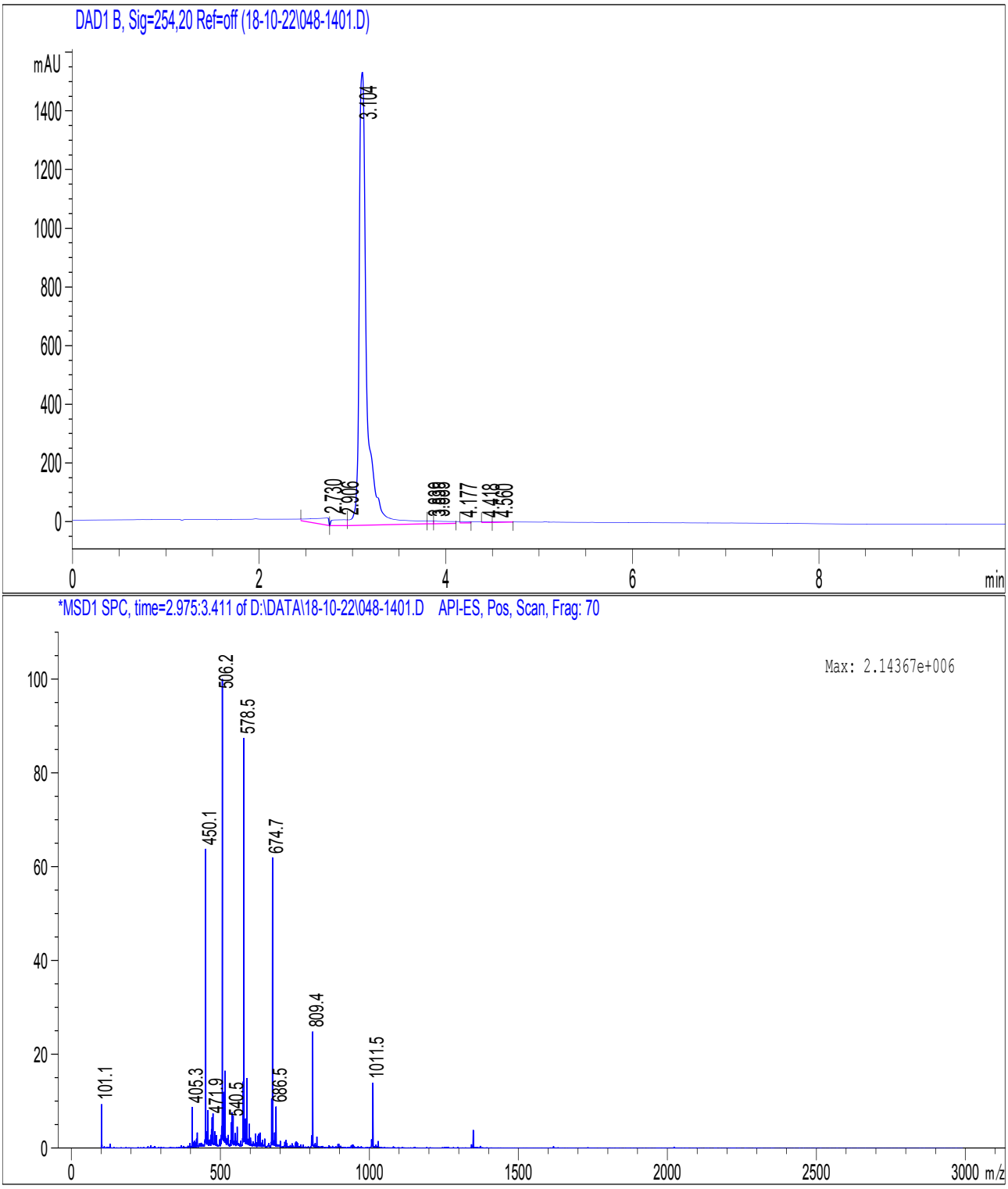

Figure S79: HPLC-MS chromatogram of purified **PNA-Hy2(6-TAMRA)**. HPLC-UV trace at 254 nm (top) and MS spectrum of the corresponding peak (bottom). Calcd MW:4043.80.

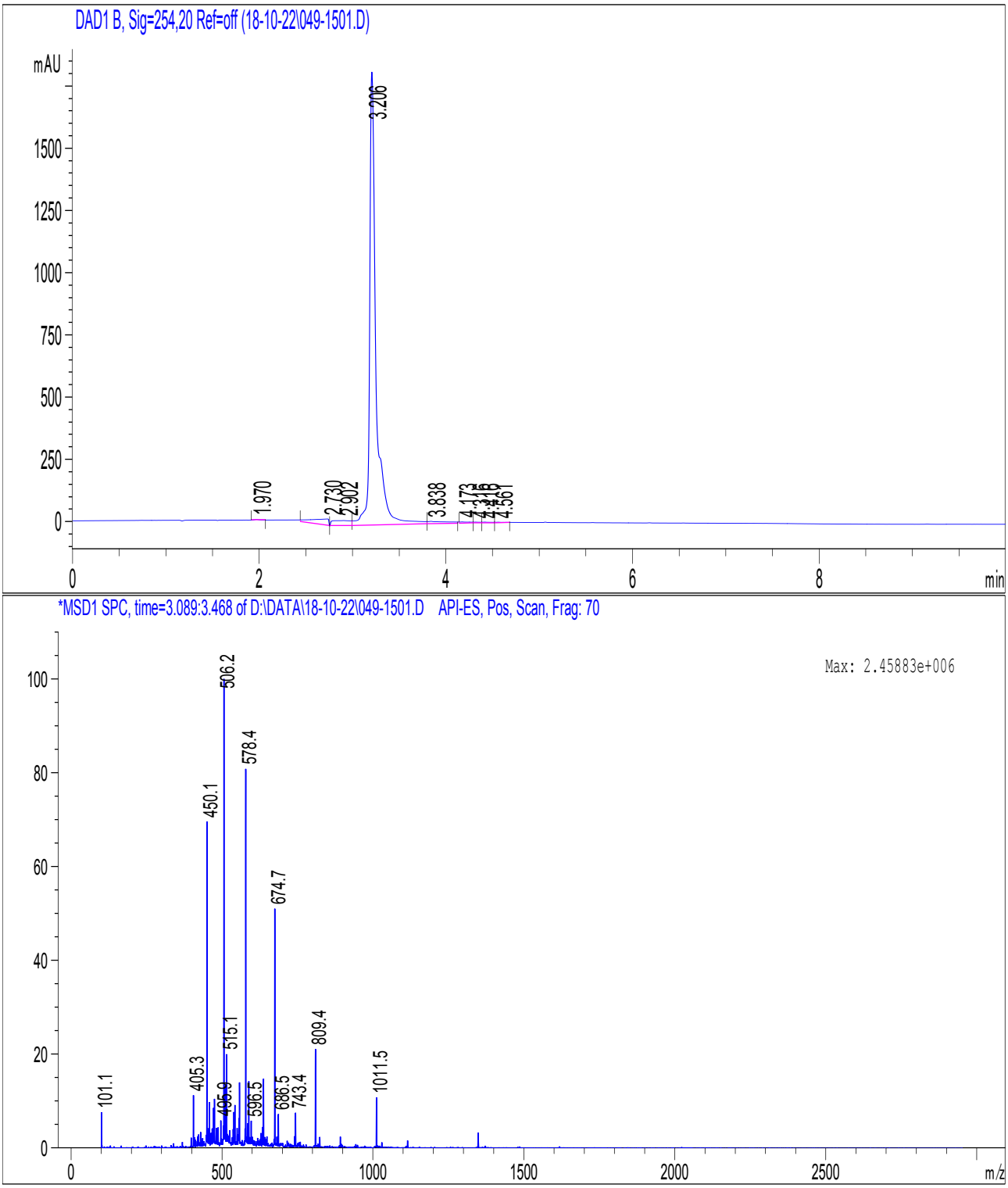

Figure S80: HPLC-MS chromatogram of purified **PNA-Hy2(5-TAMRA)**. HPLC-UV trace at 254 nm (top) and MS spectrum of the corresponding peak (bottom). Calcd MW:4043.80.

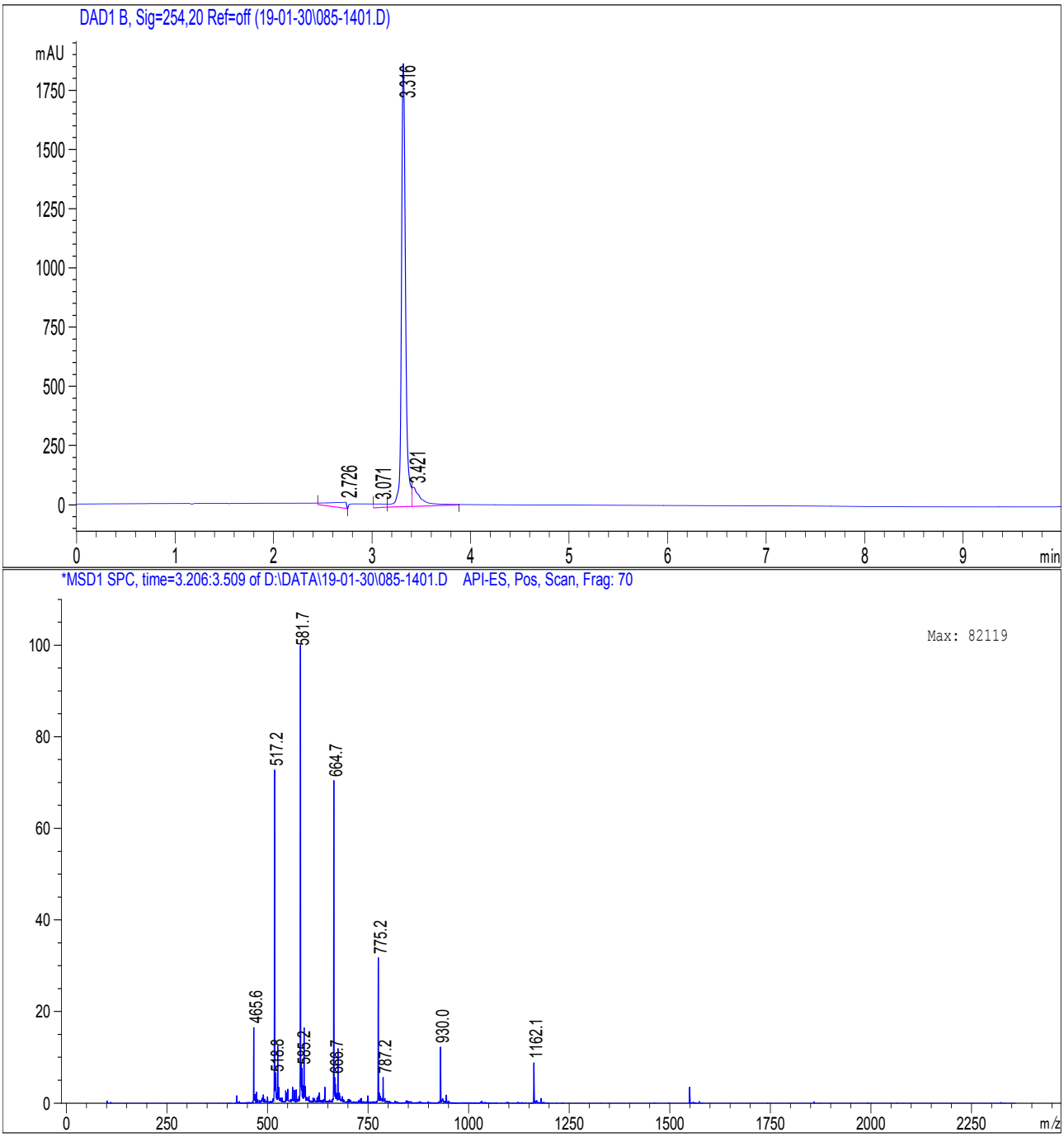

Figure S81: HPLC-MS chromatogram of purified **PNA-Hy3**. HPLC-UV trace at 254 nm (top) and MS spectrum of the corresponding peak (bottom). Calcd MW: 4645.9.

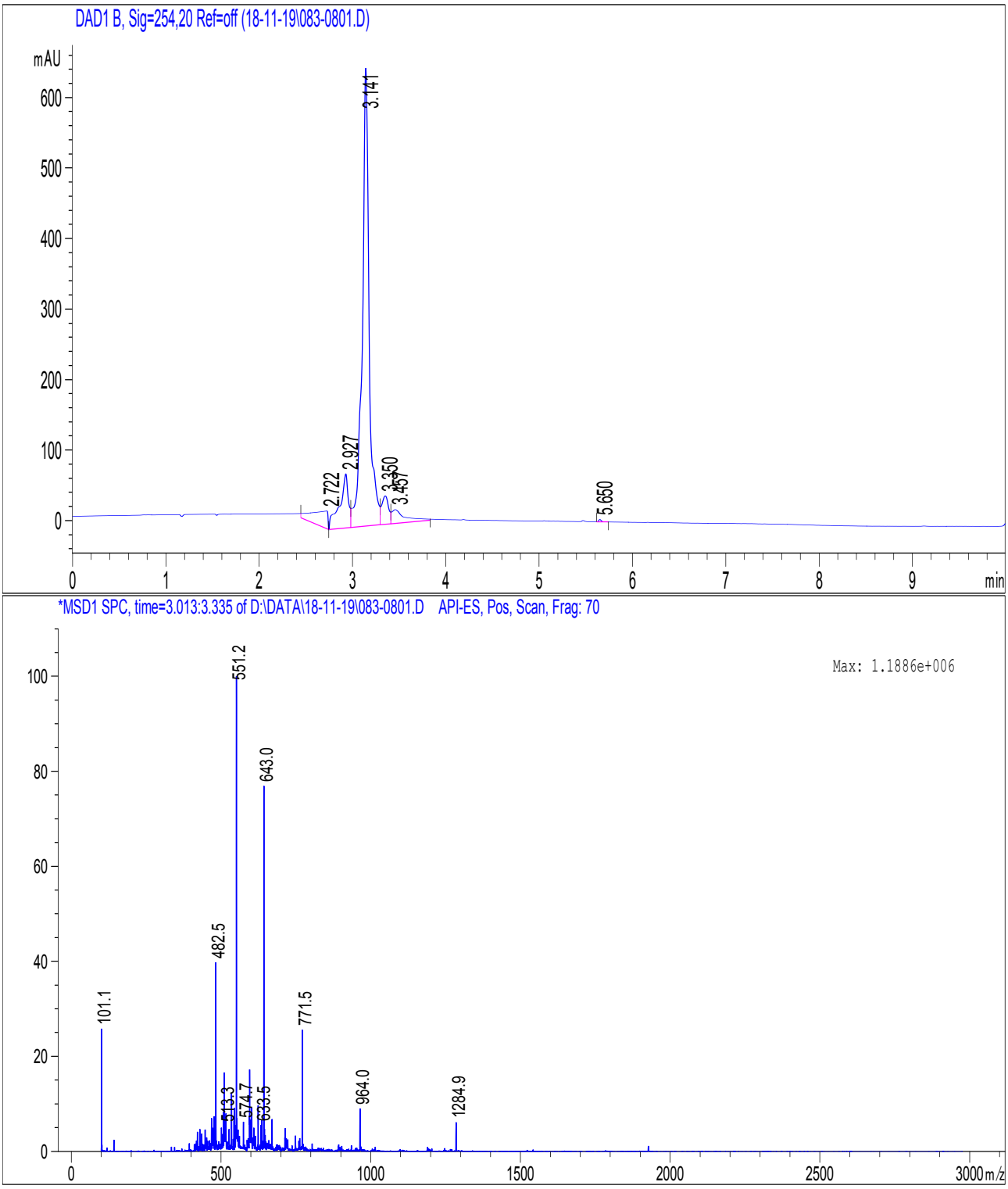

Figure S82: HPLC-MS chromatogram of purified **PNA-Sc0**. HPLC-UV trace at 254 nm (top) and MS spectrum of the corresponding peak (bottom). Calcd MW:3852.96.

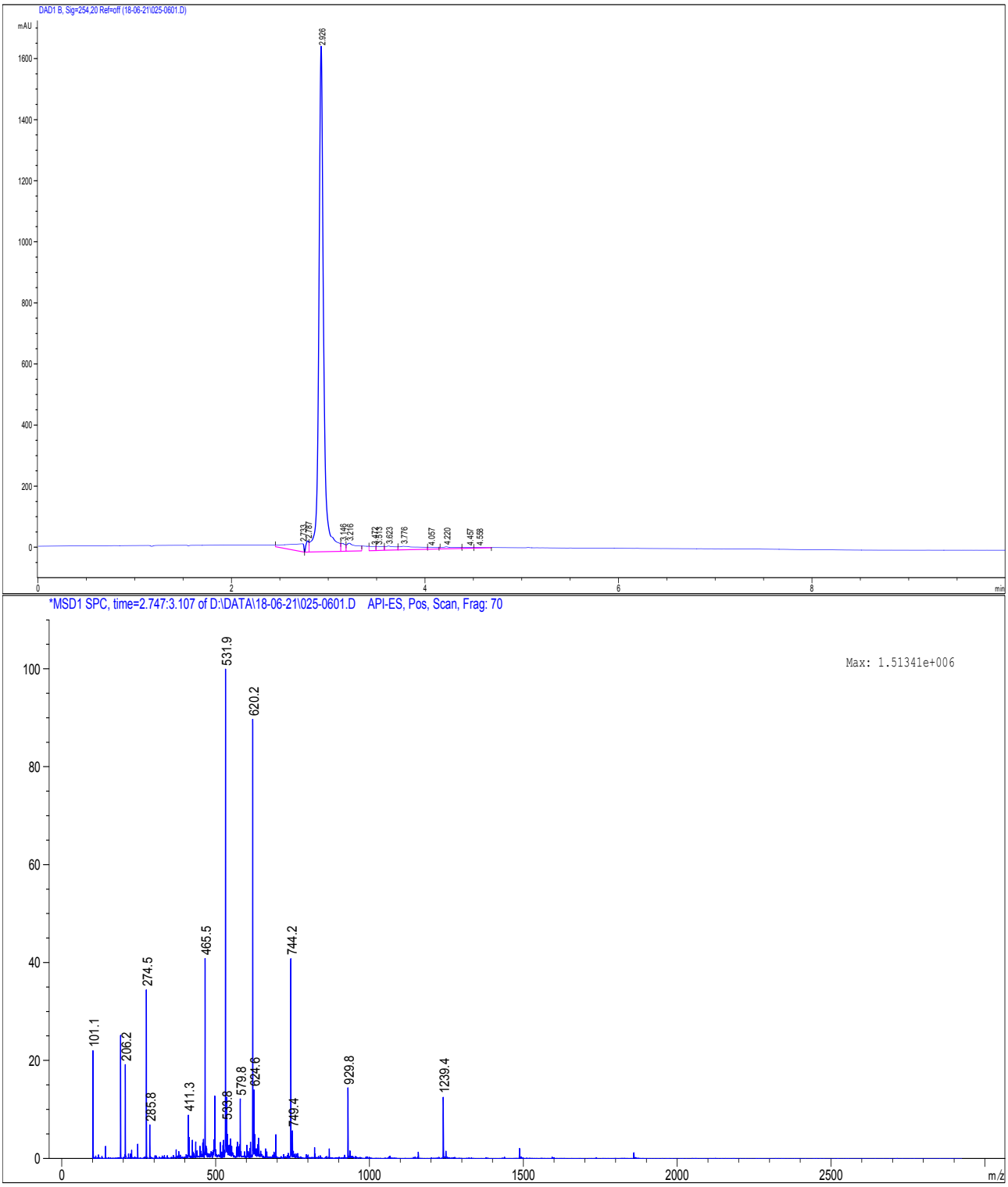

Figure S83: HPLC-MS chromatogram of purified **PNA-Sc1**. HPLC-UV trace at 254 nm (top) and MS spectrum of the corresponding peak (bottom). Calcd MW:3716.8.

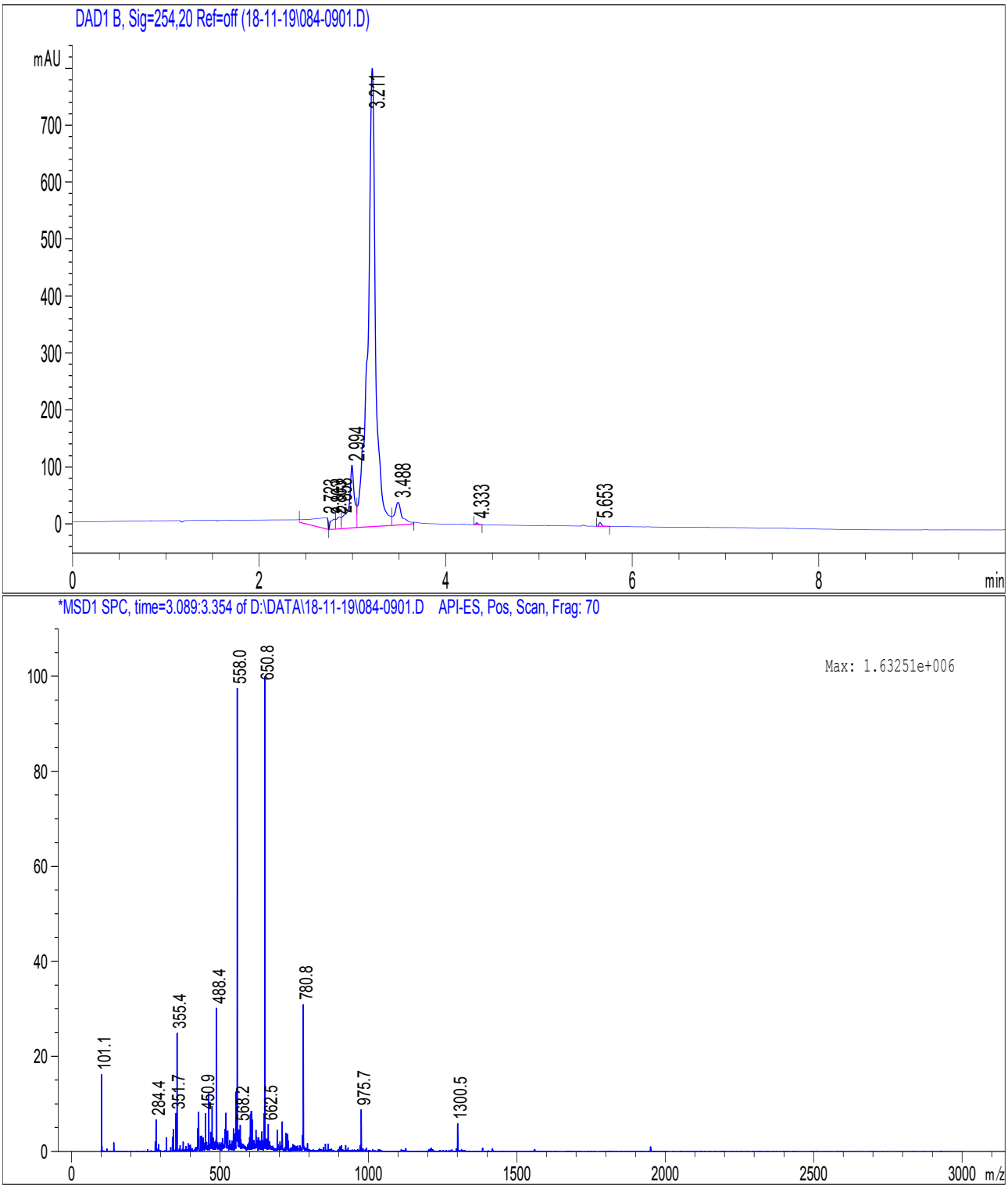

Figure S84: HPLC-MS chromatogram of purified **PNA-Hd0**. HPLC-UV trace at 254 nm (top) and MS spectrum of the corresponding peak (bottom). Calcd MW:3900.02.

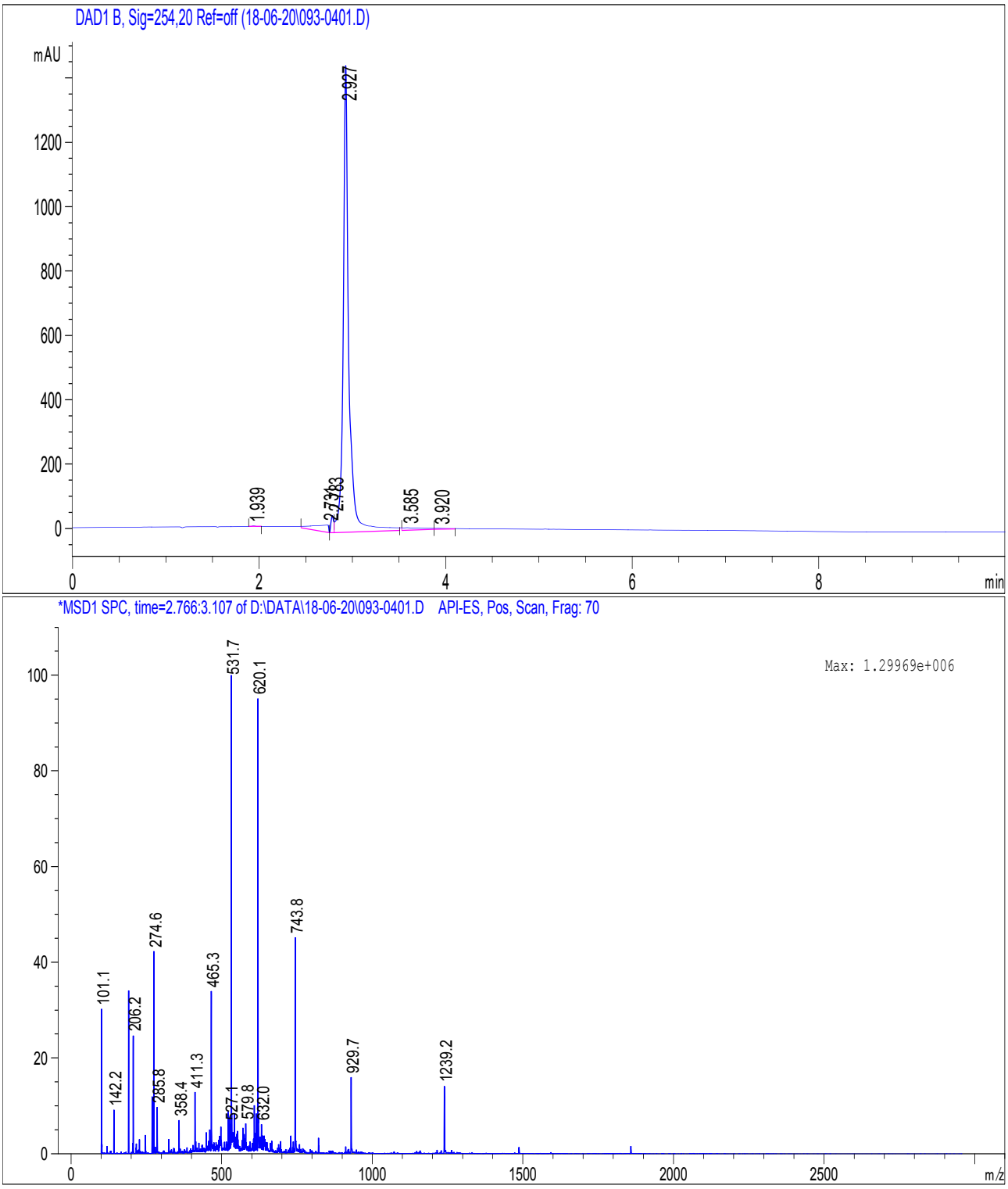

Figure S85: HPLC-MS chromatogram of purified **PNA-Hd1**. HPLC-UV trace at 254 nm (top) and MS spectrum of the corresponding peak (bottom). Calcd MW:3715.9.